TÉCNICO LISBOA

Assessing Material Costs and Deposition Rates of Automated Composite Lay-up Technologies

Gonçalo da Veiga França da Rocha e Castro

Thesis to obtain the Master of Science Degree in

Aerospace Engineering

Supervisors: Eng. António Pedro Dias Alves de Campos
Prof. Elsa Maria Pires Henriques

Examination Committee

Chairperson: Prof. Filipe Szolnoky Ramos Pinto Cunha
Supervisor: Prof. Elsa Maria Pires Henriques
Members of the Committee: Prof. Bruno Alexandre Rodrigues Simões Soares
Prof. Marco Alexandre de Oliveira Leite

January 2021

Declaration

I declare that this document is an original work of my own authorship and that it fulfills all the requirements of the Code of Conduct and Good Practices of the Universidade de Lisboa.

Acknowledgments

First of all, i would like to thank my supervisors, engineer António Campos and professor Elsa Henriques who helped me throughout the development of this dissertation providing me with their knowledge, patience and guidance which were crucial to its conclusion.

Secondly, i want to express my gratitude to my internship tutors at Embraer Évora, Pedro Albuquerque and Felipe Mutschler, whose mentorship and knowledge, although not directly involved with the matter of this thesis, gave me the tools, work method and inspiration required for the high exigence of this work. I would also like to thank my Embraer colleague Raúl Guichón for its expertise in composites technologies which revealed itself very helpfull and finally to Duarte Cacilhas, composite technician at Embraer Évora, for his suggestions on how to improve the Automated Composite Lay-up Technologies process.

My thanks to all the friends and colleagues that I was fortunate to have by my side throughout this intense but pleasant journey, without your support and friendship this would have been much tougher.

I am very grateful to my girlfriend, Joana, whose continuous encouragement and patient kept me going and focused. Finally, I want to acknowledge my father, sister and grandparents which have shown support through my whole life and have always motivated me when things were not going as expected. My deepest appreciation goes to them.

Resumo

A procura por materiais compósitos de fibra de carbono revelou grande crescimento na última década, principalmente no sector aeroespacial, por apresentarem boa relação resistência-peso. Isto torna-os ideais para uma redução do peso estrutural e do consumo de combustível comparativamente aos metais. As peças aeronáuticas feitas destes materiais são principalmente produzidas por duas tecnologias avançadas de manufatura: Automated Tape Laying (ATL) e Automated Fiber Placement (AFP). Estudos sobre a produtividade de máquinas de fabrico de compósitos e a influência dos seus parâmetros de configuração na produção de peças aeroespaciais são escassos e os modelos de deposição de compósitos publicados são bastante simples, não permitindo o estudo de peças complexas.

Esta tese determina custos de materiais, taxas de deposição e desperdício de material das tecnologias ATL e AFP para peças aeroespaciais planas de material compósito com complexidade arbitrária. Para tal, foi desenvolvido um modelo paramétrico detalhado do processo de deposição automatizado das máquinas de fabrico. Ao permitir uma simulação rápida e precisa do fabrico de peças nos estágios iniciais, o modelo auxilia na tomada de decisão quanto à seleção de tecnologia e configuração dos parâmetros da máquina. O modelo é validado com dados da literatura e dum corpo de prova aeronáutico. Vários estudos são realizados para obter taxas de deposição e desperdício de material para peças aeronáuticas representativas. As máquinas ATL em duas fases fornecem as melhores taxas de deposição embora possuam maiores taxas de material desperdiçado. O offset da primeira fita revelou-se promissor para camadas com múltiplas descontinuidades e formas complexas.

Palavras-chave: Indústria Aeroespacial, Tecnologias de Deposição Automatizadas, Custos de Material, Taxas de Deposição, Taxas de Desperdício de Material

Abstract

The demand for carbon fiber composite materials has grown considerably over the last decade, particularly in the aerospace sector, as they present high strength while yielding low weight. This makes them ideal for structural weight and fuel consumption savings compared to metals, which have been the primary aviation materials for almost a century. Carbon fiber composite aeronautical parts are mainly produced through two advanced composite manufacturing technologies: Automated Tape Laying (ATL) and Automated Fiber Placement (AFP). Studies on the productivity of composite manufacturing machines and the influence of their configuration parameters in the production of aerospace parts are scarce, moreover composite lay-up models in the literature are relatively simple, not allowing the study of more complex shapes.

This thesis assesses material costs, deposition rates and scrap levels of ATL and AFP technologies for aerospace flat composite parts with arbitrary planar complexity. For that, a detailed parametric model of the manufacturing machines' automated lay-up process was developed. The model helps decision-making regarding technology selection and machine's parameters configuration by allowing fast and accurate part manufacturing simulation in early development stages. The model is validated with literature results and data from an aeronautical specimen test part. Several studies are conducted to obtain lay-up and scrap rates for aeronautical representative parts and a first tape lay-up offset study is performed to survey technical scrap reduction. ATL two-phase systems provide the best lay-up rates while yielding the highest scrap rates. First tape offset lay-up revealed promising for plies with multiple gaps and complex shapes.

Keywords: Aerospace Industry, Automated Lay-up Technologies, Material Costs, Lay-up Rates, Scrap Rates

Contents

List of Tables

List of Figures

Nomenclature

ACMT Automated Composite Manufacturing Technologies.

AFP Automated Fiber Placement.

ATL Automated Tape Laying.

CAGR Compounded Annual Growth Rate

CF Carbon Fiber.

CFRP Carbon Fiber Reinforced Polymer.

CNC Computer Numerical Control.

CTLM Contour Tape Laminating Machine.

ESA European Space Agency.

EVTOL Electric Vertical Take-off and Landing.

FTLM Flat Tape Laminating Machine.

FW Filament Winding

GFRP Glass Fiber Reinforced Polymers.

OEM Original Equipment Manufacturer.

OOA Out of Autoclave.

Prepreg Pre-impregnated Fibre.

RTM Resin Transfer Molding

SOA State Of The Art

VARTM Vacuum Assisted Resin Transfer Molding

1. Introduction

The use of composite materials in the manufacturing industry has had a notorious growth over the last decade, in major part due to its excellent properties [1]. A composite material is a combination of two or more materials with different physical or chemical properties that forms a new material with different characteristics from the ones which it's created from. Composite materials tend to have high strength, high elasticity modulus, low density and excellent resistance to fatigue, creep and corrosion. They also have low coefficient of thermal expansion [2]. The aerospace sector in particular is one where this kind of materials shows great upside due to their high strength to weight ratio and high temperature resistance. For all the aforementioned, composites offer a great alternative to metals due to lower part count and structural weight savings enabling aircraft to consume less fossil fuels as consequence. Better fatigue resistance and corrosion suppression allows for reduced inspections providing another advantage over metals. [3].

These composite aeronautical parts are mainly produced through two automated composite manufacturing technologies: Automated Tape Laying or ATL and Automated Fiber Placement or AFP. Both are considered additive manufacturing and consist of heating and compacting synthetic pre-impregnated resin with non-metallic fibers onto a mold or surface. ATL was invented in the late 60's as an upgrade to manual lay-up as it brought more consistency to the material produced and productivity. Today, this technology has the highest productivity rate of the two for flat parts, which is measured in kg of material deposited per hour, and produces components like tail planes, wing skins and center wing boxes. Its main disadvantage is the high technical scrap rates comparing to AFP due to utilizing larger tape widths. Technical scrap is the excess material produced in the manufacturing process of a composite part. AFP lays-up material in a fiber form and took its beginnings in the late 70's, early 80's and has since then been growing quite strong. It is nowadays a well known process with high potential in the most diversified areas, especially the aerospace area. Its greatest advantage is its steering capability over contoured surfaces due to the smaller fiber tows utilized when comparing to ATL, which enables the production of parts with higher curvature. AFP is responsible for manufacturing components such as spars or fuselages in much less time comparing to its production in a metal structure, for example [4].

Both technologies require high initial investment in machines in the order of US$ 2 - 6 million for ATL and US$ 5 - 25 million depending on the machine complexity and size for AFP [5, 6]. The material used, pre-impregnated epoxy carbon fiber, called prepreg, is also expensive and finding ways to reduce cost associated with it is critical to the development of these technologies. This can be achieved by reducing technical scrap and/or by optimizing the lay-up strategy (the first can be a consequence of the latter). Technical scrap also carries an indirect cost as it has a disposal value associated. This greatly affects machine economics which is very important to manufacturing technologies as original equipment manufacturers companies (OEM's) are constantly working on developing more efficient machines.

It is of important notice that this thesis was developed as I worked as an intern at Embraer in Évora as a Product Development Engineer. I was able to interact with people highly proficient in composites

knowledge and to see, *in locu*, these automated machines perform. There is currently a lack of literature information on part lay-up rates. This mostly happens because the information is well kept within manufacturers to increase market competitiveness. Even when some lay-up rates are revealed it usually comes without disclosing the exact shape of the geometry, the lay-up speed used or the machine constraints. This means that, even though the value of the lay-up rate is revealed, it is of no use to assess that machine's productivity in relation to the production of that part. Also, for comparison purposes, either within the same automated technology or with other, it becomes useless. In addition, some information exists on how to improve machine lay-up time by optimizing lay-up paths using algorithms that reduce non-productive travel time [7], optimize the relationship between adjacent tapes in order to prevent wrinkling on complex geometries [8] or even to generate tow paths for double curved surfaces [9]. None of these touch on the subject of technical scrap reduction. Furthermore, strategies that would reduce scrap rates without making changes to the machine itself or the lamination process for a certain constant tape width could not be found. Faster machines [4] or the pursue of cheaper materials that could maintain adequate properties [10] are some of the ways to improve productivity but they don´t tackle the problem without any major breakthroughs or difficult improvements. Marsh [4] expresses that there is software that "ensured that material wastage and removal operations were minimised" but fails to explain how so. Information on how lay-up configuration is determined during the design phase of a composite part is also a very pertinent matter. Why is this relevant for technical scrap reduction? Because, at a first stage, all first tape/tows should be placed aligned with the first edge of the part in order to reduce scrap. In that manner, technical scrap for that first tape would be deemed at a minimum. Although common sense, and the so called eye test would say that that is the best way to go at it, if some thought is put into this situation, it is conceivable that an offset of the first tape/tow might have a trickle down effect on the lay-up configuration and reduce the material wasted thus improving any type of automated composite machine productivity. Could a model or a tool be capable of answering this question?

The main goal of this thesis is then to develop an algorithm capable of reproduce and simulate the lay-up process of flat laminates for both Automated Composite Manufacturing Technologies (ACMT) and provide information on lay-up and scrap rates as well as improve the latter by reducing the material wasted through improved lay-up configurations. This goal has many derivatives as the tool would be able to not only reduce the technical scrap and the material related costs but also to provide productivity data for comparison between machines for a certain flat component as well as data for the same machine with different setup configurations. Influence of machine constraints and part geometry on lay-up productivity can also be studied. Finally, the model would also serve as an estimating tool for the material costs of the lay-up of any flat composite part, as well as helping decision making regarding technology selection and machine's parameters configuration and with it, improve the efficiency of its design phase. Most manufacturers design their composite parts in a certain manner, access its production cost and set it as standard for future comparisons. Then, as the production of that part increases, the configurations are iterated as experience is gained through the operator, and scrap and cycle time are therefore reduced. In the meantime, a lot of material scrap and machine time could be saved if a tool could provide newer path information for scrap reduction. There are companies outside the machine manufacturing industry

that provide software similar/more advanced to the one intended to develop here, for licenses that cost in the range of the thousands of euros a month [11] granting the possibility of simulation without the need to buy a machine that costs millions to utilize similar software. Nonetheless, there is currently no available free tool for academic or even small companies' economic power, which could be provided by the work developed in this document.

1.1 Thesis Outline

This thesis starts in Chapter 2 with a historic perspective of composites in aviation. Secondly, global composite and carbon fiber composites market is assessed in order to grasp the importance of this work. Current state of the art machines will be described in light of a brief history through time since its first beginnings to the most technologically developed ones. Furthermore, a literature review on the lay-up process of the Automated Composite Technologies, ATL and AFP, and on lay-up productivity and current progress in software development is shown in this chapter.

In Chapter 3, the work methodology behind this thesis is described.

Chapter 4 consists of the mathematical description of the composite technologies process itself. The importance of this step is described in this section as it is the founding basis of the algorithm to be developed.

In Chapter 5, the algorithm is succinctly described. Its inputs, outputs, some important developed functions and a high-level and low-level flowcharts depicting the main script structure are shown in this section. Implementation of improvements to obtain the best lay-up configuration regarding first tape/tow is described here. Model guide and its capabilities are also discussed in this chapter.

Chapter 6 is the Results section. Here, the model is validated by crosschecking data with real part lay-ups and models from other literature. Lay-up and scrap rates are obtained for aeronautical representative composite parts and its results compared and discussed. The potential cost saving applications of the first tape/tow offset study is shown in order to access its value.

Finally, in Chapter 7 the conclusions of this thesis and future work are presented.

2. State of the Art

A composite material is, as the name indicates, the combination of two or more materials at a macroscopic scale with significantly different physical and/or chemical properties. They usually create a material with properties superior to those who compose them. Its two main constituents are designated matrix and reinforcement. The most important function of the reinforcement is to provide strength and stiffness to the material and to resist external loading. The matrix, which surrounds the reinforcement, is responsible to transfer and distribute these external loads to the fibers and also to protect them from the external environment. For the matter discussed in this thesis, composites with polymer matrix reinforced with carbon fibers, commonly denominated as carbon fiber reinforced polymers (CFRP), are of particular research interest. Different types of materials can be chosen for the matrix and reinforcement of a composite material. Also, different shapes and forms of reinforcements can be produced. All that, combined with a multitude of manufacturing processes, provides the opportunity to design a material that is unique and has characteristics adapted to any kind of application. This makes composite materials very desirable when comparing to metallic materials which are not as versatile. As an example, the combination of long unidirectional carbon fibers with an epoxy resin matrix provides high strength and stiffness while yielding low density. This is ideal for the aerospace industry as weight reduction is one of its main drivers due to high fuel costs. This type of material is most commonly used in the manufacturing methods discussed in this thesis (ATL and AFP) and is part of a group of premixed composite materials where the fibers have been pre-impregnated with a polymer matrix, often called prepreg material. Composite laminates are then a product made by stacking layers of prepreg or dry fiber material, constituting a ply, with different angles of fiber reinforcement in directions of 0, 45, 90° or -45°. After the lay-up is finished, the laminate, for a typical standard industry process, goes into an autoclave for curing purposes.

2.1 Composites in aviation - historic perspective

The history of fiber reinforced composites in the aircraft industry probably started with the invention of phenolic resin by L. H. Baekeland with a patent being filed in 1907 under the trade name ”Bakelit”. Later, in 1916, Robert Kemp also filed a patent with the name ”Structural Element” for the production of several airframe parts such as wings and fuselage with fibre reinforced phenolic resin. An example of the use of this composite material could be seen in the Fokker F18, a commercial aircraft produced in 1935, which had wings with Bakelite glued plywood [12]. In the late 1930’s, N. A. de Bruyne, an aircraft engineer known for its pioneering work in structural adhesive bonding, started investigating new, stiffer, stronger and lightweight materials with the purpose of minimizing structural weight. His efforts, alongside J. E. Gordon, a naval architect, came into fruition when they discovered that stacking impregnated phenolic resin flax thread fibers and submitting them to heat and pressure enabled the formation of a high strength, low density material [13]. This was one of the first examples of an industrial composite used in the aerospace sector and it was called prototype ”Gordon-Aerolite”. This material was present in

the design of the Supermarine Spitfire aircraft, famous for its role in the second world war [14]. Gordon was also a pioneer in understanding that composites needed to be produced in an efficient way if they were to compete with metals in part manufacturing which is still a main driver of the composites industry to this day. In 1940, Pierre Castan made an important breakthrough for the composites world with the introduction of polyester and epoxy resins [12, 13]. It enabled the production of glass fiber reinforced polymers (GFRP) in the early part of the 1950's which, a decade later, were used to produce the first fiberglass rotor. Major aircraft companies like Boeing and McDonnell were quick to acknowledge the advantages of a composite rotor structure due to structural weight reduction and thus started developing further research in the subject. When composites were incorporated on large transport helicopters in the 1980's, these enjoyed not only better performance but also required less part inspections which further reduced costs. In addition, fiberglass rotor blades improved damage tolerance relating to the array of ballistic threats, common to this type of aircraft [15].

Fiberglass composites were present, in the late 1950's, in the McDonnell Douglas DC-9 and the Boeing 707 in tertiary components like interior parts, sidewalls, bag racks and galleys, the latter with about 2% composite structural weight [15, 16]. However, a steadier utilization of composite materials in aircraft structures only materialized with the discovery of carbon fibers in the UK, in 1964, and its commercial availability in 1966 [17]. Carbon fibers were, at that time, tagged with a high price and were mainly used in high-tech and high-cost applications like military aircraft such as the previously mentioned helicopters. Its introduction to civil aviation was slow and progressive being used in a smaller scale at first. It was only in the final years of 1960's that fiberglass fibers, proving successful in interior parts, started to be applied into secondary aircraft structures like spoilers, rudders, flaps and ailerons. Example of this was the introduction of the Airbus A300 in 1972 with around 5% composites in their structural weight including GFRP fairings and radome and CFRP air brakes and rudders. Finally, in the late 1970's, with the emergence of Automated Tape Laying, carbon fibers replaced fiberglass fibers in most of these secondary structures and proved they were there to stay for the long haul. By that time, carbon fibers could be produced on larger industrial scale (first larger scale commercial production occurred in 1971 at Toray, in Japan) [12] providing manufacturing capacity to the aviation industry.

Over the next two decades CFRP were progressively introduced in primary critical structures such as stabilizers, fuselage barrels and wings. The Boeing 737 classic horizontal stabilizer and the vertical stabilizer of the A310 are references of that, happening in the middle 1980's. The latter allowed a total weight saving of almost 400kg when compared to its previous unit made of aluminum alloy. Also, the reduction from 2076 parts in metal to only 95 excluding fasteners made it much easier to produce and require less inspections. In 1987, the appearance of the A320 extended the use of composite materials to the horizontal stabilizer together with multiple control surfaces, main landing gear, nose landing gear doors, wing trailing edge panels, flap track and pylon fairings, nacelle cowling and floor panels. All these changes generated a weight saving of 800kg over its aluminum predecessor increasing the total percentage of structural weight made of composite materials to around 16%. It was estimated, at that time, that a reduction of 1 kg in weight produced a save over 2900 liters of fuel per year which represent considerate cost reductions. In the mid 1990's, the full empennage of the B777 was also made of CFRP.

It is was then clear that the use of composite materials reduced the number of parts and structural weight in aerospace applications [14, 15].

With the turn of the millennium, Airbus introduced the first fuselage applications made of CFRP. These were the rear pressure bulkhead and the keel beam on its A340 program. This trend continued in the development of its A380 aircraft, whose composite percentage was increased to just over 20% with the complete center wing box being a CFRP design. Furthermore, its rear fuselage, wing ribs and upper deck floor beams were also made of CFRP. Airbus took another step forward in the composite trend when they had its first full wing aircraft made of CFRP on its A400M, a military aircraft, in 2009. In the last decade, composite materials really took over aircraft design with complete airframes being formed of CFRP (tail, wing and fuselage) in Boeing's 787 Dreamliner in 2011 and the Airbus A350XWB in 2014, both made by a record 50 plus percent composite materials [15]. The most recent aircraft confirmed by Boeing to be introduced in 2022 is the B777X which is a newer version of the B777 with composite weight percentage raised to 30% due to wings with folding wingtips made of CFRP [18]. Aircraft structural materials breakdown of the B787 can be seen in Figure 2.1.

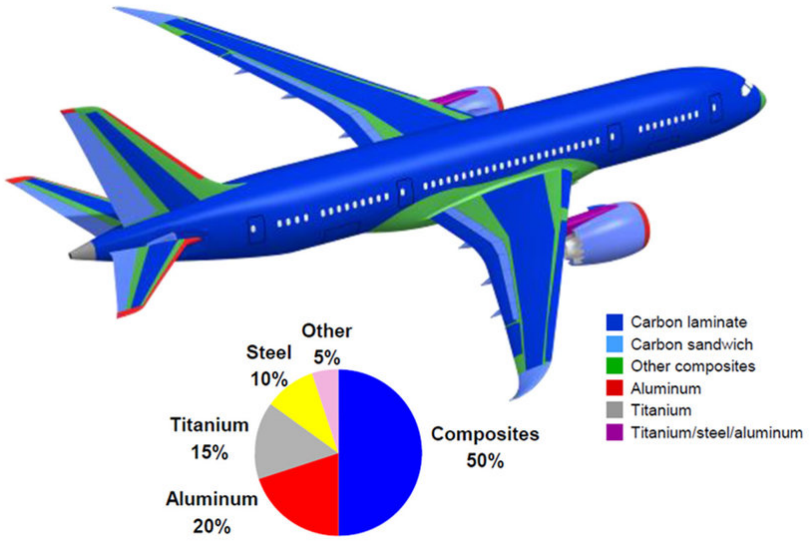

Figure 2.1: Boeing 787 structural materials [19].

Aircraft manufacturing companies all around the world also contain composite technologies in its products. Embraer, a brazilian company, has composite knowledge dating back to 1968 with the EMB-110 where composite assemblies were utilized in its airframe [20]. Recently, composite materials can be seen in their business jets Phenom 100E, 300, with around 18% and 20% respectively [21] and in the bigger Legacy 500. Their latest commercial aircraft, the E175-E2, developed to compete within the regional flights market and to be introduced into the market in 2021 has its full empennage and all of its control surfaces such as flaps, ailerons, rudder, elevator and spoilers made of CFRP [22]. Bombardier in Canada, now extinct, launched the C100 series in 2010 with 20% of the aircraft weight resultant from composite materials [23]. This value was raised to 46% with the launch of the renovated A220 by Airbus which acquired that program from Bombardier in 2016 [24]. The PJSC United Aircraft

Corporation, in Russia, is currently manufacturing the Irkut MC-21, the first aircraft with out of autoclave (OOA) composite wings made with resin infusion dry fiber, totaling its composite percentage to 40% and planned to be introduced in 2021 [25]. Last but not least, the entrance in scene by Japan's Mitsubishi Heavy Industries with the launch of its SpaceJet program in 2021-2022, an aircraft formerly known as the MRJ, with 10-15% composite airframe [26] and COMAC, in China, with the C919 jet containing 12% composite materials [27], predicted to launch in 2021. Both will prove to be major players in the aerospace composite industry. However, the introduction of any composite innovation is slow to be applied due high safety standards in the aerospace industry which justifies the high gaps in time between the introduction of new aircraft composite parts and its increased usage through the years, visibly portrayed in Figure 2.2.

In the same figure it's possible to distinct three levels of composite material structural weight percentage in commercial aircraft. The lower end, with 5% or less, translates to composite usage in secondary and tertiary structures like spoilers, fairings and cowlings. The middle tier, with around 10% structural weight made of composites, indicates its use in the empennage (e.g horizontal and vertical stabilizer) and some primary control surface such as rudders and flaps. If the wing box, meaning its skin and spars, is also made of composite materials, the structural weight percentage increases steeply into the range of 35%. Finally, adding a composite fuselage structure raises the value to 55% which is the case for the Boeing 787 and Airbus 350XWB. Weight savings for secondary structures using composite materials instead of metal alloys are around 40% and for primary structures such as wings and fuselages this value decreases to 20% [14].

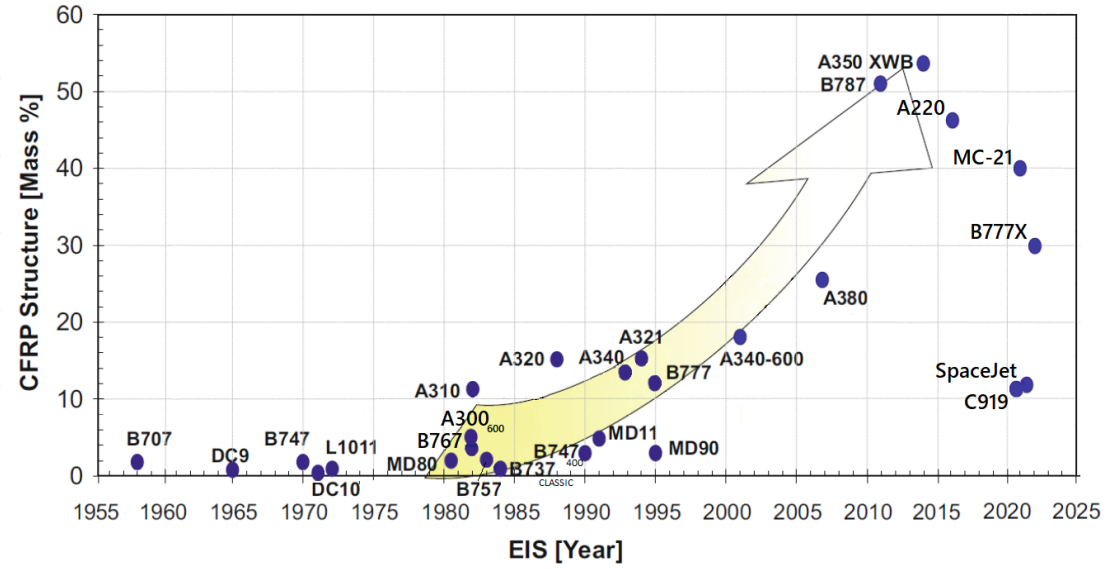

Figure 2.2: Commercial aircraft composite structural weight percentage by year of introduction. Adapted from [12].

2.2 Composites today and future trends

The global composite market size was estimated at US$ 89.04 billion in 2019 and is expected to expand at compounded annual growth rate (CAGR) of 7.6% from 2020 to 2027 as per Grand View Research report released in July 2020. The most dominant sector was the glass fiber reinforced composites with 61.8% share. Nevertheless, the carbon fiber product segment has a strong forecast for continuous growth, registering the same CAGR of 7.6% from 2020 to 2027. Thermoset resins, such as epoxies, had a remarkable share of the overall revenue accounting for 72.0% as its use in aerospace, defense and transportation applications is rising. The lay-up manufacturing process segment, in which ATL and AFP are inserted, also had the largest portion in overall revenue with 33.1 % market share [28].

2.2.1 Carbon fiber composites market

In 2018, the global carbon fiber composites demand was estimated to be 154,7 kt with a turnover of US$ 23.15 billion based on 140,6 kt and US$ 21.14 billion being achieved in 2017. This represented a CAGR of 10.03% in demand and 9.51% in turnover since 2013 which shows a healthy development of the composites industry. The matrix of composites can be of different types of materials. The most common are metal alloys (metal matrix composites, MMC), ceramic compounds (ceramic matrix composites, CMC) and polymers (polymer matrix composites) which when reinforced with carbon fibers are called CFRP as already stated in this document. As it can be seen in the Figure 2.3 the CFRP estimation for 2018 was a dominant one, gathering 82.7% (127.8 kt) market share of the global carbon fiber composites market and 71.2% of its revenue turnover [29].

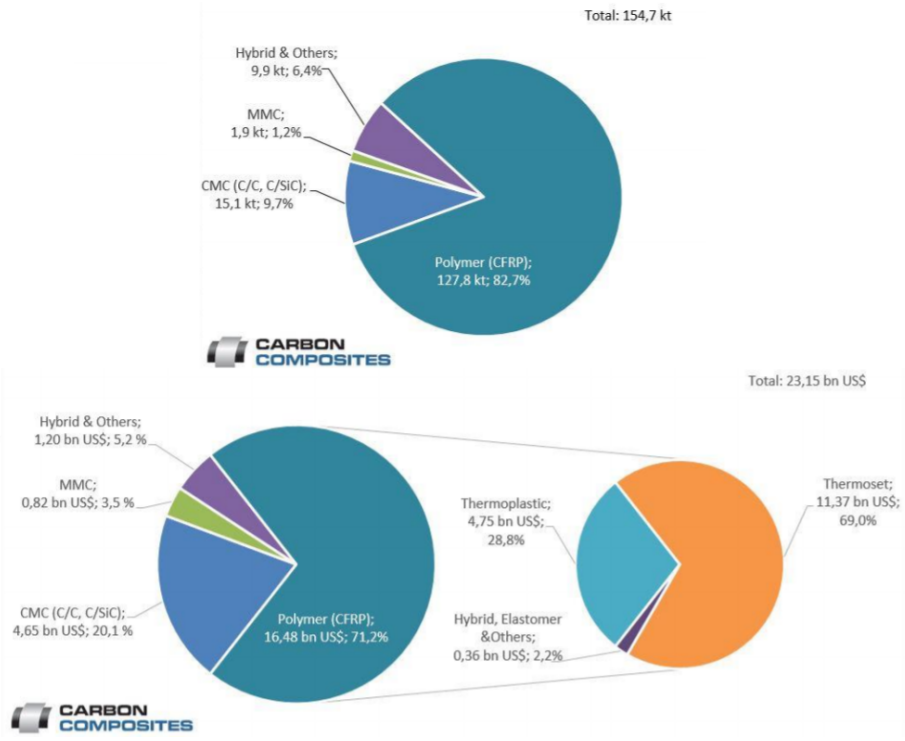

Figure 2.3: Distribution of the global carbon composites market by matrix materials with reference to demand (above) and turnover (below) - 2018 estimations [29].

An average annual growth of 11.88% since 2013 until 2018 is estimated for the global turnover of CFRP and its value was estimated to be US$ 16.48 billion in 2018 which indicated market growth for the foreseeable future. The segment with highest expression among non-polymer matrix are the CMC, mostly due to its use as high performance brake disks or materials for high temperatures. Although non-polymer matrix occupy only 17.3% in demand they settle for 28.8% of the revenues. This happens in major part because these segments contain customized solutions used in space applications and aviation which translates to higher market prices. Within the CFRP segment, thermoset matrix accounted for 69% of turnover although a steady increase is occurring for thermoplastic matrices since 2014 (24%; 25%; 26.3%; 27.6%) to 28.8% in 2018, which represents a CAGR of about 16.8% [29].

The same company who produced this data in 2018 released a report in 2019 stating that global CFRP demand was, in fact, 128.5 kt for 2019, a small raise comparing to its predictions made in 2018, as stated above. The demand for 2019 was estimated at 141.5 kt with a growth of 10.1% comparing to 2018 and netting a CAGR (2010-2018) of 12.24%, as it is shown in Figure 2.4. The CFRP turnover was approximately US$ 17.88 billion, a raise of 9.64% from the previous year and a CAGR of 11.69% (2013-2018) indicating the ascending development of the CFRP industry [30]. The major drivers of this growth are the increasing usage in the aerospace and defense sector as well as the wind energy industry [31] and the automotive sector. The latter is of particular interest as in the near future, due to Corporate Average Fuel Economy (CAFE) standards, vehicle weight will need to diminish and composite materials will become crucial in this aspect.

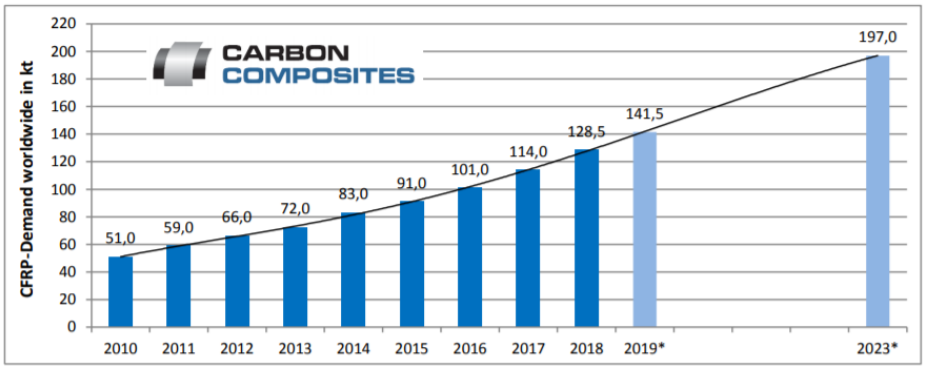

Figure 2.4: CFRP demand from 2010-2023 - 2019 (*Estimations) [30].

The carbon fiber composites demand and turnover estimations for 2018 are shown distributed by application in Figure 2.5 and Figure 2.6. The aerospace segment has established its market dominance with approximately US$ 12.91 billion (56%) generated although its demand share is predicted lower at 55.31 kt (36%). This difference can be explained by the elevated prices per kg of aerospace material due to high safety requirements and high quality parts which require expensive certifications and qualifications. The second largest sector, both regarding required quantity and turnover was the automotive sector, 37.13 kt (24%) and US$ 4.17 billion (18%), respectively. On a tertiary position, the wind energy segment has risen in market share due to almost all large dimensions wind turbine models of newer generations using carbon composites for tension and compression chords. An example of this was seen

in October 2017, when Vestas Wind Systems, the world's largest wind turbine manufacturer, started the transition to rotor blades made of carbon fiber composites supplying themselves with Hexcel Corp. [32].

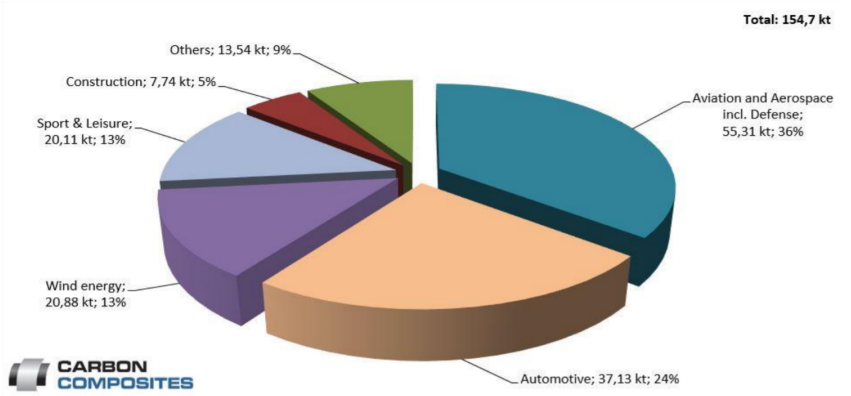

Figure 2.5: Global carbon fiber composites demand by application in 2018 [29].

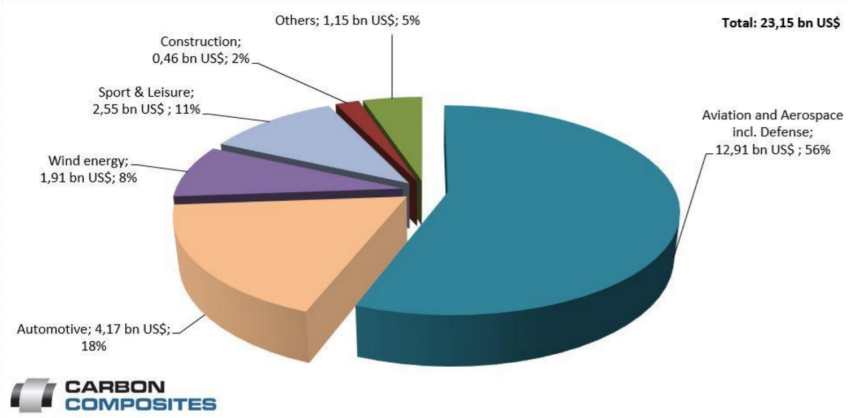

Figure 2.6: Global carbon fiber composites turnover by application in 2018 [29].

Another market study, performed by Arthur D. Little consulting in 2018 [33], also attributed the largest portion of market share of demand for carbon composite materials to the aerospace sector. In that report, market share was claimed to be close to 60% of the global carbon fiber demand by value which is in accordance with the 56% estimation of Sauer and Kühnel [29], presented above. However, there is a divergence between the studies relating to size of the aerospace sector for demand, as Arthur D. Little claims 29 kt and Sauer and Kühnel [29] predicted 55,31 kt, which can be attributed to the first study not including aerospace defense data. Furthermore, Arthur D. Little reports that the aerospace sector would be in continuous growth until 2023 at rate of 7% CAGR which indirectly influences growth for the composites market. Aircraft demand for composite materials constituted 75% of the total demand for the aerospace industry being the rest allocated to rockets, satellites, and missiles. Commercial aircraft was the most relevant slice of the aircraft segment with 90% market share [33].

A year later, in 2019, the aerospace composite segment exceeded US$ 12.7 billion, a slight decrease comparing to the 2018 US$ 12.9 billion from Figure 2.6. One other study claimed it continued to have the largest share of the advanced carbon composites market, turnover wise, comparing to the previous year [34]. The forecast for its growth between 2020 and 2026 is around 9.3% making its market value

prediction set in US$ 15.7 billion for 2026. The fastest growing segment of the aerospace composite market and still gaining popularity is aircraft exterior applications (airframe) which dominated in 2019 with around 60% of market share. Exterior parts such as fuselages, stabilizers, wings and control surfaces made of composite materials are gradually shifting to become the standard in the industry. The carbon fiber reinforced plastics sector is expected to dominate the composite aerospace market in the coming years as in 2019 it accounted for over 40% share [35]. This shows the importance of automated lay-up in composites technologies will only tend to increase in the future. The two main drivers of the aerospace market are, logically, the increase in structural weight percentage of composite material and aircraft production. Both are increasing as average composite material share of aircraft empty weight is estimated to have increased from 7% to 13% since 2010 until 2018 [33] albeit a ceiling is probably being reached for a maximum value.

As of 2018, the two main aircraft programs were the A350XWB and the B787 in commercial aviation composite market followed by the A320, B737 and A220 at a smaller scale. Focusing on the second driver, both Airbus and Boeing announced their intentions on increasing production rates of the A350XWB and B787 which are much lower comparing to their highest profit programs: the A320 and B737. Airbus was able to produce 8 A350XWB per monthly basis in 2018 [33] and projected an increase of plus 2 to reach a total production rate of 10 aircraft per month in the following year which was exactly accomplished as 112 aircraft were delivered in 2019 [36]. On the other hand, Boeing increased the production of the B787 from 12 to 14 aircraft per month from 2018 to 2019 [33], only to have them be reduced to 12 in 2020 due to the USA-China economic tension. Despite fluctuations, these big aircraft increased production contributed to a rise on the demand for composite material for commercial aircraft to over 29 kilotons in 2019 [35], matching the total composite demand for the entire aerospace sector in the previous year. Boeing also has plans to introduce a new midsize aircraft (NMA) that would fit between the B737 and B787 in terms of size and range around 2025. This new aircraft design is very significant to the composite industry because, as the next all-new aircraft, it is expected to feature major structures manufactured with carbon fiber composites. Moreover, there is expectations for the announcement of replacements of the 737MAX and the Airbus A320 which are planned to enter service around 2028. On account of that, the important question to ask is if and where composites will be used in these planes. If the answer is affirmative, it would represent a major increase in the carbon fiber market demand as the rates of the replacement aircraft would be significantly higher comparing to those of the NMA.

In the aerospace defense segment, it is predominantly aircraft programs F-35, Boeing KC46, Airbus A400M and Embraer KC-390, as well as the helicopter programs V-22 Osprey, Black Hawk, Sikorsky CH-53K and Airbus H160 that lead to a stable composite demand [29, 37]. The space industry has also contributed to the carbon composites market and is expected to have that contribution increased with the privatization and competitive environment of space enterprises. An example of that are companies like SpaceX or Blue Origin which have increased their usage of composite materials being present on panels, cargo doors or boosters in their products [29, 38, 39]. Also Orion, a program to carry astronauts into space, manufactured by Airbus Defense and Space in conjunction with Lockheed Martin and ESA is developing a carbon fiber heat shield manufactured using OOA prepreg from Toray Composites [40].

Although aircraft production may be on the rise for the near future, its maximum composite airframe structural weight percentage is probably reaching a ceiling, which is around 50%. To further increase the growth of the aerospace sector in the composite industry and to meet faster production demands, further development of current processes is needed as well as innovation from other areas like materials and new manufacturing processes. Forecasts predict that in 2020 composite manufacturing will be around 50% [41] performed by AFP and ATL machines comparing to the 33.1% overall revenue share in 2019 [28], being AFP the most dominant technology and growing faster too. This can be attributed to its greater precision over ATL and better lay-up rates for most parts while producing less waste. Nevertheless, some competitive alternatives to autoclave curing processes are increasing its relevance. Resin transfer molding (RTM) is gaining traction in the aerospace industry as manufacturers search for innovative cheaper processes.

This process starts by using AFP technology, but instead of laying the usual prepreg tows, it uses dry fibers with binder powder or, more recently, thermoplastic veils, to build a stack of plies called preform [42, 43]. The next step is to place it on a closed mold and have low viscosity resin and catalysts pumped in under low to moderate pressure and heat through injection ports or have it vacuumed in a bag on a slightly different process called vacuum assisted resin transfer molding (VARTM). In both processes, the autoclave cure is not needed reducing cycle times and reducing tooling costs. Also, dry fiber and resins used in RTM or VARTM are cheaper than the prepreg material. In addition, VARTM does not require high heat or pressure and therefore operates with even lower cost tooling, making it possible to inexpensively produce large, complex parts in one shot. RTM is used for components such as the rudders of the Boeing 757 and 777, landing gear doors for the Airbus A330/A340 and flap shroud and landing gear doors for the F/A-18 [44]. A similar but novel process to VARTM is being used to produce the CFRP wing box of the MS-21 single-aisle jet by Russian OEM and fabricator Aerocomposit. In this process, a semipermeable membrane is used to enable a consistent, robust process, delivering 100% impregnation resulting in no dry spots or voids. A robotic arm machine from Coriolis Composites is now producing the wing spar and stringer preforms at Aerocomposit, while a gantry-based machine by MTorres is laying up the wing skin preforms. OOA infusion has also been demonstrated on large tooling and structures for NASA's Space Launch System program using epoxy and bismaleimide resins [43, 45].

Future composite aircraft development will come in areas like supersonic travel, urban air mobility and all-electric commercial jets. Boom Aerospace is developing the Overture, an aircraft with a fair composite composition designed to travel at speeds up to Mach 2.2 and at heights of 18000 m. An emergent aerospace market segment is related to intra and inter-city travels on small aircraft, up to 10 passengers. Hyundai and Uber are working on a EVTOL 100 km range on charge aircraft which will require composites use to make it viable as large batteries utilized need a reduced structural weight to offset its mass. Also Boeing and Porsche are working on a EVTOL prototype. Nevertheless, certification, airspace management and safety standards will postpone entrance in commercial service likely until 2025 [46, 47]. Also Airbus with its E-Fan X hybrid-electric commercial aircraft will certainly be of major importance for composites use in electric aircraft going forward [48].

2.3 Automated Composite Manufacturing Technologies

It is important to understand how ACMT developed over time and its current state of the art (SOA) in order to deliver one of this work main goals which is to develop an algorithm capable of simulating the lay-up of any flat composite part. There are currently two main technologies to manufacture advanced composite laminates from unidirectional prepregs: ATL and AFP. Both consist of laying fiber tape, or tows for AFP, in some specific sequence and angle orientation to form a laminated composite material. ATL was originally invented to automate hand lay-up and increase its efficiency. Both technologies aim to reduce costs, enhance repeatability, reproducibility, productivity and increase part quality. Despite high initial investments in the machines, these automated processes can reduce labor hours per component, lower material scrap rates comparing to manual lay-up and also reduce the need for in-process inspection thus lowering manufacturing costs [49]. Global AFP/ATL machines market is forecasted to grow at an imposing rate over the next five years to reach an estimated value of US$ 294.7 million in 2024 [50].

2.3.1 Developments through time

Automated Tape Laying - ATL

The first reference to an ATL system dates back to 1971 with a patent assigned to Chitwood and Howeth designating a method of laminating composite tape onto a rotatable base-plate using computer numeric control (CNC) [51] although some research was already in place since the end of the 1960's [49]. In 1974, a machine was designed by Goldsworthy [52] to deliver 76 mm wide tape being capable of lay-up over curved surfaces as the head was able to turn. At that time, ATL systems were built in-house and were part of a component centered production system. Lay-up speeds were reported at 10-20 m/min which is not great but it was argued that it did not affect overall productivity [53]. Moreover, ATL could minimize lay-up errors, lay-up time and material wastage comparing to the standard hand lay-up as scrap rates were up to 30% for smaller parts and 2-4% for larger ones comparing to rates of 50-100% for hand lay-up [54]. In Figure 2.7 it is depicted the Goldsworthy prototype ATL machine which consists of spools of tape, a winder, winder guides, a compaction shoe or roller, tape cutter and a position sensor [55].

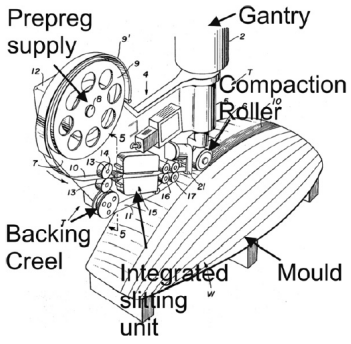

Figure 2.7: Drawing of an early ATL system [53].

In the 1980's the technology broaden itself in order to reach higher lay-up rates. Most machines available were only capable of depositing flat laminates and, in order to solve this problem, in 1984, K. L. Stone introduced a commercial ATL system from Cincinnati Milacron (now Fives Group) that was capable of laying tapes up to a curvature of 15º and follow the contour of the mold making it the first example of a Contour Tape Laminating Machine (CTLM). However, problems relating to lay-up speed, reliability and accuracy were still very critical. Furthermore, the system was not able to deliver tape with the necessary compaction pressure and breakage of the ply backing was a regular occurrence. In 1985, R. Grone and M. Grimshaw introduced an ATL system where direct lay-up force control and head normality over curved surfaces was enabled by a force-controlled Z and A axes which improved accuracy [56]. Nonetheless, ATL systems were still majorly unreliable being utilized only on simple components due to low tack levels and degradation caused by limited heating. Even though pressure control was mostly dominated by the end of the decade, the question remained on which pressure levels were actually desirable and, with the problems stated above being unresolved, the lay-up speeds remained unchanged from previous designs. At this time, tape layers were used primarily on military aircraft due to the high price of an ATL machine, tagged at US$ 3.5 million [57]. In addition, some studies, although not very reliable due to not taking into account all the variables, were questioning the desirability of automation claiming similar rates to pre-existing hand lay-up making the emergence of ATL a strenuous process [53].

In 1991, tape heating was finally introduced. It was applied first for thermoplastic lay-up and it allowed to overcome tack control past issues [58]. Further improvements from the middle 1990's until today have been fairly limited due to the appearance of AFP machines and were solely productivity driven. ATL is nowadays a standard process for prepreg lay-up, with high lay-up rates, specifically used for flat or quasi-flat large parts. It has higher scrap rates comparing to AFP but can have better lay-up rates than the latter for large flat parts [5] and it is also easier to perform offline programming. It is commonly used to manufacture parts like wing skins, illustrated in Figure 2.8, stabilizer skins or wing box centers.

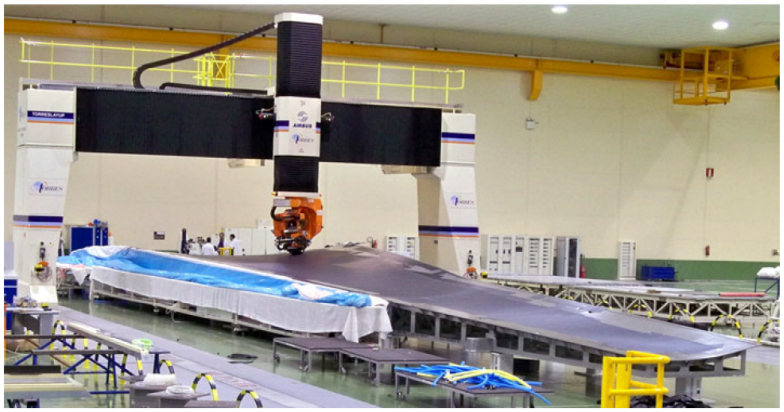

Figure 2.8: MTorres TORRESLAYUP machine manufacturing a wing skin [59].

Main manufacturers of ATL equipment are the Fives Group, Automated Dynamics and Accudyne System (USA), M.Torres Diseños Industriales S.A.U (Spain), Mikrosam AD (Macedonia) and GFM (Germany). Current SOA ATL machines like the Cincinnati CHARGER Tape Layer can deliver lay-up rates

up to 60 m/min and achieve 25 degree contours. Tape width used for this machine can vary from 3, 6 to 12 inches (76.2, 152.4 to 304.8) mm and it can provide up to 10 machine axis [60]. A strong competitor is the MTorres ATL system called TORRESLAYUP, seen in Figure 2.8, whose biggest advantage is the possibility to use different multi-tape configurations such as 4 x 152.4 mm, 4 x 76.2 mm or even 2 x 152.4 mm up to a maximum 609.6 mm wide band. This provides the ”capability to lay down several tapes simultaneously in order to boost productivity by increasing band width, scrap reduction by means of independent control of each tape and scrap reducing strategies” as stated in the machine's website [61]. It also figures 11 independent axis. Current SOA ATL machines initial cost can vary between US $ 2 and 6 million [5] depending on machine configuration, rotational ability, head configuration and cutting system. MTorres has also been developing smaller robotic flat tape layers in order to provide a cheaper machine and increase ATL versatility making it accessible to smaller companies [55].

Automated Fiber Placement - AFP

The first AFP system designed is most likely the one depicted in the Figure 2.9 which was, on theory, already capable of performing one of AFP signature tasks, the ability to lay-up material on a curved surface. At the time of its design, the tape width used measured 76 mm and some challenges arose when this tape, being somewhat to wide, had difficulties to conform over strongly curved surfaces. The solution would convey from slitting that tape into smaller 3.2 mm tows and deliver them at individual speeds by keeping the excess material on the head. Translating that idea into reality would prove difficult as further developments were stagnant at time. Nevertheless, the basic principle for future AFP machines was set.

In early 1980's, Hercules Aerospace took the development process ahead and by 1983 the first fiber placement machine was invented [62]. However, it was only by the end of that decade that the first AFP machine was made commercially available by Cincinnati Machine (now the Fives Group) [62]. They combined the cut-restart and compaction features of ATL machines and the ability to simultaneously supply different rates of material from filament winding (FW). An important amount of knowledge acquired from early ATL developments was therefore crucial to the introduction of AFP machines in the market. The limitations of the Goldsworthy machine were lifted by Evans et al. solution of keeping the slit tape on different bobbins, which worked independently [63]. In the early 1990's, AFP systems were thus capable of controlling tension, temperature and lay-up speed of each tow independently which was later perfected with the introduction of offline programming systems. Lay-up speeds were, at that time, approximately 7 m/min for AFP which would be comparable to the lower end of the spectrum of ATL productivity. That, in turn, would result in a productivity of 5 kg/h, which was fairly low. Some technical problems like reliability and accuracy were present due to unwanted tension in the tows. Combining that with the tow small width, made the systems prone to gaps in the material laid which negatively impacted the mechanical performance of the laminate [53].

Productivity saw some improvement when Measom and Sewell reported, in 1996, an increase of this value by 450% on the fabrication of a complex component using AFP compared to its production using FW and manual lay-up. Also, the scrap rate was reported to reduce from 62% to 6% [53]. The ability

to steer, which translates to the capability of laying material along curvilinear paths, was enabled by the possibility of using narrower tapes allowing AFP systems to manufacture complex composite parts that were forbidden in the past while also reducing scrap rates. Despite the rise in productivity, it was still not enough to offset the high initial capital expenditure of an AFP machine which was near US$ 6 million [57].

Figure 2.9: CORIOLIS C1 robotic arm machine [64].

Until the year 2000, AFP systems were mainly employed to military and space programs like the V-22 Osprey or the F22 Raptor due to affordability factors. Major problems like splicing errors (welding of the tape ends), dropped tows, and material changes resulted in increased downtime and consequently lowered productivity. Some of these issues were minimized with the introduction of infrared heating which allowed lay-up at higher temperatures, increased tack levels and reduced lay-up errors [65]. In 2008, it was engineered a system that was capable of splicing the tows together [66], reducing the downtime for material refilling, and also an automated inspect system to detect lay-up errors [67], reducing time for quality inspection after lay-up, therefore contributing to increase productivity. In that same year, the invention of a system with multiple placement heads, replaceable creels, and replaceable placement heads by T. Oldani and D. Jarvi [68] allowed the simultaneous use of two or more fiber placements heads, capable of independent movement from each other, to work synchronously on forming a composite part on a tool surface. However, lay-up rates were not reaching their full potential due to the inability to cut or add ”on the fly”, meaning that the machine needed to slow down from its maximum lay-up velocity in order to successfully perform the cut or add process. One year later, the same authors were able to fix this problem by creating a system that was able to determine the initial location to start the high-speed event of the cut or add operation with a suitable advance in the toolpath thus eliminating the need to reduce speed [69]. This greatly affected AFP machine productivity. Despite all these improvements in reliability and raw productivity, issues relating to the high machine and material costs comparing to other methods remained. Offline programming was, in the beginning of 2010’s, in a none optimized state with tow gaps and overlaps still being a main technical problem. As the main focus of this thesis is in the offline programming spectre, this matter will be further studied in subsection 2.3.4.

In the aerospace industry, AFP machines are commonly used to manufacture fuselage panels, examples being the production of the Airbus A350XWB and the Boeing 787 fuselage. In 2008, the latter

placed an order for six VIPER 6000 fiber placement from MAG Cincinnati to manufacture that part [70]. The ”VIPER’s enable independent control over feed, clamp, cut and start for up to 32 individual tows or slit tape. This allows automated ”on-the-fly” adjustment of fiber band width, controlled bending of fiber layout around changing contours, and precise configuration of openings (doors, hatches, etc.)” [70]. It is also able to lay-up parts with diameters up to 8 m [71]. Other SOA machines like the GEMINI hybrid model with its interchangeable heads grants the possibility to change between AFP and ATL systems in the same lay-up which ”provides flexibility to process a wider array of parts, optimizes bandwidth and lay-up capabilities, eliminates parasitic time for material loading and provides minimal capital investment which will maximize profits with one machine platform for multiple processes” as described in [72]. MTorres hybrid machine claims a similar system with head exchange within 90 seconds boosting productivity up to three times and higher scrap savings [73]. Ingersoll Mongoose Hybrid can also provide the flexibility of interchangeable heads with the advantage of having optional number of tows, ranging from 4 to 32. Moreover, it allows the use of thermoplastic materials which can reduce cycle times [74] and increase productivity. Finally, CORIOLIS C3 AFP machine is particularly suitable for big doubled curvature surfaces, claiming maximum lay-up speeds up to 1.2 m/s and accelerations of 3 m/s^2 which are the highest that could be found in all manufacturers websites. Top AFP system manufacturers are the Fives Group, the world’s largest supplier, Ingersoll Machine Tools Inc. which is involved in fiber placement since its beginnings in the early 1990’s, Accudyne System, Automated Dynamics and Electroimpact Inc., all these five companies being located in the USA. There is also Coriolis Composites technologies SAS in France, M.Torres Diseños Industriales S.A.U in Spain and Mikrosam AD in Macedonia.

Figure 2.10: Eletroimpact AFP gantry machine manufacturing a fuselage panel [75].

These companies offer systems in different types of configurations: Automated Dynamics and Accudyne only supply their systems on small gantries and industrial robots which demand lower capital investment and are better suited for specific applications. The Fives Group, MTorres, Mikrosam and Eletroimpact solely provide their systems in moving column type, winding platforms or even high rail gantries like the one in Figure 2.10 which implicate higher productivity and reliability by using more tows in the machine’s head. Coriolis and Ingersoll supply all the types stated providing higher versatility to the costumer. An example of a robotic AFP system by Coriolis Composites is depicted in Figure 2.9. Moreover, machines by Coriolis Composites, Accudyne Systems, Electroimpact, and Automated Dynamics also provide small scale lab set up for research purposes [55].

2.3.2 Process description

It is important for the purpose of this thesis to obtain a solid knowledge of the fundamentals of ACMT processes. A thorough research was conducted on the subject which complemented the already presented ATL and AFP SOA machines and history developments. In order to create an algorithm capable of the simulation of ATL and AFP lay-up of flat laminates it was essential to understand how these machines work. These technologies can be viewed as additive manufacturing since a composite laminate is made by stacking plies on top of each other, thus adding material, as opposed to machining where a part is made by removing material. Currently, a wide variety of automated composite lay-up machines exists, from robotic arms to column, table and gantry based systems, unidirectional or bidirectional lay-up, single technology or hybrid, single head to multiple heads working in sync but one set of rules is horizontal to them all. These machines lay single tape (ATL) or multiple tows (AFP) on a mold, in a defined sequence, at a certain speed, benefiting from a set axis acceleration until a layer is completed. The process is then repeated until all programmed layers are completed. These systems have some constraints in common such as the minimal course length, meaning the shortest distance that can be laid up, which consists of the distance between the machine's blade and the lay-up roller or the minimum cut-restart length which is the minimal length necessary to lay-up a tow after the previous was laid down and is dependent on the configuration of the cutting and feeding systems. The values of these constraints change from ATL to AFP and can vary within a technology. A detailed description of these technologies is presented in the next paragraphs with unique and common traits between them.

Automated Tape Laying

ATL works typically by placing a single fiber tape onto a flat or slightly curved mold or surface. ATL uses tape with 3, 6, or 12 inches (76.2, 152.4 or 304.8 mm) width. The width of the tape is normally selected taken into account the curvature of the part to be produced. ATL machines are usually mounted on horizontal gantries, typically on an open bay gantry configuration, or vertical column system due to the mass of the material and machine head. They can have up to 11 axis of movement, as the TORRESLAYUP machine discussed earlier, 6 for the machine head and 5 for the gantry movement. These machines can either be a flat tape laminating machine (FTLM) or a contour tape laminating machine (CTLM), being the latter the most used in the industry. As the name indicates, CTLM is capable of laying material in both contoured concave (up to 40º) and flat surfaces while FTLM is only capable of depositing material in flat surfaces [76].

Both ATL and AFP systems are driven by CNC that follow accurately predetermined paths, called tool paths, contouring the mold. During the lay-up of each ply, tapes are placed consecutively next to one another with a gap of 0.5-1 mm, necessary to respect variations in tape placement resultant of lay-up control error margin and tape tolerances. There are three different material delivery technologies used in ATL systems: single-phase (most common), two-phase and dual-phase. For the first, the process starts by loading the spool of material into the delivery head which is then pulled through the feed rollers and past the cutting blades. After, the prepreg has its backing paper removed and the lay-up can

begin with the tape being laid onto the tool through a silicone roller with compaction pressure and heat application. During material guiding, tack should be low to allow for smooth feeding and reliable cutting. However, adhesion to the paper has to be sufficient to ensure that the prepreg remains on the carrier during and after the cutting process. As a general rule, tack is controlled via temperature activation, based on the fact that adhesion increases with increasing temperatures. In the single-phase process the machine must slow down or stop to make the materials cuts. In the two-phase system, which is a more advanced technology, present in machines like the Forest-Liné ATLAS, from Fives, the excess material for complex course paths is pre-cut on an offline cutting machine [77]. In this case, the machine does not need to decelerate for the cutting operation reducing lay-up time and prompting productivity. Also, the after process of removing scrap is eliminated thereby heightening the savings. In contrast, this type of system has disadvantages like the increase in logistical costs and complexity due to the advanced preparation of the tapes and also some relative instability during the lay-up process. A dual-phase system is simply the combination of these two: one machine head runs a single-phase system and the other a two-phase system. This kind of material system delivery was chosen to manufacture the wings of the 787 by Boeing's subcontractors Mitsubishi and Fuji by purchasing a large Fives Forest-Liné dual-phase ATL system [49]. One unique feature of SOA ATL systems is its ability to provide net shape contours which enables the lay-up of any contour on the component without the scrap being placed on the part, contrary to AFP systems. However, net shape cutting of wide tapes may cause relatively high tape scrap rates, depending on the component geometry [78]. An example of a typical ATL machine configuration is displayed in Figure 2.11.

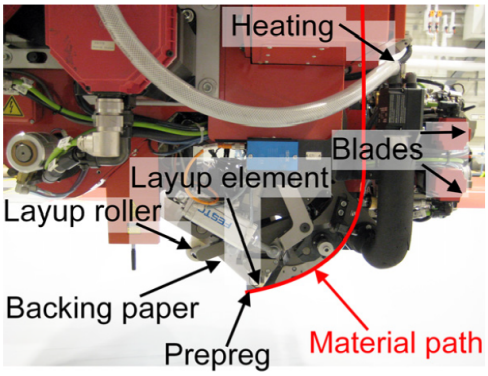

Figure 2.11: Typical ATL lay-up head configuration [53].

For the actual lay-up process, the machine starts on a standstill elevated position in relation to the mold, being this distance defined by the operator, then it begins moving by coming down and touching the mold. Subsequently, it accelerates in the lay-up plane while laying down material, until the velocity defined by the operator is reached [56, 79–82]. It can happen that the machine does not reach this speed due to a short course length. Before finishing a course, the machine starts to decelerate and cuts the material feed with rotating or pinching blades if it has a single-phase system. Scrap is then generated and it can be disposed off in different manners, either removed together with the carried paper and resulting in a lower productivity as the cutting speed is reduced or, if it would interfere with subsequent process steps, deposited outside the part on the work area after each course lay-up. If

the latter is not feasible, scrap cuts may be placed in a designated external area in a secondary lay-up process of each course resulting in a even higher decrease of productivity [78, 83]. The rest of the material is then deposited until the machine comes to a stop and lifts back to the starting height. This height, a set distance from the lay-up plan, is usually a number chosen from a set of discrete values that varies between automated composite machines and it is of high importance because it has to be far enough to avoid collision and not too far to cause unproductive travel time. After, the machine returns to the other side of the part or, if it is capable of, rotates its head, which by itself eliminates unproductive travel time, and starts the next lay-up course, repeating the whole process until finishing the ply.

SOA ATL machines also include continued visual inspection through the lay-up process to reduce error and avoid defected tape placing by automatically stopping the machine if some defect is detected [67]. Studies claim that using visual inspection during lay-up can reduce up 30% of the time to build up a part [59]. Heating tape temperatures can vary between 26ºC and 44ºC [54, 65, 84] for thermoset materials and 375ºC to 400 ºC [85] in thermoplastics, in order to control tack levels. ATL machines can reach speeds up to 1 ms^{-1} and accelerations of 1 ms^{-2} for the X and Y axis and 3 ms^{-2} in the Z axis. Its rotatory axis A and B can reach speeds of 2.6 rpm with an acceleration of 0.32 ms^{-2}. Its C axis which is the axis perpendicular to the lay-up plane can rotate up to 200 degrees with an maximum velocity of 23.6 rpm an acceleration of 0.41 ms^{-2} [77]. The compaction pressure depends on the tape width but is normally around 0.1 MPa for thermoset tapes. The minimal course length for this technology is around 100 mm for most systems [53].

Lay-up rates can vary between 10 and 150 kg/h for flat or mildly contour parts manufactured with this technology as per Hagnell and Åkermo [5], depending strongly on material width and fiber areal weight. One article [59] cites that Brock Jahner, Automated Composites Project lead at Electroimpact assured lay-up rates up to 300 kg/h for a given machine and part and configuration. Furthermore, it is also stated that this rates were dubious due to lack of information on part geometry and machine specifics [59]. This is a good example on why this thesis will bring value as the lay-up rates to be reported here will have all the other relevant information, like the part's geometry, tape width and lay-up speeds, for example, available. Another article refers the same order of values as Lukaszwecicz report, about 100 kg/h theoretical rate, but the real value was set at 25–50 kg/h for simple geometries, down to 12 kg/h for more complex preform. The reason behind this decrease is the downtime caused by spool changes and cleaning of the machine guiding elements. It also presents scrap rates in the order of 2 to 4% in larger parts up to 30% for small parts for ATL machines [54]. In 2011, Lukaszwecicz, performed a benchmark study for the manufacturing process, using ATL and AFP systems, of a simple flat rectangular geometry. The results provided lay-up rates of 29.2 kg/h for ATL and 41.3 kg/h for AFP [83]. These values will be subject of study with the tool to be developed in this thesis in order to provide a scientific basis for comparison. Results are shown in subsection 6.2.3.

Scrap rates are dependent on part size as the lay-up has a significant decrease in efficiency as the part gets smaller. As discussed previously, when fabricating smaller parts, the machine probably does not reach the desired speed and makes the process inefficient cost wise. According to Grimshaw [54], scrap rates tend to be higher for smaller parts but decrease with the part size increase, reaching a

plateau. Inversely, lay-up rates increase with part size. Grimshaw graphics are depicted in Figure 2.12 and Figure 2.13.

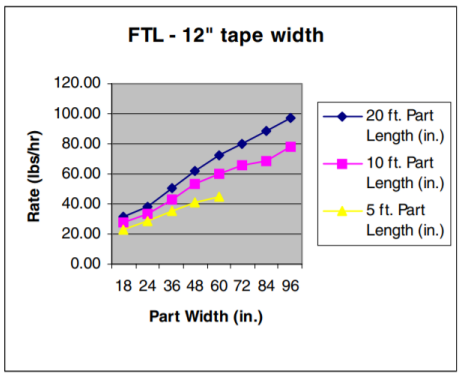

Figure 2.12: Lay-up rate variation with part size [54].

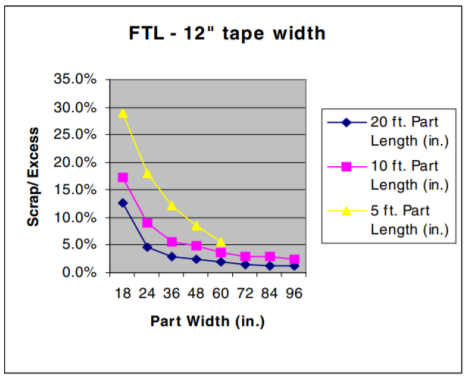

Figure 2.13: Scrap rate variation with part size [54].

One future improvement, currently in development, is related to the prepreg tape cost and width. As reported by Brosius [10] in CompositesWorld, ”if the price of industrial-grade carbon fiber were suddenly reduced by 50%, it would open big opportunities in automotive and wind energy markets” as the cost would come down. Tape width currently has a gap in the middle size of its range. Current efforts are to bring to market tapes between 0.75 inch to 1 inch (19 mm to 25.4 mm) wide on the narrow end of the spectrum, to 1.25 inches to 1.5 inches (31.8 mm to 38.1 mm) on the wider end in order to fulfill that gap [86]. One recent example of that is the Fives Lund SLALOM ATL machine which lays down 1.5 inch carbon fiber tapes taking advantage of the better allowables and tolerances for tapes and the conformability of tows while providing greater lay-up efficiency. Each tape creel is individually controlled like common AFP systems, has its own compaction roller and can be individually added or cut at ply boundary. Three 19-lane Slalom machines have already been used by Mitsubishi Heavy Industries to fabricate wing skins for the Boeing 787. Initially these machines would reach 0.6 meters per second, but current testing has them reaching speeds of 4.5 meters per second to lay or cut operations and 2.5 meters per second for adding tapes. This would mean, for sure, groundbreaking innovation for the automated composite industry [87].

Automated Fiber Placement

AFP is a similar but more advanced process than ATL because it is capable of laying small fiber tows, enabling steering and thus producing composite parts with higher degree of curvature. Material used for this technology can be impregnated tows or slit prepreg tape as well as binder powder fiber for dry fiber placement. They are usually fed into bobbins from an external creel rack or included in the placement head and provided with an inter-leaf film for the purpose of reducing tacking and friction in the material supply. The material guiding system is composed of guide pulleys or tubular guides which compensate for rotations of the placement head with respect to the creel in order to prevent rewinding of the spools caused by the motion of the machine. Some systems offer the possibility to place two material sets on the creel which automatically replaces an empty set in order to minimize material loading time and

increasing productivity [78]. An image of a typical configuration of an AFP machine head is shown in Figure 2.14. The tow width can range from 1/8, 1/4 and 1/2 of an inch (3,175, 6,35 to 12,7 mm) in single width. Also, a novel 4 mm tape width is provided by the Cincinnati Viper [71]. It also can vary in the number of tows delivered being 32 the most used in one machine head. They can range from 1, 2, 4, 8, 16, 24 or 32.

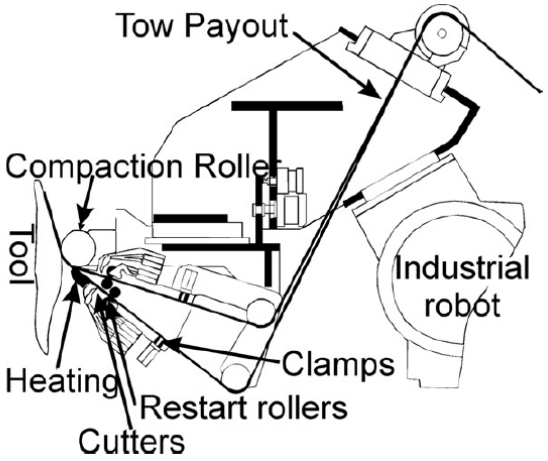

Figure 2.14: Typical AFP lay-up head configuration [53].

These tows align in parallel with low and adjustable tension and compaction pressure to form a band of fiber deposited material. Compaction is applied during lay-up in order to avoid defects by eliminating entrapped air and inner band gaps present in the plies and also ensures accurate position and sufficient adhesion between tows and component. Usually, heat is introduced into the compactor to reduce resin viscosity of the tows. Increased tack provides better and quicker adhesion of the fibers to the mold providing reliability and flexibility in fiber steering. Each tow can be controlled individually allowing independent cut, positioning and restart [69, 88]. This makes this process very convenient for laminating contoured and tapered parts with constant ply thickness due to its steering capability. Furthermore, it allows almost no excess length at component edges reducing scrap rates. The complexity of the part's geometry and its in-plane curvature impose a physical constraint which translates into a limit on the minimum steering radius desired for each tow, which in turn, affects tow number and width selection [5].

Generally, geometries that have more complex curvature require narrower tows reducing productivity. For AFP systems, the performed cuts can only be done transversely thus the shape placed is not net shape. Highly complex cuts, such as the ones that can be achieved using ATL technologies, cannot be performed because the material is not supported by carrier paper during cutting. The maximum cutting speed is very important to a machine's productivity as it should accompany a rise in lay-up velocity for optimum lay-up. The latter is fundamental for the cut "on the fly" concept and it only exists on AFP machines. There are current some limitations regarding compaction roller diameter and head geometry which limits female mold radii that can be used for parts built with this technology. Geometrical features like difficult double curvatures, tight corners and steep ramps as well as tapered laminates can be challenging, even for AFP technology. All of these factors influence productivity.

SOA commercial machines can deposit material up to 1.2 ms^{-1} with head axis accelerations up to 3 ms^{-2} [64]. Rotational speeds and accelerations vary more by company and therefore are not quoted. Due to the cut "on the fly" feature, AFP tends to have lower minimal course length than ATL, normally around 50 mm [53] for smaller robotic arms and 90 - 124 mm for larger machines [64]. AFP lay-up rate can range from 2 to 150 kg/h [5] with an example of the Boeing 787 complex fuselage having a lay-up rate of about 8.6 kg/h in 2006 [89]. Current scrap rates for AFP machines range from 2 - 5 % as per [90, 91] nearing net shape lay-up capabilities. One article [92] claims dry AFP scrap rate of 3% which demonstrates that rates are similar for dry fiber placement comparing to prepreg type. Current efforts to further broaden the use of this technology are focused on versatility, with tape width varying from 1/2 to 2 inch (12.7 to 50.8 mm) being researched, affordability as Mikrosam is developing a machine that would require significantly less initial invest with a price tag around half a US$ million [93] and efficiency as some experiments could reproduce a smaller AFP module with a lay-up speed up to 3 ms^{-1} and acceleration of 10 ms^{-2} [94].

2.3.3 Lay-up productivity

One of the main goals of this thesis, due to lack of literature information on the subject, is to provide a tool horizontal to both technologies that can simulate the lamination process and provide lay-up rates, among other relevant information, of any flat composite part geometry. This is important, not only because most of this information is well kept within manufacturers but also because it is industry norm that when lay-up rates are revealed, as examples presented in this document, it usually comes without revealing the exact shape of the geometry, the lay-up speed used, machine constraints such as the minimal course length, or the cut-restart length. This means that, even though the exact value of the lay-up is revealed it is of no use to assess that machine's productivity in relation to the production of that part. In addition, for comparison purposes, either within the same automated technology or with other, it becomes useless. The tool to be developed in this thesis should diminish this problem as both technologies can be compared and the influence of machine constraints and part geometry on lay-up productivity can be studied.

Some academic literature such as Lukaszewicz [83] provided some insight on composite lay-up productivity by automated technology regarding lay-up speed and part size variation. However, the study is somewhat limited due to the simplicity of the part geometry used, and more importantly because of the simple equations on what it was based on. Further investigation on this subject can be seen in chapter 6. Nonetheless, this benchmark work was given high relevance by industry experts and researches as it is cited multiple times in articles and papers which reveals the impact and importance of this data on the composite industry and just how imperative it is to provide a more accurate and broader tool to perform this kind of research.

Usually, comparison of equipment and technologies in the industry is done through productivity expressed in kg/h. However, productivity expressed in this unit is not realistic because it depends on a variety of factors like the total lay-up width, machine configuration and system technology, material and areal weight, part complexity and size and programming and lay-up strategies. Lengsfeld and Lacalle

[78] were keen on this subject as they developed a more reliable form to compare lay-up rates between systems and net machine capacities for a given part geometry. The basis for comparison is performed through the areal lay-up rate (typically measured in m^2/h). This unit ends up being independent of material, areal weight and tape width which allows comparison of productivity between different processes, ATL or AFP, and technologies (machine manufacturers) for a certain composite component.

As referred in this document, common lay-up technologies can reach up to 1.2 m/s in lay-up velocity. However, this maximum speed can only be achieved for certain phase of the component lay-up. Due to short courses, curvatures, empty runs, transition movements the average lay-up speed is much lower reducing productivity. This speed allows for the determination of absolute machine capacities and it not only takes into consideration the velocity per se, but also additional process operations during lay-up that reduce productivity. These parameters are:

Reduced process velocity

- Acceleration and deceleration phase during lay-up such as the end and beginning of each course;
- Performing cuts as velocity needs to reduce for net shape cuts (ATL) and systems which don´t possess cut ”on the fly”;
- Material and process related velocity reduction like high complexity part or limited tack;

Non-productive time

- Machine travel time such as transition between tape courses, sequences and additional time caused by non-optimized lay-up strategy;
- Non-productive process steps like the lay-up of scrap on an external scrap area (ATL example).

Some future challenges to the automated placement systems would be reducing non-value-added operations like inspection time, time projection which, according to a recent study, correspond to 22% and 30% of the lay-up cycle time, being only 27% to the lay-up itself. The objective is to increase run time to 77% and completely eliminate laser projection and operator-induced stoppage by using servo-driven creels, 100% in-process inspection and data management [95].

2.3.4 Programming and optimization

ACMT are controlled by CNC programming. Parameters such as the lay-up path definition, non-productive travel time optimization or even sequence determination is often determined in this phase. The process normally starts with a composite part design model using CAD software prior to layer geometries and stacking definition. After finalizing part geometry, ply thickness and contour are the next logical step. In continuation, the desired ply orientation is assigned to each ply geometry: 0°, 45°, 90°, or -45º are the industry norm. The main goal of offline programming is to make sure surfaces and contours defined in the ply book are completely covered with prepreg material with its corresponding fiber orientation. Furthermore, scrap can be minimized [78], herein one of this thesis goals is inserted, and also the lay-up should be optimized in terms of part quality and productivity. Existing independent

commercial software and also machine manufacturers software specifically developed for that system serve this purpose as they allow for the generation of courses and complex lay-up strategies to pursue those requirements. Many of the parameters which are set during this phase significantly effect how the machine lays up the part as well as the rate at which it is laid.

The programming stage takes into account numerous parameters and strategies that are important for the subsequent lay-up process. Some of these options include: initial start of lay-up and staggering of plies; distance between tapes/tows; lay-up and scrap strategies like complex course paths on curves, both geodesic and non-geodesic, as well as curve offsets; sequential order and orientation of courses; control of machine and process parameters (pressure, temperature, lay-up speed, compaction and tape tension); course generation, calculation, and, if necessary, simulation of trajectories (position and orientation of tool center point), collision analysis, determination of the synchronized positioning of all machine axes and generation of part program; feed rate optimization strategy. The set-up of the various lay-up parameters and strategy is strongly dependent on both the lay-up technology chosen and the component geometry. Also, the options offered by the utilized software and the skill of the programmer can play a significant role on the quality of such optimization [78]. Simulating the manufacturing process provides essential information such as material lay-up rates and scrap factors [54]. In addition, after optimization is performed on a part lay-up, operator to operator variation is eliminated and the program can be executed as many times as needed with virtually no variability therefore enhancing reliability and reproducibility [59, 96]. Furthermore it prevents waste of material and machine time in dry run testing [97]. Nonetheless, there is a learning curve for operators in part optimization which takes time for experience to be gained. This happens at the cost of productivity and scrap material.

Crosky et al. [90] stated that ”improved software capabilities to integrate CAD, mechanical analysis, trajectory design, optimization, and manufacturing process modelling will be a driving force to increase industrial implementation of fibre placement”. As its proposed in this document, some research is to be developed in this area of interest. In addition to a tool capable of the already explained simulation and providing lay-up and scrap rates, the other proposed idea comprises a focus on reducing material scrap by searching an optimized lay-up strategy when it comes to the initial tape lay down of each continuous part of each ply (it can happen that a part has a ply which is not continuous, meaning that it has lay-up gaps in a certain direction). Usually, the left boundary of each first tape laid coincides with the left boundary of the part geometry because, in such manner, scrap is being diminished as that is the ideal position for scrap reduction. However, with the first tape being set that way, the rest of the lay-up in that ply may not be optimized for scrap reduction as an offset in the outer direction of the ply might have a trickle down effect on setting the consequent adjacent tapes for a better material usage, therefore diminishing scrap. This effect increases as tape width and part size also increases. Results on this study are presented in chapter 6. In 2017, Potter [98] commented on the importance of early stages decisions in development of composite products being supported from modelling and simulation of composites design and manufacture. He goes further by stating that there is still a long way to go in ”analytical, numerical and predictive tools associated with composites design and manufacture” [98].

3. Methodology

The following chapter tries to clarify the methodology that was applied to develop the model that sustain this thesis. After technologies' SOA exposure and detailed description, it is then necessary to understand and structure what is required to achieve the proposed objectives of this work.

First, the necessity to develop a model/tool that could accurately calculate the results proposed on this document was understood, meaning the lay-up and scrap rate and material costs of any flat composite part deposition. With a solid model that was able to realistically simulate the deposition processes developed, some features could then be introduced in order to improve the lay-up strategy. The tool should be capable of suggesting a more efficient way to perform the lamination process. This could be either by making it less costly or making it faster. Cost wise, the only way to reduce, by analyzing the deposition process alone, was to decrease the technical scrap as this parameter is highly costly. One square meter of aerospace grade material can cost between 34 and 420 euros per kg for the higher tier [99] and another study cites an average price of 71 euros per kg for aerospace grade carbon fiber [100]. For a medium size part of 10 square meters, using the latter average price value and an average areal weight of 0.6 kg/m^2 [101, 102], with a technical scrap of around 10% which is standard for ATL with 40 layers, the total scrap cost is equal to 2840 euros plus the cost of disposing it. It is then highly relevant to reduce this value. Consequently, although with less impact, by having less scrap the machine will deposit less material and therefore the lamination process will take less time generating cost savings in electricity and machine usage. It was understood to be difficult to attain a method of reducing cycle time purposes as current SOA machines have this parameter highly developed on an efficient basis and no strategies could be thought in order to suggest improvements on the subject.

The next logical step was to elaborate an algorithm that was capable of reproducing the desired outputs using the inputs and constraints needed. Therefore, a research of these technologies was performed to understand how the deposition processes work and the machine and part constraints that would serve as inputs. The algorithm then needed to answer the following questions for a certain desired flat part:

- Given the proper inputs how much would the lay-up manufacturing process cost, material wise?
- Given the proper inputs how much time would it take to perform the lay-up?
- For some lay-up velocity, axis acceleration and tape width what is that machine configuration productivity values in terms of kg/h?
- For some constant inputs which tape width is the best suited from a material cost or time saving perspective?
- For some constant inputs which lay-up paths configuration presents the best solution for technical scrap saving regarding first tape/tow offset?

The first approach was to obtain primary values for any kind of black and white image in 2D. These values would be the area of the total material deposited including technical scrap, its cost, and the cycle time for its production. In the beginning phase were addressed constraints related to the deposition process itself, its specifications, such as the tape width to use or the minimum cut restart length for a given lay-up. The following step was to define the tool inputs. Which inputs were program intrinsic, which were machine related and which were user/part specifications. Then it was studied how the provided part image should be processed. One initial perceived limitation was on how the pixel problem could be approached. Should the pixel resolution be a standard 1:1 scale, meaning one pixel was 1x1 mm^2 or should this option be user customized? Due to the different widths of tape/tow used in these technologies, and being these sizes usually a multiple of the lowest size for each technologies, a pixel resolution being a sub multiple of the tape width used for that simulation was chosen in order to not loose image information in the conversion. The pixel resolution was then decided to be a user option because letting it be a standard resolution could drastically increase the simulation time for parts with larger areas. Having obtained the boundaries of the part, the tool would be able to lay down the tapes or tows inside those limits from one edge of the part to the other respecting the plies orientations given as inputs. The sum of the area of those tapes/tows would total the material deposited. Knowing the material areal weight, its price per kg and the disposal cost per kg, the material manufacturing costs could now be computed.

Secondly, and having obtained accurate results regarding the simulated deposited material, the area of the part to be studied and its technical scrap for any chosen tape width, the second item regarding cycle time could be addressed. This was the most time consuming part of the algorithm due to highly complex logic behind the method of translating the real time process to discrete logic steps. To start, the deposition process had to be described by simple equations in order to grasp a mathematical form to represent it. This is shown in detail in the next chapter. Having formulated those equations, an algorithm could be developed to obtain the time spent in laying up the material. A more precise approach was then taken by making the algorithm work for both technologies since the lay-up time calculation is different for both processes, being the initial calculation method only suitable for ATL technology. This new improvement of the model was of high difficulty because there were new inputs introduced like the initiation and cutting speed for AFP technology. Furthermore, the fact that each deposition creel can cut, stop and start a tow deposition independently of the each other but the speed at which all of them perform must be the same and the introduction of constraints such as the minimum distance between cutting and feeding an individual tape/tow should highly enhance the difficulty of the algorithm's development. In a later stage it was realized the importance of calculating lay-up time with the effect of machine acceleration since the earlier time results were somewhat inaccurate and low.

The item before last referring to the best tape width suited for a particular machine configuration and for a desired part was answered based on iterating the model developed for the desired tape widths. The model then presents all outputs for the different tape widths and the user should select either the fastest one, which had a smaller cycle time, or the less costly, material wise. With the cycle time now obtained and having the value of the deposited mass the lay-up rate could be found representing the selected

machine configuration efficiency for that certain part. The first four items were therefore addressed.

The algorithm was developed through multiple increments until the desired outcome was attained, with a high-level flowchart representing its main structure and inputs/outputs being elaborated. Secondly, multiple functions based on the referred equations needed to be developed to reproduce the envisioned results. After the model had a solid working principle, it was then necessary to validate it. This was achieved by comparing its results such as the lay-up rates, material deposited, technical scrap and other time parameters to others retrieved from research papers/thesis and also from one Embraer's specimen part test. By having a good agreement between results it also validated the algorithm's image process system as the parts would have approximate areas as well as scrap rates and cycle times. All the answers related to this topic were discussed in chapter 6.

Once the software was validated some simulations were performed for representative aeronautical composite parts in order to obtain values for lay-up and scrap rates. Furthermore, it allowed the comparison between different machine's configurations and technologies and also to grasp the full potential of the tool developed by analysing all the results provided. The last thing to be implemented was the tape offset study for technical scrap reduction. After careful consideration and conversations with composite machine operator at Embraer's facilities in Évora, it was understood that some optimization could be done as the software they used to forecast and simulate the deposition did not provide the best location for the first tape/tow laid in order to reduce material costs. The software had as standard procedure to start the deposition with the first tape/tow aligned with one of the part's edges. This method of deposition is not necessarily the most efficient one because having an offset of the first tape/tow can mean a better configuration by reducing scrap. With this feature developed the model could then, not only provide the best tape width selection as well as dictate the optimal lay-up strategy for the first tape/tow. It was then important to implement it in the algorithm that was to be implemented with MATLAB software. In Figure 3.1, there is an illustration of the research methodology and how the final outcome was attained.

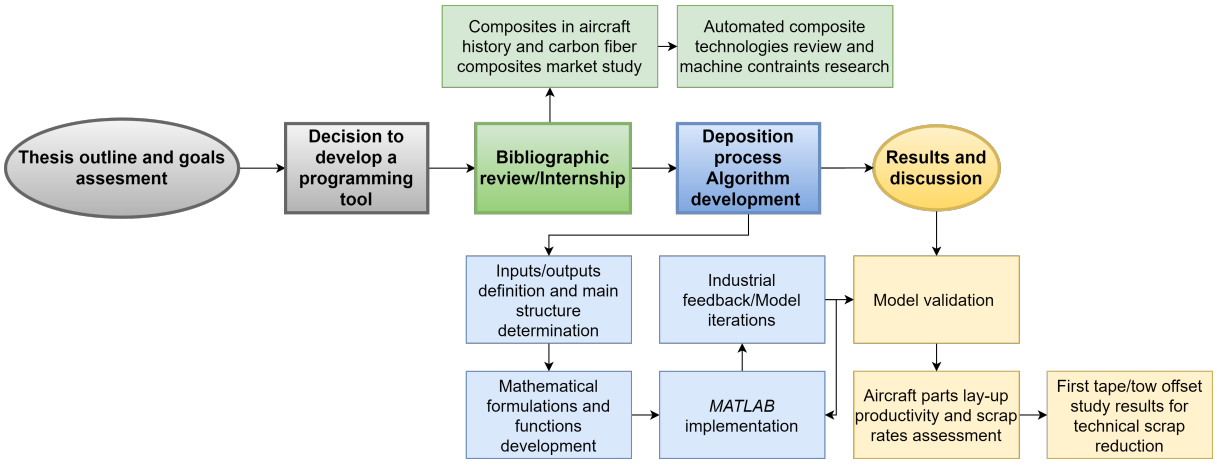

Figure 3.1: Work methodology.

4. Process Mathematical Formulations

In this section, the mathematical equations that describe the lamination process are presented. This constitutes the first step in transforming the mechanical process which is the composite material deposition in an array of mathematical formulas that can represent it and contribute towards developing a realistic simulation tool. These equations are a translation of what was previously explained, i.e., the fundamental parameters which rule the deposition process and would serve as the basis for the algorithm. The equations can be divided into five different global prisms: material and technical scrap, distances, times, lay-up productivity and material costs. All the knowledge and information that allowed the development of the work presented in this chapter were acquired through observation of AFP and ATL machines lay-up at Embraer's facilities in Évora and literature and video reviews available on the internet.

All equations are based on a 2D coordinate system where abscissas increase from left to right and ordinates from top to bottom shown in Figure 4.1. This referential coordinate system changes from each course to the next and has its ordinates axis aligned with the left boundary of each tape or first tow and its parallel to the direction of the lay-up course or the angle reference of that ply. The deposition process is modelled with each ply starting on the left side of the part and progress from left to right. Also, the machine is set as starting from a top reference at the beginning of each ply and then lay-up material in a top to bottom motion, having the ordinates of the machine head location increase through each course deposition. After the first tape/tows being laid, the machine then progresses based on its settings to turn the machine head if bi-directional lay-up is selected, otherwise it returns back to a top position. The location of the machine head is defined as the middle point of all its creels. For ATL technology, for example, if the tape width selected is 304.8 mm, the location of the machine head in the referential is the middle point of that tape meaning the 152.4 mm point mark. For an AFP technology, taking as an example a machine utilizing 24 tows at once, its abscissas reference point is at the end of the 12^{th} tow, as it is its middle point.

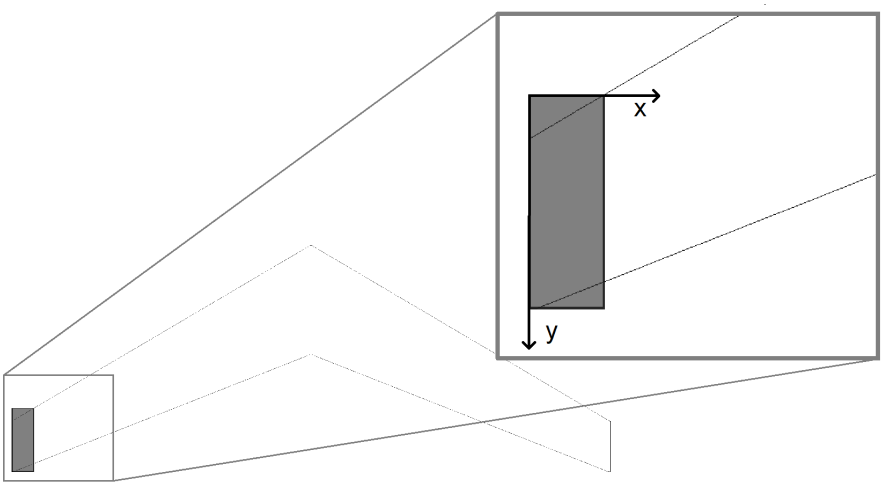

Figure 4.1: Model 2D coordinate reference system.

4.1 Material and Technical Scrap

The first parameters to formulate, as explained in the previous chapter, were the total material deposited and the technical scrap of any lay-up deposition. The material deposited in each lay-up course was quite simple to translate into an equation since it is given by the multiplication between the tape/tow width utilized and its length. This is only possible due to the simple rectangular geometry of each tape/tow. The area of each individual tape/tow is then summed for each ply to obtain the total deposited area in the laminate. The formula for the total material deposited in the lay-up of any flat part is described in Equation 4.1. Knowing the area of the part to be laminated, the technical scrap can be obtained by subtracting that value times the total number of plies of that part from the total material deposited, expressed in Equation 4.2, and its percentage in Equation 4.3. The areas are expressed in m^2.

$$Mat_{dep} = T_{width} \sum_{Ply_i=1}^{n_{Plies}} \sum_{r=1}^{n_{Tape/Tows}} (T_{length_r})_{Ply_i} \tag{4.1}$$

$$Tech_{Scrap} = Mat_{dep} - Area \times n_{Plies} \tag{4.2}$$

$$\%Tech_{Scrap} = \frac{Tech_{Scrap}}{Mat_{dep}} \times 100 \tag{4.3}$$

4.2 Lay-up Process Distances

In order to obtain the time spent by the machine in the lay-up process, the distance travelled by its head needs to be calculated. In AFP technology, as referred in previous chapters, the machine starts the process as it accelerates from an idle position and reaches a speed called initiation speed. This is the speed the machine needs to be at when any of its creels is initiating the deposition of a tow or completing a minimum course length for each tow initiation. This means that AFP machines, when initiating a tow, need to be, not only at that initial speed when the compaction roller hits the mold to start laying a tow but also maintain that speed for the minimal course length for method 1. For method 2, the machine starts from an idle position at the part's edge and the machine only reaches its initiation speed after. If it reaches before travelling the minimum course length it maintains that speed value until reaching that length. If the machine reaches the minimum course length first (not common), it can accelerate to lay-up speed right away.

Tow ordinates are represented by set A and B. Set B depicts the ordinates of each tow starting location and A the ordinates of each tow finishing location. Both of these sets represent a portion of the lamination process where the machine head travels at initiation or cutting speed, respectively. After all tow courses of a said set B finish depositing the minimal course length, the machine can accelerate to its configured lay-up speed. The initiation speed distance is then the distance travelled by the machine from idle position until it reaches initiation speed and also the distance it tracks when it moves at that

exact speed. Two methods exist to calculate this distance which are dependent on machine configuration: method 1 has the machine starting the acceleration from idle before reaching the part in order to attain initiation speed on the exact location of the part's edge; method 2 has the machine starting the acceleration from an idle position on the exact location of the part's edge. It can happen that the machine accelerates to its lay-up speed because all the minimal course lengths were completed for all but one tow, because that tow is only to be initiated further in the course deposition. That would mean the existence of two sets B because the machine was at initiation speed in two different non continuum sections of that part deposition. This usually does not happen in real lamination but as the tool is designed to be able to encompass all these technical details it was relevant to predict this event. The distance travelled at initiation speed is thus, mathematically, the difference between the maximum ordinate and minimum ordinate of set B, plus the distance to reach initiation speed ($D_{reach_{is}}$) plus a minimal course length for method 1, shown in Equation 4.4; and the difference between the maximum ordinate and minimum ordinate of set B plus a minimal course length for method 2 and is displayed in Equation 4.5.

The distance travelled at cutting speed, analogously, is the distance between the point where the machine reaches cutting speed and the point where it stops. For this parameter two methods can also be applied in the same fashion: method 1 has the machine at cutting speed past the part's edge and only after it travels the required distance to stop (D_{reach_0}); method 2 has the machine stopping at the part's edge. Method 2 is used for single-phase ATL machines and also some AFP systems. Moreover, it was the chosen method for the validation test of Lukaszewicz [83] model in chapter 6. The cutting speed distance for method 1 can be calculated by the difference between the maximum ordinate and minimum ordinate of set A, described in Equation 4.6, and the difference between the maximum ordinate and minimum ordinate of set A for method 2, shown in Equation 4.7. The machine slows down from its lay-up speed to reach cutting speed with a distance offset relating to the point where the first tow of that course is design to end. This distance offset is the length required to decelerate from lay-up speed to cutting speed. After the first tow is cut and placed in the mold the others follow the same logic. If, as also explained for set B, there is a bigger difference than the minimal course distance between cuts of the machine tows, the machine would accelerate back to its lay-up speed only to reach cutting speed again further down the path and another set A would be generated. It is also important to refer that the imposition of having the machine going back to its lay-up speed or transitional speed on the explained situations and generating more than one set A or B was implemented in order to study the most efficient configuration of a determined machine as it could easily be set to maintain initiation or cutting speed for those situations. However, for the basis of the proposed algorithm, these discussed distances were defined in such manner.

Finally, the distance travelled at lay-up speed is the modulus of the difference between the minimum ordinate of set A and the maximum ordinate of set B minus the minimal course length as depicted in Equation 4.8. This comprehends the distance travelled by the machine from the point at which accelerates to lay-up speed from initiation speed or cutting speed to the point where it slows down to cutting speed or initiation speed. The index j raises until $N\_Courses$ is reached which is the total number of courses in a determined ply.

$$Method\ 1 - Dist_{ispeed\_AFP} = \sum_{Ply_i=1}^{n_{Plies}} \sum_{j=1}^{N_{Courses}} [max(B_j) - min(B_j) + Min_{length} + D_{reach_{is}}]_{Ply_i} \quad (4.4)$$

$$Method\ 2 - Dist_{ispeed\_AFP} = \sum_{Ply_i=1}^{n_{Plies}} \sum_{j=1}^{N_{Courses}} [max(B_j) - min(B_j) + Min_{length}]_{Ply_i} \quad (4.5)$$

$$Method\ 1 - Dist_{cspeed\_AFP} = \sum_{Ply_i=1}^{n_{Plies}} \sum_{j=1}^{N_{Courses}} [max(A_j) - min(A_j) + D_{reach_0}]_{Ply_i} \quad (4.6)$$

$$Method\ 2 - Dist_{cspeed\_AFP} = \sum_{Ply_i=1}^{n_{Plies}} \sum_{j=1}^{N_{Courses}} [max(A_j) - min(A_j)]_{Ply_i} \quad (4.7)$$

$$Dist_{lspeed\_AFP} = \sum_{Ply_i=1}^{n_{Plies}} \sum_{j=1}^{N_{Courses}} [|min(A_j) - max(B_j)| - Min_{length}]_{Ply_i} \quad (4.8)$$

$$A = \{y_1, ..., y_k\} \qquad B = \{y_1, ..., y_k\} \qquad k \in \{1, ..., N_T\}$$

If a determined course does not have the necessary length to reach lay-up speed the tool has the machine simulated to, in accordance to the distance that remains when subtracting the initiation speed and cutting speed distance from the course distance, accelerate to a speed inferior to that of the lay-up speed and then decelerate to reach cutting speed. If a situation occurs where the machine does not have enough course distance to transition from initiation speed to cutting speed the machine is set to maintain through that full course at the lowest value of those two speeds. All distance parameters will be expressed in meters.

For ATL technologies more variety in the deposition process was found. As exposed in Chapter 2 there are single and two-phase feeding systems where, for the first case, the machine needs to slow down to a stop to cut the tape, then it accelerates to its cutting speed, stops again, and then lays down the rest of the tape at its cutting speed and comes to a halt again. A similar procedure also happens when it starts each ply. A constant time for ATL single-phase systems course initiation and cutting will then be necessary as an input. The distance travelled while at or getting at initiation speed is shown in Equation 4.9 and was assumed to be two times the minimal course length as standard, although some machines have different values. It is then multiplied by the total number of tapes utilized. Furthermore, for single-phase systems, the distance travelled at cutting speed is the same as the one travelled at initiation speed as the distance is the same two minimal course lengths multiplied by the total number of tapes. The distance run at lay-up speed for single-phase systems is simply the difference from the maximum ordinate and minimum ordinate minus four times the minimal course lengths. Its formula is

shown in Equation 4.10. For two-phase systems, where the tapes are pre-cut, the machine does not need to stop nor it has initiation or cutting speed, only a lay-up velocity. The machine simply starts from an idle position on the exact point the lay-up is designed to start until it reaches its lay-up speed and comes to a stop on the exact location where the lay-up ends as shown in Equation 4.11.

$$Dist_{ispeed\_ATL\_singleph} = Dist_{cspeed\_ATL\_singleph} = \sum_{Ply_i=1}^{n_{Plies}} \sum_{j=1}^{N_{Courses}} (2 \times Min_{length})_{Ply_i} \tag{4.9}$$

$$Dist_{lspeed\_ATL\_singleph} = \sum_{Ply_i=1}^{n_{Plies}} \sum_{j=1}^{N_{Courses}} [(y_{max_j} - 2 \times Min_{length}) - (y_{min_j} + 2 \times Min_{length})]_{Ply_i} \tag{4.10}$$

$$Dist_{lspeed\_ATL\_twoph} = \sum_{Ply_i=1}^{n_{Plies}} \sum_{j=1}^{N_{Courses}} (y_{max_j} - y_{min_j})_{Ply_i} \tag{4.11}$$

4.2.1 Transitional course Distances

The distance between the end of one course deposition and the start of next constitutes the transitional tape/tow distance parameter, defined in this thesis. This course transition can be made in one of two ways. The machine can opt to start the next course in the same side of the part were it previously ended (bi-directional lay-up) or to transition to the opposite side of the part and start the next course deposition. For the first case it would require a capability to rotate the machine head at least 180º.

Following the same logic as in previous formulas, sets A and B are defined representing the ordinates in a 2D plane of one side (beginning) and the ordinates of the other side (end), respectively. The course transitional distance can then be described as the square root sum of the quadratic difference between ordinates and abscissas of finishing and starting point courses. The distance in abscissas is a constant value and can be given by the number of tape/tows times the length of each tape/tow. When this transition is done in the same side of the part the difference in ordinates is done in set A, if it is performed in the bottom side of the part, shown in Equation 4.12, or in set B if it is done in the upper side of the part, shown in Equation 4.13. On the other hand, when the transition is done on opposite sides, the difference in ordinates is between the maximum ordinate of set A of the finishing course and the minimum ordinate of set B of the next course deposition which can be described as the transitional distance bottom up, relating to the reference system, and is described in Equation 4.14. The distance up bottom is the reverse of the previous formula being the ordinates difference between the minimum value of the set B and the maximum value of the next set A, described in Equation 4.15. N_T differs from $n_{Tape/Tows}$ (Equation 4.1) as the first represents the number of tows or tape used for each course deposition and the latter the total number of tape/tows deposited for the whole lamination.

$$Dist_{trans\_bottom} = \sum_{Ply_i=1}^{n_{Plies}} \sum_{j=1}^{N_{Courses}-1} [\sqrt{(max(A_j) - max(A_{j+1}))^2 + (N_T \times T_{width})^2}]_{Ply_i} \tag{4.12}$$

$$Dist_{trans\_up} = \sum_{Ply_i=1}^{n_{Plies}} \sum_{j=1}^{N_{Courses}-1} [\sqrt{(min(B_j) - min(B_{j+1}))^2 + (N_T \times T_{width})^2}]_{Ply_i} \tag{4.13}$$

$$Dist_{trans\_bottom\_up} = \sum_{Ply_i=1}^{n_{Plies}} \sum_{j=1}^{N_{Courses}-1} [\sqrt{(max(A_j) - min(B_{j+1}))^2 + (N_T \times T_{width})^2}]_{Ply_i} \tag{4.14}$$

$$Dist_{trans\_up\_bottom} = \sum_{Ply_i=1}^{n_{Plies}} \sum_{j=1}^{N_{Courses}-1} [\sqrt{(min(B_j) - max(A_{j+1}))^2 + (N_T \times T_{width})^2}]_{Ply_i} \tag{4.15}$$

$$A = \{y_1, ..., y_k\} \qquad B = \{y_1, ..., y_k\} \qquad k \in \{1, ..., N_T\}$$

4.2.2 Transitional gap Distances

When a discontinuity exists in a ply, the machine needs to travel through a horizontal or longitudinal gap. The same logic for transitional course distance applies to this case with the difference being in the abscissas. The machine head can finish a course and transition through the horizontal gap to start the next course deposition on the same side where it finished or return to the opposite longitudinal side, also through the horizontal gap, to start the next course. For this procedure new sets need to be created. These are the sets C and D which contain the abscissas of all tape/tows starting and finishing locations. Set C represents the abscissas of the points (for all AFP tows) or point (for a single ATL tape) of the bottom side of the course deposition. Set D represents the location abscissa(s) of the upper side of the course deposition for each tow or tape. A and B represent the same as in the previous equations. These locations points are always midpoints of those tows or tape, meaning its half length point. Here, the index l is introduced as to represent the index of the gap being counted on a certain Ply_{index} ply.

Regarding the abscissas part of the equations, as the ordinates are similar to previous equations, is important to refer that for the location of the machine, whether it be finishing or starting, the midpoint of both sets D and C needs to be found. As an example, for better illustration, let's take set C for AFP technology. This set represents all the bottom midpoint location abscissas of the tows of a certain *l* course deposition before or after a horizontal gap transition. For gap transitional distance calculation only certain j course depositions are of interest from the set $N\_courses$ which are represented here as a l index belonging to the set $N\_courses_{H\_Gap}$. All other sets represented in this sub section are also indexed in $N\_courses_{H\_Gap}$ because they change from gap to gap or from l to $l + 1$. To calculate the distance the machine travels in the x axis, the midpoint of set C has to be calculated. This translates to subtracting the minimum abscissa of set C from the maximum abscissa of the same set, divide it by

two and sum that value to the minimum abscissa. This point represents the location of the center of the machine relating to the x axis whether it is finishing a course prior to the gap transition or starting one after the gap transition. The same logic applies to the calculation of the machine's center location related to the x axis for the upper side of the part. If the machine is to transition on the bottom side of the part, through the gap, the set C for tape/tows *l + 1* must be used. If the machine is to transition on the upper side of the part, through the gap, set D with tape/tow *l + 1* should be used instead. For the ordinates, to calculate a horizontal transitional gap distance in the upper side of the part, instead of subtracting the minimum ordinate from set A of tow/tape *l + 1*, it must be subtracted from set B, as explained in previous similar equations. Equation 4.16 and Equation 4.17 represent a horizontal gap transition on the bottom side and upper side of the part, respectively.

If the machine is to transition from the bottom side, through a horizontal gap, to the upper side of the part the formula to look at is the Equation 4.18. Reversely, if the transition happens from the upper to bottom side of the part the formula that represents it is the Equation 4.19. If the machine needs to travel through a longitudinal gap another two sets representing the starting ordinates and abscissas of the tows or tape after the gap. These will be designated as sets E and F, respectively. Set A and will maintain the same meaning as in previous formulas and another set G needs to be created representing the abscissas prior to the longitudinal gap. The formula for longitudinal gap transitional distance is shown in Equation 4.20. In this case the index will be m which indicates the number of the longitudinal gap of said course deposition, which can be more than one up to $N\_courses_{V\_Gap}$.

$$Dist_{horz\_gap_{bottom}} = \sum_{Ply_i=1}^{n_{Plies}} \sum_{l=1}^{N\_courses_{H\_Gap}} [((max(A_l) - max(A_{l+1}))^2 + ((min(C_{l+1}) + \tag{4.16}$$

$$((max(C_{l+1}) - min(C_{l+1}))/2)) - (min(C_l) + ((max(C_l) - min(C_l))/2)))^2)^{1/2}]_{Ply_i}$$

$$Dist_{horz\_gap_{up}} = \sum_{Ply_i=1}^{n_{Plies}} \sum_{l=1}^{N\_courses_{H\_Gap}} [((min(B_l) - min(B_{l+1}))^2 + ((min(D_{l+1}) + \tag{4.17}$$

$$((max(D_{l+1}) - min(D_{l+1}))/2)) - (min(D_l) + ((max(D_l) - min(D_l))/2)))^2)^{1/2}]_{Ply_i}$$

$$Dist_{horz\_gap_{bottom\_up}} = \sum_{Ply_i=1}^{n_{Plies}} \sum_{l=1}^{N\_courses_{H\_Gap}} [(max(A_l) - min(B_{l+1}))^2 + ((min(D_{l+1}) + \tag{4.18}$$

$$((max(D_{l+1}) - min(D_{l+1}))/2)) - (min(C_l) + ((max(C_l) - min(C_l))/2)))^2)^{1/2}]_{Ply_i}$$

$$Dist_{horz\_gap_{up\_bottom}} = \sum_{Ply_i=1}^{n_{Plies}} \sum_{l=1}^{N\_courses_{H\_Gap}} [(max(B_l) - min(A_{l+1}))^2 + ((min(C_{l+1}) + \tag{4.19}$$

$$((max(C_{l+1}) - min(C_{l+1}))/2)) - (min(D_l) + ((max(D_l) - min(D_l))/2)))^2)^{1/2}]_{Ply_i}$$

$$Dist_{long\_gap} = \sum_{Ply_i=1}^{n_{Plies}} \sum_{m=1}^{N\_courses_{V\_Gap}} [(max(A_m) - min(E_{m+1}))^2 + ((min(G_{m+1}) + \tag{4.20}$$

$$((max(G_{m+1}) - min(G_{m+1}))/2)) - (min(F_m) + ((max(F_m) - min(F_m))/2)))^2)^{1/2}]_{Ply_i}$$

$$A_l = \{y_1, ..., y_k\} \qquad B_l = \{y_1, ..., y_k\} \qquad E_l = \{y_1, ..., y_k\} \qquad k \in \{1, ..., N_T\}$$

$$C_l = \{x_1, ..., x_k\} \qquad D_l = \{x_1, ..., x_k\} \qquad F_l = \{x_1, ..., x_k\} \qquad G_l = \{x_1, ..., x_k\}$$

4.2.3 Transitional ply Distances

The last distance to be studied and formulated is the distance the machine travels when starting a new ply. The same rationale applies here. The main difference is that the sets used are from consecutive plies. For bottom up ply transition (machine finishes last tape/tows of one ply at the bottom side of the part and starts the next ply in its top side) the Equation 4.21 is the one to look at. The distance travelled in the y axis is the difference between the highest ordinate from set A of the last tape/tows of one ply and the lowest ordinate from set B of the first tows/tape of the next ply. The distance in the x axis is the difference between the abscissas' midpoint of set C of the last tows/tape of one ply and the abscissas' midpoint of set D of the first tows/tape of the following ply. Formulas that describe the up down transitional distance, up up or down down are not inserted here due to repetition purposes.

$$Dist_{trans\_ply\_bottom\_up} = \sum_{Ply_i=1}^{n_{Plies}-1} [(max(A_{N_{Courses\,Ply_i}}) - min(B_{1_{Ply_i+1}}))^2 + \tag{4.21}$$

$$((min(C_{N_{Courses\,Ply_i}}) + ((max(C_{N_{Courses\,Ply_i}}) - min(C_{N_{Courses\,Ply_i}}))/2)) -$$

$$(min(D_{1_{Ply_i+1}}) + ((max(D_{1_{Ply_i+1}}) - min(D_{1_{Ply_i+1}}))/2)))^2)^{1/2}]_{Ply_i}$$

$$A = \{y_1, ..., y_k\} \qquad B = \{y_1, ..., y_k\} \qquad k \in \{1, ..., N_T\}$$

$$C = \{x_1, ..., x_k\} \qquad D = \{x_1, ..., x_k\}$$

4.3 Manufacturing Process Times

All time parameters related to the deposition process itself are based on an uniformly accelerated movement as the machine usually has at least three different free axis which can be individually configured. The other three axis, referent to the machine rotational movements were not formulated as usually when the machine rotates it is simultaneously moving up and down and solely with the formulation of the latter movement the time spent on both actions can be obtained. The values for axis acceleration, lay-up, initiation and cutting speed as well as retracting and approaching speed can then be different in all axis. The two main time parameters of automated tape deposition are the cycle time and the lay-up time. The first includes the second and constitutes the time the whole process takes from the moment the machine is being prepared and configured for a part lamination (setup time), through the lamination process itself (lay-up time), to finally the time needed to change tape/tow rolls in the machine creels when they run out. Its formula can be seen in Equation 4.22. All time parameters have as its base unit the second.

$$Cycle_{time} = Setup_{time} + Layup_{time} + Rolls_{ch_{time}} \tag{4.22}$$

The lay-up time consists of the time on part and the time off part. Its corresponding formula is the Equation 4.23. The first is the time the machine spends on actual lamination, meaning the time the machine is laying composite material along its tool paths, seen in Equation 4.24. The second is the time spent in processes such as tape/tow transitions, horizontal and longitudinal gaps, ply transitions and in head approach/retract procedures, shown in Equation 4.25. The time on part parameter can then be split into the time the machine spends accelerating to and at initiation speed, the time the machine spends decelerating from cutting speed to a stop and at cutting speed and also the time the machine time takes to accelerate and decelerate from initiation or cutting speed, respectively, to and at lay-up speed. For ATL two-phase systems it consists solely on the time the machine takes to accelerate from a standstill position to lay-up speed and the time it takes to decelerate from it to a stop.

The parameters described in the previous paragraph can be obtained applying the formulas that describe an uniformly accelerated movement having the distance variable of those formulas be the ones described in Equation 4.4 - Equation 4.21 and the velocity variable used according to the situation. For example, to calculate T_{ispeed} for AFP technology the distance used in the movement formulas should be the one obtained by formula Equation 4.4 or Equation 4.5. Initial velocity is zero and the velocity to be reached is the initiation speed defined. The acceleration used is the one configured for the axis in which the machine is performing the course deposition. Transitional time formula is the one illustrated in Equation 4.26. As for the approach and retract time, as the name indicates, it is the time the machine spends to descend from neutral position to start a tape/tows course and the time the machine takes to return to that same neutral position after finishing that course and is shown in Equation 4.27. It can be divided in approach and retract time as these processes can be carried at different speeds (approaching and retract speed). For these times a different acceleration is used as its movement axis is a different

one. For the specific case of the single-phase ATL system, the time the machine spends when initiating a course or stopping to cut material needs to be added to the Equation 4.24 as it is normally a specific constant time for each machine that covers the (defined as standard here) two minimal course lengths.

$$Layup_{time} = T_{on\_part} + T_{off\_part} \tag{4.23}$$

$$T_{on\_part} = \sum_{Ply_i=1}^{n_{Plies}} (T_{lspeed} + T_{ispeed} + T_{cspeed})_{Ply_i} \tag{4.24}$$

$$T_{off\_part} = T_{transitional} + T_{appr\_retr} \tag{4.25}$$

$$T_{transitional} = \sum_{Ply_i=1}^{n_{Plies}} (T_{tow/tape\_tr} + T_{gap\_tr} + T_{ply\_tr})_{Ply_i} \tag{4.26}$$

$$T_{appr\_retr} = \sum_{Ply_i=1}^{n_{Plies}} \sum_{j=1}^{N_{Courses}} [(T_{approach} + T_{retract})_j]_{Ply_i} \tag{4.27}$$

To calculate the time needed to change material rolls it is first necessary to obtain the number of rolls required for a certain composite deposition. The number of rolls required is directly related to the length of tape used in each machine creel. As such, the material deposited per machine creel is just the individual sum of the tape/tow length deposited in each ply by each creel. An identification of which creel is responsible for each tape/tow course is thus required. This is represented by the same *k* index as it represents the index of creel from the set $\{1, ..., N_T\}$. Each k creel will have courses whose index belongs to the set $\{j, .., N_{Courses}\}$. This is especially relevant for AFP technology since ATL technology only has one creel. This parameter is evaluated in meters and the number of material rolls required can then be determined. It is given by the sum of the division of the number of creels (which is equivalent to the number of tows or tape per course, N_T) by the length of one material roll. The formulas which represent this are the Equation 4.28 and Equation 4.29. The final parameter of the cycle time can now be calculated. For ATL technology, the time to change tape rolls is equal to number of rolls required minus the one roll already placed prior to lay-up, times the time to change a single roll, $Roll_{ch\_time}$ which is written in Equation 4.30. For AFP technology, the time for creel changes has to be added. If the rolls changing is to be done all at once in order to save time, $(N_{rolls_{req}} - N\_heads)$ is to be divided by the number of machine creels and rounded up which corresponds to formula Equation 4.31.

$$Dep_{per\_creel} = \sum_{Ply_i=1}^{n_{Plies}} \sum_{j=1}^{N_{Courses}} \sum_{k=1}^{N_T} [(T_{length_k})_j]_{Ply_i} \tag{4.28}$$

$$N_{rolls_{req}} = \sum_{k=1}^{N_T} \frac{Dep_{per\_creel_k}}{Roll_{length}} \tag{4.29}$$

$$Rolls_{ch_{time_{ATL}}} = (N_{rolls_{req}} - 1) \times Roll_{ch\_time} \tag{4.30}$$

$$Rolls_{ch_{time_{AFP}}} = \frac{(N_{rolls_{req}} - N_T) \times (Roll_{ch\_time} + (N_T \times Creel_{ch\_time}))}{N_T} \tag{4.31}$$

4.4 Lay-up Productivity

Indirect parameters such as the total mass deposited in the process is obtained by multiplying the material areal weight, which usually comes in kg/m^2, by the total material deposited obtained in Equation 4.1 and is shown in Equation 4.32. Other mass parameters are the scrap mass, Equation 4.33, and the lay-up rate, Equation 4.34, of the process which is viewed as an important benchmark reference. It translates the machine productive efficiency for one specific composite part.

$$Total_{mass} = M_{aweight} \times Mat_{dep} \tag{4.32}$$

$$Scrap_{mass} = M_{aweight} \times Tech_{scrap} \tag{4.33}$$

$$Layup_{rate} = \frac{Total_{mass}}{Layup_{time}} \tag{4.34}$$

4.5 Material Costs

Other indirect parameters are costs as they can be divided in material costs and scrap costs seen in Equation 4.35. The material cost is easily computed by multiplicating the total material deposited obtained in Equation 4.1 by the material unit cost, Mat_unit_{cost}, given in €/kg, and is shown in Equation 4.36. In Equation 4.37 is described the cost that manufacturers pay to dispose of its technical scrap and is obtained by multiplicating the scrap disposal cost per unit, $Scrap\_unit_{cost}$, given in €/kg, by the scrap mass, obtained in Equation 4.33.

$$Total_{cost} = Mat_{cost} + Scrap_{cost} \tag{4.35}$$

$$Mat_{cost} = Mat\_unit_{cost} \times Mat_{Dep} \tag{4.36}$$

$$Scrap_{cost} = Scrap\_unit_{cost} \times Scrap_{mass} \tag{4.37}$$

5. Algorithm Development

5.1 Overview

The focus of the algorithm to be developed is to fully model the automated deposition process present in AFP and ATL technologies for flat laminates. In this process a robotic head deposits, ply by ply, several tape/tows of composite material at different angles of orientation. The process is repeated n times until completion, being n the number of layers or plies. This is a process with parameters that can be divided into inputs and outputs and will be described in this section. Furthermore, the input parameters can also be divided into machine constraints, part specifications like the number of plies and its orientations and also model setup variables. In addition, the outputs are divided into time, material and cost related results. The main concept of the algorithm is depicted in a high-level flowchart in Figure 5.1, which is divided into part drawing input, image processing, part manufacturing simulation, results processing, and relevant outputs.

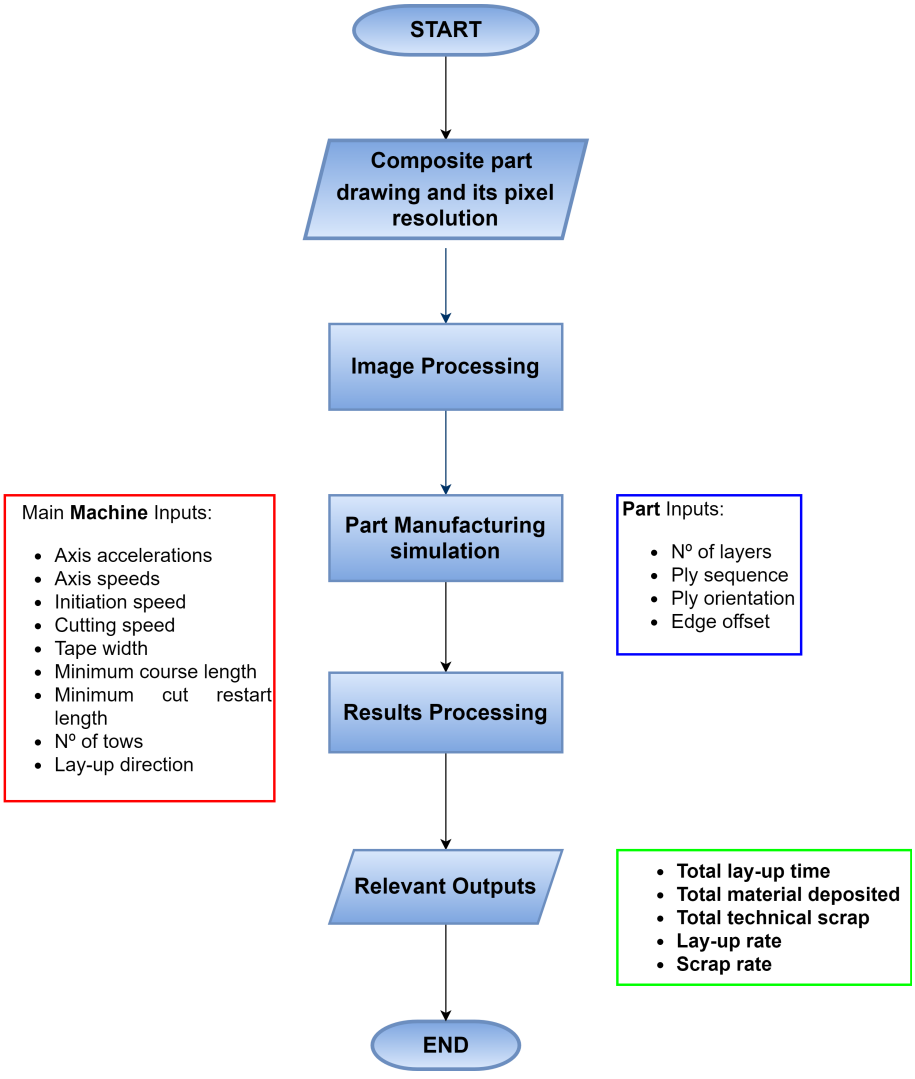

Figure 5.1: High-level algorithm description.

5.2 Model Inputs and Outputs

In this section, model inputs and outputs will be introduced and its relation succinctly explained. The inputs, as referred, can be divided into machine constraints, composite part specifications and tool setup options. The model outputs can be seen as the simulation process results.

First and foremost, a two-dimensional image of the composite part to be study should be created if not available already. This can be done with any 2D image editing software. It is important to have dimensional measurements of the part so to compare with the tool's results. The main benefit of using *Paint* software is the fact that it enables image pixel resolution customization which is crucial as the tool requires it as an input. A part offset is also industry norm, meaning an offset that is established on the part's edges in order to avoid defects in the following trimming operation, and constitutes another input if the user decides to use it in the simulation in case. An example of this feature is shown in Figure 5.2 and Figure 5.3, a simple rectangular part and an aircraft horizontal stabilizer, where the offset is seen in black.

Figure 5.2: Part image offset of 20 mm with original area of 1 m^2.

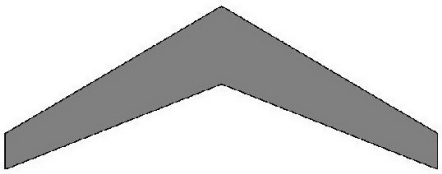

Figure 5.3: Part image offset of 20 mm with original area of 8 m^2.

Further, the plies angle orientation as well as its sequence should be determined in order to provide it as inputs. One characteristic of this model is the possibility to have different part images associated to determined plies. This could prove to be beneficial as different plies can have assigned to them different part geometries, due to, for example, specific reinforcement zones or ply specific holes. Material unit cost and areal weight, the number of parts to be produced and the unit cost of scrap disposal finalize the part input parameters. These are summarized in Table 5.1.

Table 5.1: Part input parameters.

Symbol	Description	Unit
$Part_{image}$	Composite part 2D image	-
P_{res}	Image pixel resolution	mm/pixel
P_{Offset}	Part offset	mm
N_{Plies}	Number of plies	-
Seq_{Ply}	Sequence and order of plies angle orientation	º
Mat_unit_{cost}	Material unit cost	€/kg
$Scrap\_unit_{cost}$	Scrap disposal unit cost	€/kg
$M_{aweight}$	Material areal weight	kg/m^2
N_{part}	Number of parts	-

The tool allows for some user customization as it provides additional options to the simulation. Firstly, and in order to save computational time, an option to display the lay-up was added. By selection the option *N* it was estimated that the computational time reduces by half and this value increases exponentially with the increase of image size. This is very relevant as the simulations are memory intensive due to constant image processing performed in this model. Furthermore, if the option was selected as *Y*, a second option to see the lay-up simulation be performed ply by ply is available. If the latter is not selected, the tool will show a better approximation to reality as the deposition will be shown as a ply being added on top of the previous plies. These options also enable a clearer understanding of how the tapes/tows are being placed. Figure 5.4 - Figure 5.7 show ply by ply lay-up in the four different angle orientations for ATL and Figure 5.8 - Figure 5.11 for AFP lay-up with the direction of the lay-up described.

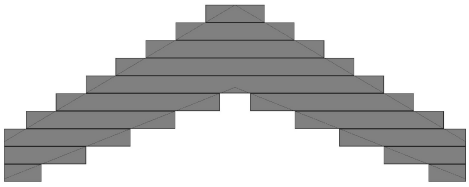

Figure 5.4: Example of ply Lay-up 0º - ATL (top to bottom).

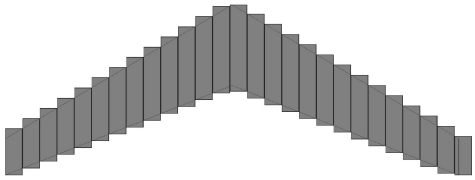

Figure 5.5: Example of ply Lay-up 90º - ATL (left to right).

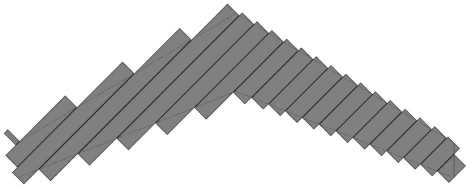

Figure 5.6: Example of ply Lay-up 45º - ATL (right to left).

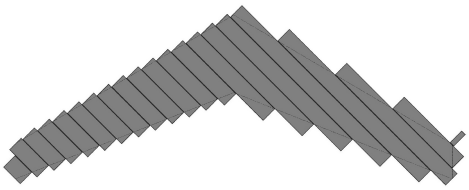

Figure 5.7: Example of ply Lay-up -45º - ATL (left to right).

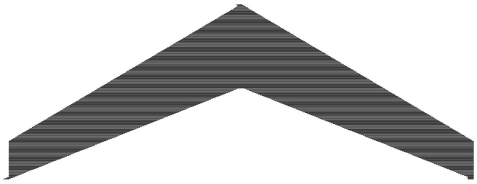

Figure 5.8: Example of ply Lay-up 0º - AFP (top to bottom).

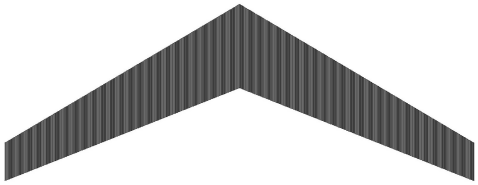

Figure 5.9: Example of ply Lay-up 90º - AFP (left to right).

A third option enables the user to see the machine toolpaths which is industry norm [103]. This enables the visualization of where the machine head will effectively pass in each course deposition. In Figure 5.12 and Figure 5.13 examples of this feature are shown for AFP and ATL technology, respectively. On the left image, the machine performed 8 lay-up courses with 32 creels and 12.7 mm tape

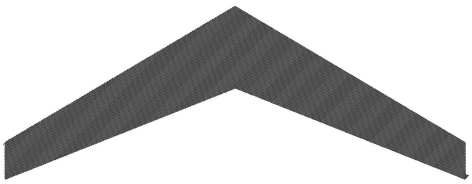

Figure 5.10: Example of ply Lay-up 45º - AFP (right to left).

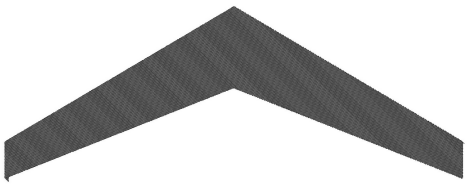

Figure 5.11: Example of ply Lay-up -45º - AFP (left to right).

width and on the right one it performed 10 courses with one creel and 304.8 mm of tape width. During the algorithm implementation some image scaling tests were performed since the simulation time was very high for small pixel resolution. The purpose was to assess if scaling up the images was effective in reducing the simulation time while maintaining the initial values fidelity. It was found that the scaling was not possible due to the area of the part not corresponding to the exact intended value as information would get lost in the scaling up process. This was particularly evident with complex part geometries. Because of that, no scaling option was introduced in the model.

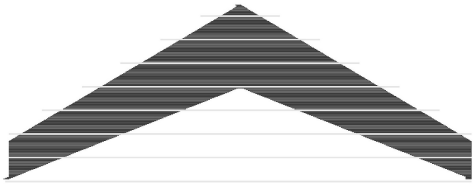

Figure 5.12: Lay-up toolpaths AFP.

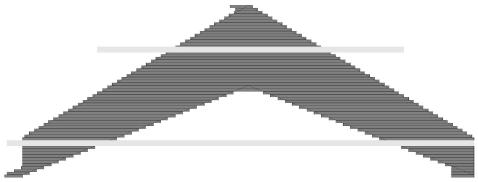

Figure 5.13: Lay-up toolpaths ATL.

As one of the proposed goals for this work, an option to find the best lay-up configuration regarding the first tape/tow is also available. This was decided to be made as an option an not imposed to all simulation as this process is very time consuming due to the high number of iterations performed. The number of iterations is also a user option and each one means a new lay-up simulation for all the plies with the first tape/tow having an offset ”away” from the part increased by one comparing to previous iteration until it reaches the number of iterations provided by the user. This offset value is a multiple of the pixel resolution, as it is the minimum value it can be represented. In addition, a tape/tow longitudinal alignment option is provided. This is related to the existence of longitudinal gaps in the direction of a course path that are misaligned. By enabling this option the machine will align with the part after the longitudinal gap at the cost of increasing lay-up time, reducing productivity but also reducing otherwise technical scrap. An example of a part lay-up ply with this kind of longitudinal gap misalignment is shown in Figure 5.14. This is the same horizontal stabilizer shown in previous images with two random longitudinal cuts. The same ply part image with the option set as a *Y* for this option is shown in Figure 5.15. It can be seen that all three separated sections have its first tape aligned with its first vertex, which in this case is the top one as the lay-up is being performed perpendicular to a top to bottom direction. On the contrary, in Figure 5.14, only the middle section has its first tape aligned. The other two areas have the tapes laid down according to the paths defined by the alignment of the first tape of the middle

section with its upper part edge. Further insights on this matter can also be consulted in section 5.3. Main simulation results are presented in MATLAB's command window but in order to save the full output information in an *excel* file an option is provided to the user for that purpose. All these inputs are summarized in Table 5.2.

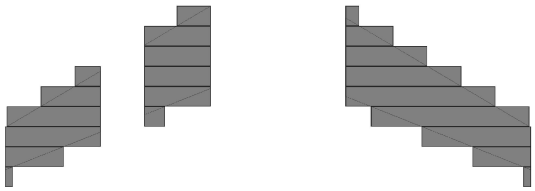

Figure 5.14: Example of ply Lay-up 0º (top to bottom) without longitudinal gap alignment.

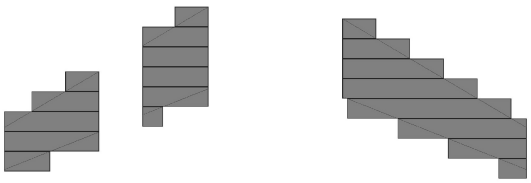

Figure 5.15: Example of ply Lay-up 0º (top to bottom) with longitudinal gap alignment.

Table 5.2: Tool setup parameters.

Symbol	Description	Unit
$Disp_{lamin}$	Show lay-up simulation	Y/N
$Ply\_by\_ply_{disp}$	Display lay-up ply by ply	Y/N
$Tool_{path}$	Show machine toolpath	Y/N
$First_{tape/tow_{opt}}$	First tape/tow optimization	Y/N
$N_{Iterations}$	Number of iterations to perform	-
$Vert_{align}$	Longitudinal lay-up alignment	Y/N
$Excel_{creator}$	Excel file creation	Y/N

Machine inputs are crucial to the development of this tool. These parameters, shown in Table 5.3, allow for the lay-up simulation of a composite part using any type of automated deposition machine which is crucial to enable comparison between systems for the same composite part production. On one hand, we have parameters regarding machine speed and acceleration constraints. These were chosen not to follow the traditional isometric system axis which represent how the system works in reality but instead acceleration was divided into the lay-up acceleration, which translates to the acceleration in the direction of the course lay-up; the acceleration for transitional movements, here, the direction is whichever is the shortest path for the machine for that transitional movement; and the vertical acceleration which, in this case, matches one of the "real" machine axis and is responsible for movements perpendicular to the lay-up plane. It is of important note to highlight that the axis acceleration for transitional movements is no more than the combination of the two axis of the machine system usually denominated as x and y. Only two axis are necessary for this case because the parts to be simulated are flat. For simplification purposes, the combination of accelerations turns into one constant value for all transitional movements. On the other hand, for speed parameters, the same logic applies, having initiation, cutting, lay-up, transitional and approaching and retracting speed to provide as inputs. The first three have already been extensively explained in previous chapters so no further explanation is needed. Approaching and retracting speed is the speed at which the machine approaches the mold from a higher standstill position,

called the approaching distance, and the retracting speed is the speed at which the machine, after a course deposition, returns to a determined height, called the retracting distance. For simplification reasons, rotational speed and acceleration are not inputs because for the approach and retraction time count, which is the only purpose of these parameters, the approach and retract speed given should account for head rotational movements and do not constitute the ”real” vertical machine axis speed.

Table 5.3: Machine input parameters.

Symbol	Description	Unit
a_{lay}	Lay-up axis acceleration	mm/s^2
a_{tr}	Transitional axis acceleration	mm/s^2
a_{vert}	Vertical axis acceleration	mm/s^2
v_{lay}	Lay-up speed	mm/s
v_{tr}	Transitional speed	mm/s
v_{init}	Initiation speed	mm/s
v_{cutt}	Cutting speed	mm/s
v_{app}	Approaching speed	mm/s
v_{ret}	Retracting speed	mm/s
d_{app}	Approaching distance	mm
d_{ret}	Retracting distance	mm
T_{width}	Tape/Tow width	mm
Min_{len}	Minimum course length	mm
Min_{cut_rest}	Minimum cut-restart length	mm
N_T	Tape/Tows number	-
$Layup_d$	Layup direction	Bi/uni directional
ATL_{phase}	ATL system feeding phase	Single/two-phase
ATL_{str_time}	ATL single-phase course starting time	s
ATL_{cutt_time}	ATL single-phase course cutting time	s
$Course_{start/finish}$	Course start and finish location	Prior & after (1)/at the part's edge (2)
$Roll_{ch\_time}$	Single roll change time	s
$Creel_{ch\_time}$	Creel change time	s
$Roll_{length}$	Single roll length	m
$Setup_{time}$	Machine setup time	h

The minimum course length and minimum cut-restart length given as inputs should be a multiple of the chosen pixel resolution in order to not ”lose” material in the mathematical conversion. For example, if a pixel resolution chosen is 4 mm/pixel and the tape width is 75 mm, translating the latter to pixels it equals 18.75 pixels. Pixels are indivisible in this tool for the purposes already explained and cannot be other number than integers. If the approach is to round it up to 19 pixels, that would translate to a bigger than 75 mm tape width used in the algorithm and the accuracy and aim of this tool would be affected. The same would happen if the rounding was to be done by default as some information would be lost. For that reason, a multiple must be provided. Furthermore, the tape or tows number to be used, which correspond to the number of creels in the machine head, and the lay-up direction (uni or bidirectional) also constitute tool inputs. The ATL feeding phase, which will enable or not the initiation and cutting course time values for ATL simulation, should also be provided as an input. As explained in chapter 4,

some machines start the course lay-up from a standstill position prior to the part's edge in order to hit initiation speed when the machine reaches it, and some have it starting in the exact coordinates of the part's edge. The same logic applies to the finishing of a course lay-up. This feature is then an input as well. 1 value must be typed for prior and after option and 2 value for at the part's edge option. For single-phase ATL machine's the machine start and finish position is by default the one which starts and finishes at the part's edges and new parameters like a course starting constant time and a course cutting time need to be added. This happens because these type of machines have specific procedures when starting and finishing each course lay-up which varies between machines but have a constant time for them. These values are then introduced as machine inputs when this type of machine is to be used. Finally, the single material roll and creel change time and the machine setup time are also inputs for the tool to function properly. System performance characteristics such as head rotation speed and acceleration are relevant for cylindrical parts but they do not carry any relevance for flat parts which are object of study in this thesis. As such, and also due to previously explained reasons, they were not included. After the simulation is performed, the results should be processed and the outputs presented. As explained earlier in the chapter, the tool will work by calculating the time spent at or reaching lay-up speed. The same works for initiation, cutting, transitional, approaching and retracting speed. Time on part and off part is then calculated. Furthermore, with the calculated rolls changing time and given setup time, the cycle time for the production of the composite part can be assessed. Regarding material outputs, the total material deposited as well as the technical scrap incurred constitute the major outputs of this section. The original area of the part as well as its area with offset is also displayed here as outputs in order to compare with the real area which is user knowledge. Following, the technical scrap percentage, the number of rolls required, which is necessary for the calculation of the rolls changing time, the total material and scrap mass along with the deposition or lay-up rate are calculated. These outputs are shown in Table 5.4 - Table 5.6.

Table 5.4: Model outputs - Time.

Symbol	Description	Unit
$Cycle_{time}$	Cycle time	h
$Layup_{time}$	Lay-up time	h
$T_{on_{part}}$	Time on part	h
$T_{off_{part}}$	Time off part	h
T_{lspeed}	Time at lay-up speed	h
T_{ispeed}	Time at initiation speed	h
T_{cspeed}	Time at cutting speed	h
T_{trans}	Time at tr. speed	h
T_{trans_h}	Time at tr. speed - Horz. gaps	h
T_{trans_v}	Time at tr. speed - Long. gaps	h
T_{trans_t}	Time at tr. speed - Tape/tow	h
T_{trans_p}	Time at tr. speed - Ply to Ply	h
$T_{app/ret}$	Time at appr./retr. speed	h
$T_{c_{rolls}}$	Rolls changing time	h
T_{sim}	Simulation time	h

Table 5.5: Model outputs - Costs.

Symbol	Description	Unit
$Scrap_{cost}$	Tech. scrap disposal cost	€
Mat_{cost}	Material cost	€
$Total_{cost}$	Total material costs	€

Table 5.6: Model outputs - Material.

Symbol	Description	Unit
$A_{original}$	Part's original area	m^2
A_{offset}	Part's area with offset	m^2
$P_{original}$	Part's original perimeter	m
P_{offset}	Part's perimeter with offset	m
Mat_{dep}	Material deposited	m^2
$Tech_{scrap}$	Technical scrap deposited	m^2
$\%_{scrap}$	Technical scrap percentage	%
$Mass_{dep}$	Total Mass deposited	kg
$Mass_{scrap}$	Technical scrap mass	kg
N_{rreq}	Nº of rolls required	-
$Layup_{rate}$	Lay-up rate	kg/h
Fig_{dep}	Figure(s) with material deposited	-
$Fig_{dep\_per\_creel}$	Figure with distribution of material deposited per creel	-

The changing rolls process was modelled to be done in simultaneous for all creels in the case of AFP technology as for ATL it is usually only one creel being used. In addition, the tool will save a figure of the lay-up simulation, either ply by ply or the "real" deposition process, depending on the user selected option. Furthermore, a figure of the material deposited per creel or tow number is also obtained. This last figure will provide insight on which creel is most utilized and will help further planning and strategy. Finally, costs for technical scrap disposal and material deposited will be calculated. The second value has the total material deposited included, meaning effective part material and technical scrap. Finally, there is the total cost which is the sum of the previous two parameters. There is also a cost related to the electricity spent by these machines while performing the lay-up but it cannot be calculated without a thorough study of the machine to be used. As such, it is not object of study in this work. Time on part, off part, material deposited and scrap percentage are also presented by ply values. The side in which each ply starts, the total laid courses, the total number of tape/tows and the length of each of those tape/tows are also presented for each ply. This information can be useful if a certain ply or a certain course within a ply requires more detailed attention. Further insights on script structure is shown in Appendix A.

5.3 First tape offset study for Technical Scrap reduction

In this section, the process behind the choice for a lay-up path that enables technical scrap reduction is explained. It is typical in the aerospace industry to manufacture a part with a certain lay-up configuration and tape width that is decided in its design phase. The lay-up paths are then iterated through the production of multiples of that part. In the meantime, a lot of technical scrap is overly produced because, although current software enables the simulation of any kind of lay-up paths and give the optimum path for a time and material saving perspective, it does not in one "take" calculate the lay-up configuration from a perspective of where to place the initial tape/tow. As explained, one of the intents of this thesis is to discover if the adjustment of the first tape/tow has a significant impact in scrap reduction. This process

can, however, be manually performed by the machine technician using his experience and know-how by trial and error which could be very inefficient. It was decided to perform this study solely for ATL systems since for AFP, with the small tow width, the effect of offsetting the first tow of each ply would have negligent effect on scrap saving. However, for ATL which uses tape widths up to 304.8 mm the study could potentially have more impact.

To implement this study in the algorithm some changes had to be made. First, a new loop enclosing the previous two loops was created in order to perform iterations. After a first iteration is performed, meaning the run of both previous cycles, denominated ***iteration_index_0***, where the tool runs its full main script, all the outputs related to the standard lay-up configuration path regarding the first tape placement of each ply are stored in the excel file. By standard it is understood as the first tape placement having its left edge aligned with the part's left edge. As explained, the algorithm is set to read the image from left to right at all times, being this the reason the left edge is discussed and not right or bottom/top. For a second iteration and so forth, until the last iteration number is reached, which is user defined, the tool will perform a whole new lay-up part simulation having the first tape offset the left edge of the part by x value. This x value would be a multiple of the pixel resolution, which is the minimum distance that can be represented in the image for that situation. For example, for the second iteration, read in the algorithm as ***iteration_index_1***, would have the offset be 1, which is the iteration index number, times the pixel resolution, in millimeters. The logic will then follow this example for the next iterations.

The material deposited in each ply is then stored in a matrix for each offset increment. When all iterations are performed, the tool will access that matrix and select the ideal first tape offset for each ply, regarding technical scrap reductions. A final simulation is then performed with the optimal first tape lay-up offset paths. The value obtained for the total material deposited is then saved and compared to the standard one to calculate material cost savings. If a part has a discontinued horizontal or longitudinal gap, (meaning a gap between two not connected lay-up areas of a ply) multiple iterations have to be performed for that ply in order to evaluate the effect of each first tape offset for each non connected lay-up section. The material cost saving effect for parts with plies like those potentially increases. Results for this study are presented in section 6.4.

6. Results and discussion

6.1 Overview

In this section, the tool will be validated at a first stage with empirical and theoretical models. Then, it will be used to assess cycle time and material costs as well as lay-up rates for four different aeronautical composite parts: a wing flap, a vertical and horizontal stabilizer and finally, a wing skin. Furthermore, the study related to first tape offset will be presented along with its results on technical scrap reduction.

6.2 Validation

6.2.1 Embraer's specimen test

In order to validate this model and evaluate its performance, comparison with experimental and published data was conducted. The first comparison consists of an Embraer's specimen test which is a machine check-up test to assess if everything is working properly to perform the lay-up of the company's composite parts. The data was collected *in situ* through the machine's software during my internship at Embraer's facilities in Évora. I was able to see the lay-up process of the part here studied and watch how it performed. The composite part characteristics are as specified in Table 6.1 and machine inputs in Table 6.2. Parameters like the time off part, which includes all transitional parameters and approach and retract time, also setup time and time to change rolls were not provided to me as, at the time, they were not yet relevant to the model. Only inputs and outputs which are required for the validation of the results provided are then referred. Figure 6.1 illustrates the part's geometry.

Table 6.1: Embraer's composite part data.

Parameter	Value	Unit
$Part_{image}$	Figure 6.1	-
N_{Plies}	24	-
Seq_{Ply}	[45, 0, -45, 90] x 3, sym.	º
$M_{aweight}$	0.296	kg/m^2

Table 6.2: Embraer's machine data.

Parameter	Value	Unit
a_{lay}	315	m/s^2
v_{lay}	416.67	mm/s
v_{init}	300	mm/s
v_{cutt}	283.33	mm/s
v_{app}	83.33	mm/s
v_{ret}	166.67	mm/s
T_{width}	6.35	mm
Min_{len}	101.6	mm
Min_{cut_rest}	101.6	mm
N_T	16	-
$Layup_d$	Uni directional	-
M_{Offset}	20	mm
$Course_{start/finish}$	At part's edge	-

This part had a particular geometry for the lay-up of plies at 45 and -45º angles. A type of "ears" was added at the top left and bottom right corners with 25x75 mm dimensions. Its lay-up was needed in

order to use it as a pickup zone to remove the part from the mold without touching the effective laminated area. Consequently, for the lay-up of those plies the part to use is depicted on Figure 6.2. For the other plies, at 0º and 90º angles the part image to use is the one of Figure 6.1. Here, the tool's capability discussed in the previous chapter of being able to lay-up different part geometries in different plies has achieved its purpose.

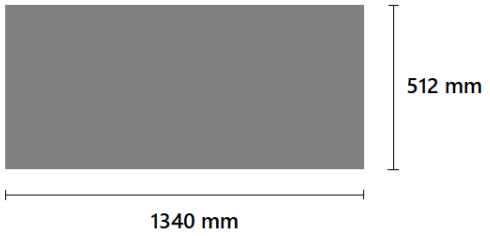

Figure 6.1: Embraer's specimen geometry for lay-up at 0º and 90º plies.

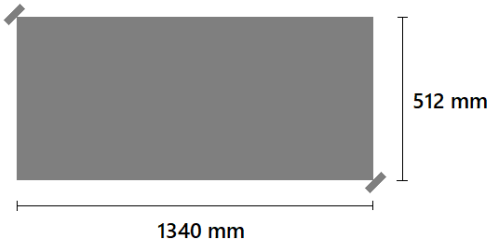

Figure 6.2: Embraer's specimen geometry for lay-up at 45º and -45º plies.

Three conclusions can be reached when analyzing Table 6.3. For one, the tool is assessing geometries correctly since the difference between the part area and $A_{original}$ calculated by the model is the same. Here, the original part area can be split in the area for the two images. One without and one with the 45º and -45º angles plies with the area of the "ears" included. Areas with offset are also very similar, with the difference of 0.39% only for the 45/-45º plies, which shows the tool's ability of resizing an image to the right amount, to deliver an offset, was accomplished. Then, the difference between actual material deposited and Mat_{dep} is practically null, 0.21% to be precise, which indicates that the algorithm developed to simulate the lay-up is very close to reality. This means that machine input constraints, part specifications and tape/tow allocation are correctly affecting the tool's outcome. Possible algorithm faults are being covered due to the simplicity of the part being studied. Because of this, more complex geometries were studied and presented in the next section. The third conclusion is that the time on part necessary to complete one full lay-up is almost exactly the same as the calculated $T_{on_{part}}$ with 0.41% difference, although there is a slight difference on the part areas. This variable only takes into account the time the machine is effectively laying tape/tow and doesn't account for other times such as the time for the machine to start another ply deposition and transition through each course (transitional time), or the time it takes to approach and retract. As such, the lay-up rate shown in Table 6.3 also does not take these parameters into account. Because of this, the rate of deposition was set on approximately 23 kg/h which is about double the value for normal lay-up rates for this machine's configuration. The other outputs, $Mass_{dep}$, $Tech_{scrap}$ and $\%_{scrap}$ are a consequence of the previous discussed outputs. The small percentage differences for all outputs, with the highest being 0.71% for the lay-up rate, indicates a successful tool development for the parameters tested. A more complex geometry will provide a harder test to this tool and other parameters such as the time off part which includes all transitional times as well as approach and retract time and the time to change tape/tow rolls still need to be validated. Nonetheless, the primary structure for a successful tool is now attained.

Table 6.3: Embraer's specimen validation data.

Parameter	Embraer's Data	Model output	Unit	Difference
$A_{original_{0°\_90°}}$	0.686	0.686	m^2	-
$A_{original_{45°\_-45°}}$	0.690	0.690	m^2	-
$A_{offset_{0°\_90°}}$	0.762	0.762	m^2	-
$A_{offset_{45°\_-45°}}$	0.766	0.769	m^2	0.39%
Mat_{dep}	18.547	18.586	m^2	0.21%
$Mass_{dep}$	5.491	5.502	kg	0.20%
$Tech_{scrap}$	2.082	2.077	m^2	0.24%
$\%_{scrap}$	11.226	11.175	%	-
$T_{on_{part}}$	0.244	0.243	h	0.41%
$Layup_{rate}$	22.504	22.664	kg/h	0.71%

6.2.2 Soares et al horizontal stabilizer

The next part to be analyzed was the horizontal stabilizer present in Soares et al. [104]. The purpose of this comparison was to validate the model with more complex geometries. The geometry and its measures are shown in Figure 6.3.

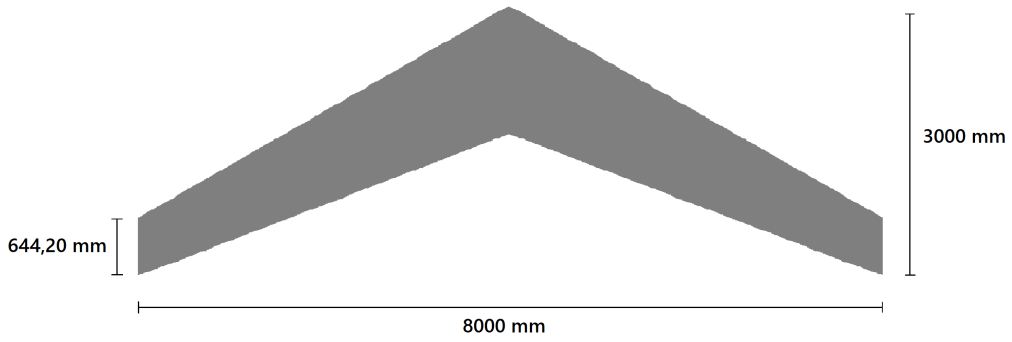

Figure 6.3: Horizontal Stabilizer part geometry [104].

Table 6.4 and Table 6.5 contain the data used as reference for comparison. This information was also obtained from the referred article as tape width used, minimal course length, number of tows, uni directional lay-up and offset are all in accordance.

Table 6.4: Horizontal stabilizer part input parameters [104].

Parameter	Description	Unit
$Part_{image}$	Figure 6.3	-
N_{Plies}	40	-
Seq_{Ply}	[0, 90, 45, -45] x 5, sym.	º
$M_{aweight}$	0.3	kg/m^2

Table 6.5: Horizontal stabilizer machine input parameters [104].

Parameter	Description		Unit
	AFP	ATL	
T_{width}	12.7	300	mm
Min_{len}	100	100	mm
Min_{cut_rest}	100	100	mm
N_T	24	1	-
M_{Offset}	0	0	mm

The ply sequence, number of plies and material areal weight are also given in [104]. In the article both technologies are assessed and, as such, both technologies will also be compared using the model developed here. Time related outputs will not be compared here because there is no reference to the speeds and accelerations used as inputs in the referred paper. By comparing values from the article and the results from the tool it can be seen that, again, and now with a more complex geometry the correct reading of the part boundaries and consequent lay-up is being done properly since the difference between material deposited is less than 1.76% in all four ply orientations in both technologies. The results of this geometric comparison are shown in Table 6.6. The technical scrap in AFP technology presents a larger difference between tool results and the data from the article, being that difference around 35%. This happens because the values are very small and a difference between small values results in a high difference percentage. Nonetheless, it represents no major error in the tool's algorithm and therefore it has minor relevance. All other parameters have a very good accordance to the data from the Soares et al. [104] since there is no higher difference than 1.76% for both technologies.

Table 6.6: Horizontal stabilizer validation - ATL vs AFP.

Parameter	**[104] - ATL**	**Model - ATL**	**Dif.**	**[104] - AFP**	**Model - AFP**	**Dif.**	**Unit**
$A_{original}$	8.26	8.266	0.07%	8.26	8.266	0.07%	m^2
Mat. at 0º	10.6	10.63	0.28%	8.37	8.349	0.25%	m^2
Mat. at 90º	9.43	9.596	1.76%	8.31	8.304	0.07%	m^2
Mat. at 45º	10.06	10.056	0.04%	8.37	8.332	0.45%	m^2
Mat. at -45º	10.06	10.056	0.04%	8.37	8.332	0.45%	m^2
Mat_{dep}	401.39	404	0.65%	334.19	333.18	0.30%	m^2
$Mass_{dep}$	120.42	120.59	0.14%	100.25	99.95	0.3%	kg
$Tech_{scrap}$	71.04	71.34	0.42%	3.84	2.52	35.38%	m^2
$\%_{scrap}$	17.7	17.746	-	1.15	0.757	-	%

6.2.3 Lukaszewicz's model

Lukaszewicz's test part was crucial to the validation of this model since it provides scientific background to this thesis once the comparison is validated. The part used for the comparison was a simple rectangular piece, similar to the one used in Embraer but larger in size. This study was part of his doctoral thesis in [83]. One of the purposes of his research was to develop and accurate way to calculate the lay-up time and scrap rates of a simple composite part in relation to their aspect ratio and part size as to establish a productivity benchmark for AFP and ATL technologies. In the document, a model was also developed through some simple equations. Furthermore, parametric studies were done in his work based on extrapolations from this one initial study. In Figure 6.4, the composite part characteristics are displayed. The machine used as base for the benchmark comparison was the MTorres TORRESLAY machine because it was the one used at Airbus which was an associate of the thesis discussed here. Part material areal weight, number and plies sequence is displayed in Table 6.7. Technical data for that MTorres system is shown in Table 6.8 as per [83].

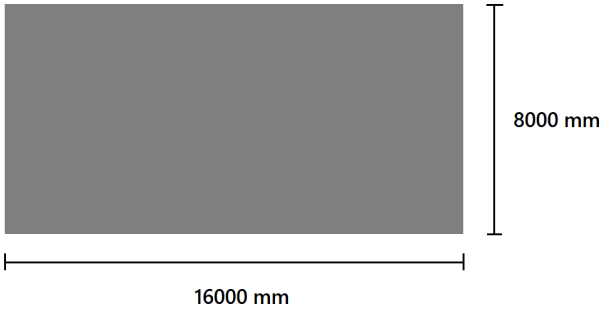

Figure 6.4: Lukaszewicz's part geometry [83].

Table 6.7: Lukaszewicz's part data [83].

Parameter	Value	Unit
$Part_{image}$	Figure 6.4	-
N_{Plies}	8	-
Seq_{Ply}	[0, 45, 90, -45], sym.	º
M_{a_weight}	0.412	kg/m^2

Table 6.8: Lukaszewicz's machine data [83].

Parameter	Description		Unit
	AFP	ATL	
a_{lay}	2000	500	mm/s^2
v_{lay}	1000	1000	mm/s
T_{width}	6.35	302.4	mm
Min_{len}	50	100	mm
N_T	32	1	-
Cutting ply time	0	6	s
Start laying shoe time	5	5	s
$Roll_{ch\_time}$	300	300	s
$Creel_{ch\_time}$	15	-	s

The machine used for this benchmarking had a specific procedure applied at the finish of each tape course during ATL lay-up. After a tape course has been laid, the machine head advances to a position outside the part and deposits a sequence with minimal course length. The reason for this step was unclear to Lukaszewicz but is one of the possibilities for scrap lay-up described in subsection 2.3.2. Also, the time for starting and stopping the ply using a laying shoe and the time for cutting the tape were added to the results presented in the document. For AFP lay-up, only the time for starting a course was added (although the time to start a ply being described as 0 s for AFP lay-up), as the time for deceleration was included in the lay-up time. For comparison purposes, the time for starting a ply with laying shoe, the time for stopping a ply course, the time for cutting a ply and the time for removing scrap had to be subtracted from Lukaszewicz's results for ATL in order to make a viable comparison. As these are constant values, there was no need to compare them. What it matters for comparison purposes are the values for $T_{on_{part}}$ of ATL lay-up which illustrate the lay-up time in itself. For AFP, the time for starting a ply is the only parameter to be removed for the same reasons explained for ATL technology.

Both technologies are said to have the machine starting from an idle position on the exact starting point of the part's edge. This is of important notice as to have the value 2 for the input $Course_{start/finish}$ for the tool developed in the AFP comparison, as explained in section 5.2. In this situation, the ATL system feeding phase is single-phase, evidence of that is the parameters already referred here as the

time to start a laying shoe. However, it is said in the document that the ATL machine also starts from the exact part's edge which should not happen because the time to start and stop a laying shoe should 'consume' a part of the course's length and that is not the case for the study referenced. As such, for comparison purposes, as said, those values have to be removed from the results shown in the document and the course is assessed as starting and finishing at the part's edges. This means that the comparison, although Lukaszewicz's ATL data is for a single-phase feeding system, will be performed as the machine being a two-phase system due to the fact that the single-phase system is modelled in tool as its initiation and cutting operations 'consuming' parts of the course length, which is not the case here. As such, ATL two-phase was selected because it starts exactly at the part's edges. The time taken for secondary operations, such as the time for roll change in ATL lay-up, or creel changes in AFP lay-up, is also added to the total time in the document. The rolls length is considered to be 240 m which a value referenced in Soares et al. [104] article as Lukaszewicz [83] has no value referenced for that parameter.

The methodology for having a logical comparison and further validation between the results of the tool and the results from Lukaszewicz [83], depicted in Table 6.9 and Table 6.10, is explained in the following paragraphs.

Table 6.9: Lukaszewicz's time results [83].

Ply Orientation	ATL	AFP	unit
0º	3785	1720	s
90º	6581	2133	s
45º	7157	2128	s
-45º	7157	2128	s
Totals	24680	8109	s
$T_{c_{rolls}}$	4418	16346	s
$Layup_{time}$	29098	24455	s

Table 6.10: Lukaszewicz's material results [83].

Parameter	ATL	AFP	unit
$A_{original}$	128	128	m^2
$Mass_{dep}$	441	427.5	kg
Mat_{dep}	1070.39	1037.62	m^2
$\%_{scrap}$	4.5	1.3	%
$Tech_{scrap}$	48.168	13.489	m^2
$Mass_{scrap}$	19.845	5.558	kg
$Layup_{rate}$	54.4	62.4	kg/h

ATL lay-up validation

To start, 0º ply orientation results were analyzed. As cited in Lukaszewicz [83] the lay-up time for one single tape course including acceleration and deceleration is 18 seconds and the total number of tapes laid for one single ply is 27. There are 2 plies with 0º angle orientation so the total lay-up time for 0º angle orientation is given by Equation 6.1.

$$Layup_{time\_0} = (18 \times 27) \times 2 \quad \Leftrightarrow \quad Layup_{time\_0} = 972\,s \tag{6.1}$$

This is the value used to compare with the output from the model developed here. In contrast, the total time for 0º angle ply orientation according to, Table 6.10, is 3785 seconds. Then, the time to start a tape course, the time to stop it, the time to cut the tape and finally the time to remove scrap should be added to the value obtained in Equation 6.1. The corresponding values for them are, as referenced in [83], 5 seconds, for the time to stop the course there is no reference on the document so it was assumed

as 3.59 s, explained in Equation 6.2, 6 seconds and 37.5 seconds, correspondingly.

$$(N_{Courses} \times n_{Plies})(Tape_{Layup\_time\_0} + time_{start} + time_{stop} + time_{cutting} + time_{scrap}) = 3785\,s \quad (6.2)$$

$$\Leftrightarrow \quad (27 \times 2)(18 + 5 + time_{stop} + 6 + 37.5) = 3785\,s \quad \Leftrightarrow \quad time_{stop} = 3.59\,s$$

The same methodology was applied to the other three orientations and the value for a single tape course for each of them was extrapolated since it is not given in the document. The total number of tape courses per orientation was obtained by dividing the total perpendicular length of the part relating to the machine lay-up direction (obtained by the tool) by the tape width, or 304.8 mm. For 0º angle orientation plies, the total number of courses laid by the machine is 27, 53 for 90º angle plies and 57 for 45º and -45º angle orientation plies. The lay-up times per ply are then obtained as shown in Equation 6.3 - Equation 6.6. The values of the lay-up course time for 45º and -45º angle plies are give as an average value because the course lengths varies within the lay-up. Contrary to that, the course lengths do not vary for 0º and 90º angle plies and the values given are not an average but a constant.

90º degree Plies:

$$(53 \times 2)(Tape_{Layup\_time\_90} + 5 + 3.59 + 6 + 37.5) = 6581\,s \quad \Leftrightarrow \quad Tape_{Layup\_time\_90} = 9.991\,s \quad (6.3)$$

$$Layup_{time\_90} = 9.991 \times 53 \times 2 = 1059.05\,s \quad (6.4)$$

45º/-45º degree Plies:

$$(57 \times 2)(Avg_{Tape_{Layup\_time\_45}} + 5 + 3.59 + 6 + 37.5) = 7157\,s \quad (6.5)$$

$$\Leftrightarrow \quad Avg_{Tape_{Layup\_time\_45}} = 10.69\,s$$

$$Avg_{Layup_{time\_45}} = 10.69 \times 57 \times 2 = 1218.66\,s \quad (6.6)$$

Having the values of a single tape course deposition time for each angle orientation it is then possible to calculate the total time on part as the sum of all plies lay-up time, seen in Equation 6.7.

$$T_{on_{part}} = 972 + 1059.05 + 2 \times 1218.66 = 4425.5\,s = 1.241\,h \quad (6.7)$$

The time off part will not be compared between the two models since there is no data for reference in [83]. The closest parameter that could be taken as time off part would be the time for removing scrap. However, in the model developed here, the time off part corresponds to the sum of the transitional time and the approach/retract time and does not foresee a parameter of time for laying scrap, as technical

scrap is modelled to always be laid in a continuous form in each course deposition at the part's boundaries. Because of this, the comparison is not viable for this parameter and therefore it could not be validated. However, if other time related parameters are validated there is a strong basis to claim that this parameter could be validated as well since the equations which they are all based on (see chapter 3) have the same supporting logic. The total lay-up time consists only of the time on part for this example. Finally, the cycle time for this study will then be the lay-up time plus the time for changing tape rolls. The total cycle time presented in Table 6.9 for ATL is 29098 seconds. The time for changing rolls is already provided by the paper being the difference between the total cycle time and the lay-up time, shown in Equation 6.8.

$$29098 - 24680 = 1.227\,h \tag{6.8}$$

Furthermore, the quantity of material laid in the scrap lay-up procedure needs to be assessed in order for the comparison to work. For that purpose, the total number of courses laid also needs to be calculated. As cited in [83], the scrap laid has a length equal to the minimal course length. Equation 6.9 and Equation 6.10 illustrate the calculations.

$$(27 + 53 + 57 + 57) \times 2 = 388 \;\; tape\,courses \tag{6.9}$$

$$388 \times (0.1 \times 0.3024) = 11.73\,m^2 \tag{6.10}$$

The scrap lay-up procedure adds 11.73 m^2 of material that is not foreseen by the model developed here. Because of this, this value needs to be subtracted from the total mass deposited referred in the document, seen in Equation 6.11. New values are then obtained for Mat_{dep} using Equation 6.12 and $Tech_{scrap}$ using Equation 6.13. The lay-up rate, obtained for comparison purposes, will just be the total material deposited divided by the time on part plus the time to change tape rolls, seen in Equation 6.14.

$$441 - 11.73 \times 0.412 = 436.17\,kg \tag{6.11}$$

$$1070.39 - 11.73 = 1058.67\,m^2 \tag{6.12}$$

$$48.168 - 11.73 = 36.438\,m^2 \tag{6.13}$$

$$436.17/2.468 \; = 176.71\,kg/h \tag{6.14}$$

Comparison between the model results and Lukaszewicz's extrapolated values in previous paragraphs is shown in Table 6.11 below. By analyzing the table a conclusion could be reached about the comparison. Most data had a good agreement with differences up to 4-5% with the exception of the time on part at 45º and -45º plies and the technical scrap.

The first difference, after thorough examination of the algorithm developed, can be attributed to the simplicity of the numerical model developed by Lukaszewicz. For 0º and 90º plies there is almost identical lay-up time for both models but for 45º and -45º angles there is not. This can be due to the higher complexity on calculating course distances at those angles, especially for corner distances, with the equations developed in [83], that although work for 0º and 90º (simpler course geometries), might not work for more complex path geometries, said 45º and -45º angle plies. The 9.47% difference in time on part for these plies and the consequent 5% difference in the global time on part is thus a result of the previously explained.

The value obtained for the time to change tape rolls in Lukaszewicz [83] was 1.227 h which is near 1.25 h. The latter corresponds to the time to change 15 tape rolls as each change requires 300 s. The difference of 4.89% between models, which corresponds exactly to 300 s, or the time to change one roll, is most likely related to the logic behind this parameter calculation. In the tool developed in this thesis, the time to change tape rolls always assumes there is already one roll set for the machine to use. As such, the calculation of the time to change tape rolls always considers one less roll from the total required. That can be the justification for this difference. The other option is that the roll length is different from 240 m as a difference of 10 m in length would bump up the rolls required to 16 and then the time to change tape rolls, seen in Table 6.9, would be in accordance to the logic used in this thesis as the difference would be null.

Table 6.11: Lukaszewicz's ATL validation.

Parameter	Lukaszweciz's Data [83]	Model output	Unit	Difference
$Time_{on\_part}$	1.241	1.179	h	5%
$A_{original}$	128	127.98	m^2	0.02%
$Time_{on\_part}$ - 0º	972	972.36	s	0.04%
$Time_{on\_part}$ - 90º	1059.05	1060.32	s	0.12%
$Time_{on\_part}$ - 45º/-45º	1218.66	1103.28	s	9.47%
Mat_{dep}	1058.67	1049.88	m^2	0.83%
$Mass_{dep}$	436.17	432.55	kg	0.83%
$Tech_{scrap}$	36.438	26.077	m^2	28.43%
$\%_{scrap}$	3.44	2.48	%	-
$T_{c_{rolls}}$	1.227	1.167	h	4.89%
N_{rreq}	15	15	-	-
$Layup_{rate}$	176.71	184.38	kg/h	4.34%

The second and biggest difference between these two models is in the technical scrap value, with 28.43%. This could be related to the use of an offset on the part geometry that was not referenced in the document. To verify this hypothesis a simulation was done adding 20 mm offset to the part in question. The new calculations are shown in equations Equation 6.15 - Equation 6.20. The total number of courses for 90º angles plies changed from 53 to 54 with the inclusion of the 20 mm edge offset. This means that there are 2 more total tape courses and therefore there is more material deposited as scrap.

$$(27 + 54 + 57 + 57) \times 2 = 390 \ \ tape\, courses \tag{6.15}$$

$$390 \times (0.1 \times 0.3024) = 11.79\,m^2 \tag{6.16}$$

$$441 - 11.79 \times 0.412 = 436.14\,kg \tag{6.17}$$

$$1070.39 - 11.79 = 1058.6\,m^2 \tag{6.18}$$

$$48.168 - 11.79 = 36.378\,m^2 \tag{6.19}$$

Finally, the new lay-up for comparison basis would compute:

$$436.14/2.468\ = 176.72\,kg/h \tag{6.20}$$

The results, shown in Table 6.12, reveal that adding 20 mm of part offset translates into a better comparison between models as the technical scrap difference reduces from 28.43% to less than 1.6%. Moreover, material and mass deposited difference both reduce from 0.83% to 0.2% which indicates the strong possibility of the inclusion of this part offset reflected on Lukaszewicz's lay-up results. Having conducted several comparisons, ATL technology simulation performed by the tool developed in this thesis can then be safely validated.

Table 6.12: Lukaszewicz's ATL validation with 20 mm part offset.

Parameter	Lukaszewicz's Data [83]	Model output	Unit	Difference
$Time_{on\_part}$	1.241	1.189	h	4.19%
$A_{original}$	128	127.98	m^2	0.02%
A_{with_offset}	128.96	128.99	m^2	0.02%
$Time_{on\_part}$ - 0º	972	974.04	s	0.21%
$Time_{on\_part}$ - 90º	1059.05	1083.96	s	2.35%
$Time_{on\_part}$ - 45º/-45º	1218.66	1110.48	s	8.88%
Mat_{dep}	1058.6	1060.75	m^2	0.20%
$Mass_{dep}$	436.14	437.03	kg	0.20%
$Tech_{scrap}$	36.378	36.943	m^2	1.55%
$\%_{scrap}$	3.44	3.48	%	-
$T_{c_{rolls}}$	1.227	1.167	h	4.89%
N_{rreq}	15	15	-	-
$Layup_{rate}$	176.72	185.50	kg/h	4.97%

AFP lay-up validation

For AFP technology the same validation methodology was applied with the difference being the non-inclusion of the time to cut a ply, the time to stop the laying shoe and the time for laying scrap, present in Table 6.8, since the machine in cause does not apply the same specific procedure as the previously discussed ATL system.

Primarily, the average time for each course laid must be obtained for each ply orientation as well. The value for 0º ply orientation is given in the document as 16.5 seconds. Knowing the total courses per ply orientation, obtained by the tool, it is possible to calculate the required values. For 0º angle orientation plies, the total number of courses laid by the machine is 40, for 90º is 79 and for 45º and -45º is 84. The calculations are illustrated in equations Equation 6.21 - Equation 6.28.

$$(N_{Courses} \times n_{Plies})(Tape_{Layup\_time\_0} + time_{start}) = 1720\,s \quad \Leftrightarrow \quad (40 \times 2)(16.5 + 5) = 1720\,s \tag{6.21}$$

$$Layup_{time\_0} = 16.5 \times 40 \times 2 \quad \Leftrightarrow \quad Layup_{time\_0} = 1320\,s \tag{6.22}$$

$$(79 \times 2)((Tape_{Layup\_time\_90} + 5) = 2133\,s \quad \Leftrightarrow \quad Tape_{Layup\_time\_90} = 8.5\,s \tag{6.23}$$

$$Layup_{time\_90} = 8.5 \times 79 \times 2 \quad \Leftrightarrow \quad Layup_{time\_90} = 1343\,s \tag{6.24}$$

$$(84 \times 2)(Avg_{Tape_{Layup\_time\_45}} + 5) = 2128\,s \quad \Leftrightarrow \quad Avg_{Tape_{Layup\_time\_45}} = 7.67\,s \tag{6.25}$$

$$Layup_{time\_45} = 7.67 \times 84 \times 2 \quad \Leftrightarrow \quad Layup_{time\_45} = 1288.56\,s \tag{6.26}$$

Having obtained the average values for a single tape course deposition for each angle orientation, it is now possible to calculate the total time on part for AFP technology:

$$1320 + 1343 + 2 \times 1288.56 = 1.455\,h \tag{6.27}$$

Finally, the cycle time for this study will then be the lay-up time, which for the interest of this study consists only of the time on part for the reasons already explained, plus the time for changing tow rolls and subsequent bobbin of the creels. The total cycle time, presented in Table 6.9 for AFP, is 24455 seconds which equals 6.79 hours. The time for changing tow rolls and creels adjustment is the difference between the total cycle time and the lay-up time:

$$24455 - 8109 = 4.54\,h \tag{6.28}$$

The comparison results is presented in the Table 6.13. It can be seen that, overall, the difference between parameters is not higher than 4% except for the same values already discussed for ATL technology comparison, the time on part for 45º and -45º angles plies and the technical scrap. The values for these differences are 7.05% for both plies and 90.34% for the latter. The difference in the time on part parameter for these plies has, most likely, the same explanation given for ATL lay-up, which is that the simple equations developed in [83], could not accurately calculate these values as they could for 0º

and 90º angles plies. It is with confidence that this affirmation is made since the tool developed here, by almost exactly calculating the same values as Lukaszewicz's for 0º and 90º plies, which were thoroughly verified, must also correctly calculate the values for 45 and -45º angle plies, since the calculation method is the same for all plies and the referential used for its calculations is always aligned with the direction of the lay-up. In contrast, Lukaszewicz's time data calculations for 45 and -45º angle plies are done utilizing a referential with its axis aligned with the other two angle plies which probably induces the reported error difference. Another assurance that the tool is behaving according to expectations is the correct calculation of the size of the longest course of 45º and -45º angle plies which is as described in [83] as 11.62 m for ATL and 11.32 m (11.37 m in the tool) for AFP. The latter difference is justified because Lukaszewicz does not take into account the extra crenulation of AFP course length and does for ATL, which essentially corresponds to adding the value of the tape width to each course length. Another evidence that Lukaszewicz's values for 45º and -45º angle plies might be in fault is the slight increase in time on part from ATL to AFP, since the ATL machine performs 57 courses and the AFP machine performs 84. Although AFP machine has an acceleration about four times higher, the 27 extra courses performed in AFP should justify a much higher increase in time on part than the 5.74% registered.

Regarding the number of rolls required, the results are 681 rolls for Lukaszewicz's AFP lay-up, which was extrapolated here from the total material deposited and using a value of 240 m per roll. For the tool, the result was 684 rolls. The difference in the time to change rolls operation of about 0.22%, or 0.01 h, can be translated to the 15 seconds it takes for the creel change of the three rolls required which differ between both studies.

Table 6.13: Lukaszewicz's AFP validation.

Parameter	Lukaszewicz's Data [83]	Model output	Unit	Difference
$Time_{on\_part}$	1.455	1.506	h	3.51%
$A_{original}$	128	128.01	m^2	0.01%
$Time_{on\_part}$ - 0º	1320	1319.64	s	0.03%
$Time_{on\_part}$ - 90º	1343	1342.56	s	0.03%
$Time_{on\_part}$ - 45º/-45º	1288.56	1379.4	s	7.05%
Mat_{dep}	1037.62	1025.36	m^2	1.18%
$Mass_{dep}$	427.5	422.45	kg	1.18%
$Tech_{scrap}$	13.49	1.303	m^2	90.34%
$\%_{scrap}$	1.3	0.127	%	-
$T_{c_{rolls}}$	4.54	4.55	h	0.22%
N_{rreq}	681	684	-	0.44%
$Layup_{rate}$	71.31	69.78	kg/h	2.15%

Of important reference is that, for the case of AFP technology, in contrast to ATL, some machine creels might deposit more material than others because of the uneven material lay down. The value obtained in the tool has that taken into account but the value obtained for Lukaszewicz's AFP lay-up was obtained by dividing the total material deposited in an even manner between all creels. This could justify that difference. Nonetheless, this small difference still allows the validation of the time to change rolls operation for AFP assuming each roll length was actually 240 m, which is not referred in the document.

This, of course, assuming the logic for calculating the tow rolls is in accordance to this thesis, already discussed for the changing tape rolls operation of ATL technology. The very high difference in technical scrap is probably justified again by the utilization of an offset which is not referred in document.

Another simulation was therefore performed with the inclusion of a 20 mm offset for AFP technology and the results are shown in Table 6.14. After the 20 mm part offset simulation was performed, it was understood that a simulation with 30 mm was required as the 20 mm part offset values did not have a good agreement with the values obtained by Lukaszewicz's AFP lay-up. For 30 mm, the technical scrap difference between studies reduces from 90.34% to 16.5% which indicates a better value agreement. A higher offset for AFP than for ATL might be due to higher tow tolerances and the smaller width from the first to the latter, justifying a higher part edge offset and thus indicating a good comparison between the model developed in this thesis and Lukaszewicz [83] data for both technologies. The model can therefore be safely validated for AFP technology as well.

Table 6.14: Lukaszewicz's AFP validation with 20 and 30 mm part offset.

Parameter	[83] Data	20 mm offset	Diff.	30 mm offset	Diff.	Unit
$Time_{on\_part}$	1.455	1.513	3.99%	1.520	4.47%	h
$A_{original}$	128	128.01	0.01%	128.01	0.01%	m^2
A_{with_offset}	128.96/129.44	128.92	0.03%	129.38	0.05%	m^2
$Time_{on\_part}$ - 0º	1320	1322.64	0.20%	1324.2	0.32%	s
$Time_{on\_part}$ - 90º	1343	1348.56	0.41%	1368.6	1.91%	s
$Time_{on\_part}$ - 45º/-45º	1288.56	1388.04	7.72%	1390.2	7.89%	s
Mat_{dep}	1037.62	1032.62	0.48%	1035.31	0.22%	m^2
$Mass_{dep}$	427.5	425.44	0.48%	426.55	0.22%	kg
$Tech_{scrap}$	13.49	8.57	36.47%	11.26	16.53%	m^2
$\%_{scrap}$	1.3	0.830	-	1.087	-	%
$T_{c_{rolls}}$	4.54	4.55	0.22%	4.55	0.22%	h
N_{rreq}	681	704	3.38%	704	0.29%	-
$Layup_{rate}$	71.31	70.17	1.60%	70.27	1.46%	kg/h

6.3 Lay-up and Scrap rates for aeronautical representative composite parts

In this section, the full potential of the model developed will be shown as four different aeronautical composite parts will be studied. The parts will be shown by order of increasing area, starting with a simple wing flap, then a horizontal and vertical stabilizer and finally a wing skin. The parts are merely representative as its measures do not correspond to any specific aircraft. The full output information will be presented for the first example and for the following parts only the most relevant outputs like the lay-up and scrap rates, total material deposited and material costs, cycle time and lay-up time will be displayed. All parts will be simulated with 40 plies with the same [45, 0, -45, 90] degree angle orientations. Material areal weight of 0.6 kg/m^2, material cost and scrap disposal cost of 71 and 3 €/kg.

The parts will be tested for both technologies with ATL being tested for single and two-phase systems

and AFP tested for pre and at start location options. AFP and ATL two-phase are also simulated for uni and bi directional lay-up. For AFP technology, the simulations will be performed with tow width of 12.7 mm and 32 tows which are the maximum available values as the parts to be simulated are large enough to justify it. For ATL technology, this value will also be the highest available of 304.8 mm and a single tape. Both technologies will be setup with values for acceleration and velocities of standard maximum values. The values used for initiation and cutting speed were chosen on a 2/3 rule of the lay-up speed as the parts to be simulated are flat. For the approaching and retracting distance, the value could be selected between 100 - 200 mm. The latter was selected to opt as a more cautioned approached. Minimum course and minimum cut restart length were chosen as the standard value of 101.6 mm. For the ATL single-phase system an average value of 4 seconds was used for its starting and cutting course time. Finally, the roll and creel changing time were selected based on Lukaszewicz [83] values, being these values 300 and 15 s, respectively. The roll length and setup time were adopted from Soares et al. [104] reference values, at 240 m and 2 h. These parameters are shown in subsection A.1.4.

6.3.1 Wing flap

The first example used was a wing flap illustrated in Figure 6.5. The dimensions used for this part are similar to those of a medium size aircraft. The outputs will be divided into two tables in each example to facilitate its reading. The first table in each section sums up the parameters which are characteristic of each technology and do not vary within it. In the wing flap example this first table is the Table 6.15 which contains parameters such as the original and offset area and perimeter, common to both technologies, the material and technical scrap deposited area and mass as well as the technical scrap percentage.

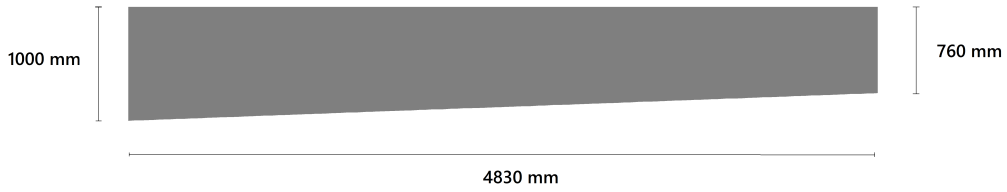

Figure 6.5: Wing flap part geometry.

Table 6.15: Model results ATL vs AFP - Wing flap.

Symbol	A_{orig}	A_{offs}	P_{orig}	P_{offs}	Mat_{dep}	$Tech_{scrap}$	$\%_{scrap}$	$Mass_{dep}$	$Mass_{scrap}$
ATL	4.27	4.50	11.43	11.55	215.92	45.04	20.86	129.55	27.02
AFP					181.66	10.78	5.94	109	6.47
Unit	m^2	m^2	m	m	m^2	m^2	%	kg	kg

In this case, the full output information is shown in Table 6.16, except for the T_{trans_h} and T_{trans_v} parameters, which were omitted, as there is no gaps in this part, and therefore, the machine does not consume any time translating over the gaps. In this table, more detailed information can be seen and several observations can be made with this data. On a larger scale, comparing technologies, the first

remark that can be made is that, as expected, the cycle times are higher for ATL technology versus AFP technology, although the ATL two-phase system with bi-directional lay-up has similar values to those of AFP systems. This is due to the higher axis accelerations used in AFP and the higher bandwidth of 406.4 mm (32 * 12.7 mm) versus 304.8 mm in ATL. These accelerations affect all time parameters like the time on and off part, the approach and retract time and the transitional time, all faster in AFP, as seen in the Table 6.18. The time to change rolls is higher for AFP (64 rolls for 32 tows) when comparing to ATL (3 rolls for a single tape) because of the time required to adjust each AFP machine creel, although AFP only changes the 32 tows rolls simultaneously once comparing to twice for ATL. Nonetheless, this time parameter has less impact on the cycle time when comparing to the faster acceleration and larger bandwidth of AFP.

The material deposited is, as predicted, higher in ATL (215.92 m^2) than for AFP (181.66 m^2), due to AFP being able to cut and lay independent tows. Even though having a higher maximum bandwidth, AFP technology is able to adjust it as suited, laying down less scrap in consequence, 45.04 m^2 (20.86%) vs 10.78 m^2 (5.94%). The technical scrap percentages are then in accordance to the reference made in subsection 2.3.2. Consequently, the material costs are higher for ATL than for AFP. Finally, the lay-up rates are higher in ATL two-phase systems despite the higher cycle times. This happens because, while having greater cycles times, this technology also deposits more material and, as a consequence, more technical scrap as well and thus boosting higher lay-up rates.

Table 6.16: Model detailed results - Wing flap.

Symbol	**ATL single**	**ATL two**	**ATL two bi-dir.**	**AFP**		**AFP bi-dir.**		**Unit**
$Course_{s/f}$	2	-	-	1	2	1	2	
$Cycle_{time}$	4.095	3.079	2.875	2.821	2.782	2.733	2.703	h
$Layup_{time}$	1.928	0.912	0.708	0.604	0.566	0.516	0.478	h
$T_{on_{part}}$	1.343	0.328	0.328	0.270	0.232	0.270	0.232	h
$T_{off_{part}}$	0.585	0.585	0.380	0.334	0.334	0.246	0.246	h
T_{lspeed}	0.059	0.328	0.328	0.107	0.091	0.107	0.091	h
T_{ispeed}	0.642	-	-	0.102	0.085	0.102	0.085	h
T_{cspeed}	0.642	-	-	0.062	0.056	0.061	0.056	h
T_{trans}	0.338	0.338	0.133	0.182	0.182	0.094	0.094	h
T_{trans_t}	0.322	0.322	0.118	0.175	0.175	0.087	0.087	h
T_{trans_p}	0.015	0.015	0.015	0.007	0.007	0.007	0.007	h
$T_{app/ret}$	0.247	0.247	0.247	0.152	0.152	0.152	0.152	h
$T_{c_{rolls}}$	0.167	0.167	0.167	0.217	0.217	0.217	0.217	h
N_{rreq}	3	3	3	64	64	64	64	-
$Scrap_{cost}$	81.07	81.07	81.07	19.4	19.4	19.4	19.4	€
Mat_{cost}	9198	9198	9198	7739	7739	7739	7739	€
$Total_{cost}$	9279	9279	9279	7758	7758	7758	7758	€
$Layup_{rate}$	31.641	42.075	45.064	38.641	39.177	39.884	40.326	kg/h

When comparing values within a technology other insights can be discussed. ATL single-phase reveals itself the less efficient system with the lowest lay-up rate of all with a rate of 31.641 kg/h. This is derived from the high initiation and cutting times comparing to other systems. In addition, the time off

part for systems which are uni-directional (0.585 h for ATL and 0.334 h for AFP) is significantly higher than that of the same system but with bi-directional lay-up (0.38 h for ATL and 0.246 h for AFP). This is due to a reduction in the transitional tape/tow time from uni to bi-directional lay-up, 0.322 h to 0.118 h, in ATL, and 0.175 h to 0.087 h, in AFP. Finally, regarding the location of course start and finish, with option 1 being to start a course lay-up before the part's boundaries and finishing after and option 2 starting and finishing at the part's boundaries, its selection affects the time on part parameter, as by selecting option 2, that parameter is reduced and consequently the cycle time is smaller because course length to run diminishes. One aspect that can be improved is the calculation of the initiation and cutting time of bi-directional systems. The model, as developed, does not take into account that the coordinates reverse when bi-directional system is chosen and, as such, calculates these parameters as if the system was uni-directional. For this case, the error induced is minimum because initiation and cutting speeds are similar. The error will increase with the increase of the difference between these speeds. The distribution of material deposited per creel for AFP lay-up is shown in Figure 6.6. Only the first four plies are shown for discussion purposes as these depend on which side of the part the deposition starts. Despite the uneven distribution of plies of 0º angle, the global creel distribution evens up, as there is a small difference of 20 m of material deposited between creels 1-18 and 19-32, which assures that, at the moment the rolls are changed, there is not much material left on one particular roll thus assuring less material wastage.

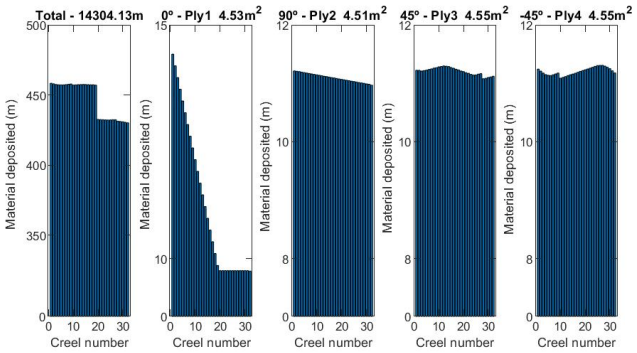

Figure 6.6: Wing flap AFP creels material distribution.

6.3.2 Horizontal stabilizer

The second part to be simulated was the horizontal stabilizer of Figure 6.3. This part is bigger than the wing flap with almost double its size, 8.27 m^2 comparing to 4.27 m^2. The same trend observed for the wing flap can be seen here. ATL two-phase has higher lay-up and scrap rates and material costs comparing to AFP, and ATL single-phase has the smaller lay-up rate of all systems for this part. ATL single-phase lay-up has a higher transitional time than ATL tow-phase uni-directional lay-up because, in the first case, the machine stops and retracts when facing a longitudinal gap, which is the case for this part.

Table 6.17: Model results ATL vs AFP - Horizontal stabilizer.

Symbol	A_{orig}	A_{offs}	Mat_{dep}	$Tech_{scrap}$	$\%_{scrap}$	$Mass_{dep}$	$Mass_{scrap}$	$Scrap_{cost}$	Mat_{cost}
ATL	8.27	8.67	419.67	89.02	21.21	251.8	53.41	160.23	17878
AFP			349.39	18.74	5.36	209.6	11.24	33.73	14884
Unit	m^2	m^2	m^2	m^2	%	kg	kg	€	€

Table 6.18: Model detailed results - Horizontal stabilizer.

Symbol	ATL single	ATL two	ATL two bi-dir.	AFP		AFP bi-dir.		Unit
$Course_{s/f}$	2	-	-	1	2	1	2	
$Cycle_{time}$	6.652	4.732	4.335	4.403	4.344	4.161	4.103	h
$Layup_{time}$	4.236	2.315	1.918	1.753	1.694	1.511	1.453	h
$T_{on_{part}}$	2.424	0.613	0.613	0.510	0.451	0.510	0.451	h
$T_{off_{part}}$	1.812	1.702	1.305	1.243	1.243	1.002	1.002	h
T_{trans}	0.749	0.668	0.272	0.454	0.454	0.212	0.212	h
$T_{app/ret}$	1.063	1.034	1.034	0.789	0.789	0.789	0.789	h
$T_{c_{rolls}}$	0.417	0.417	0.417	0.65	0.65	0.65	0.65	h
N_{rreq}	6	6	6	6	128	128	128	-
$Layup_{rate}$	37.852	53.219	58.079	47.615	48.258	50.373	51.091	kg/h

6.3.3 Vertical stabilizer

The vertical stabilizer represented in Figure 6.7 is bigger than the previous horizontal stabilizer with a bit over double its area, 19.62 m^2, to be exact. The trend remains the same as in the previous examples, but technical scrap percentage is reduced to half the values for both technologies from 21.21% to 10.74% in ATL, and from 5.36% to 2.54% in AFP. For this case, ATL two-phase uni-directional system was surpassed by both simulated AFP bi-directional systems which shows that with increase part size the latter overcomes the first. The results are shown in Table 6.19 and Table 6.20.

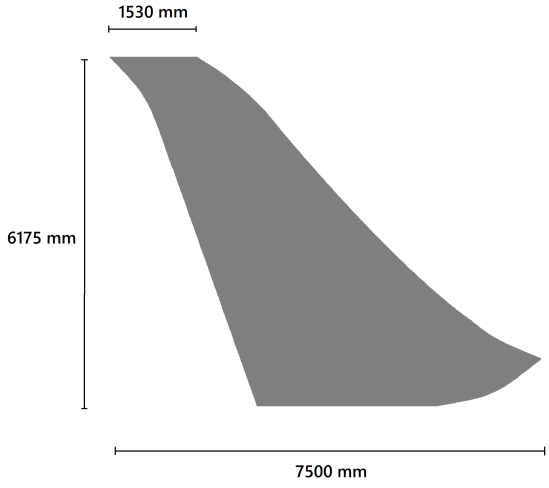

Figure 6.7: Vertical stabilizer part geometry.

Table 6.19: Model results ATL vs AFP - Vertical stabilizer.

Symbol	A_{orig}	A_{offs}	Mat_{dep}	$Tech_{scrap}$	$\%_{scrap}$	$Mass_{dep}$	$Mass_{scrap}$	$Scrap_{cost}$	Mat_{cost}
ATL	19.62	20.06	879.3	94.42	10.74	527.58	56.65	169.95	37458
AFP			805.3	20.44	2.54	483.19	12.26	36.79	34307
Unit	m^2	m^2	m^2	m^2	%	kg	kg	€	€

Table 6.20: Model detailed results - Vertical stabilizer.

Symbol	ATL single	ATL two	ATL two bi-dir.	AFP		AFP bi-dir.		Unit
$Course_{s/f}$	2	-	-	1	2	1	2	
$Cycle_{time}$	8.313	6.271	5.513	6.213	6.136	5.717	5.639	h
$Layup_{time}$	5.313	3.271	2.513	2.480	2.403	1.983	1.906	h
$T_{on_{part}}$	3.015	1.051	1.051	0.872	0.795	0.872	0.795	h
$T_{off_{part}}$	2.298	2.219	1.462	1.608	1.608	1.111	1.111	h
T_{trans}	1.116	1.042	0.285	0.7	0.7	0.204	0.204	h
$T_{app/ret}$	1.182	1.178	1.178	0.908	0.908	0.908	0.908	h
$T_{c_{rolls}}$	1	1	1	1.733	1.733	1.733	1.733	h
N_{rreq}	13	13	13	288	288	288	288	-
$Layup_{rate}$	63.461	84.134	95.692	77.77	78.748	84.521	85.679	kg/h

6.3.4 Wing skin

The final and larger example, the wing skin shown in Figure 6.8. This part, in the same fashion, doubles the area of the previous vertical stabilizer with 32.23 m^2. For this case, the scrap rate was expected to further reduce comparing to the previous example, as the wing skin is double in size, and scrap percentage tends to lower with increase part size. However, the scrap percentage increased about 2% for ATL and 0.25% for AFP. This is most likely due to the part's geometry which is more complex than the previous one. This particular aspect is also responsible for the lower lay-up rates comparing to previous examples but ATL two-phase boosts the highest production lay-up rates. Results are displayed in Table 6.21 and Table 6.22.

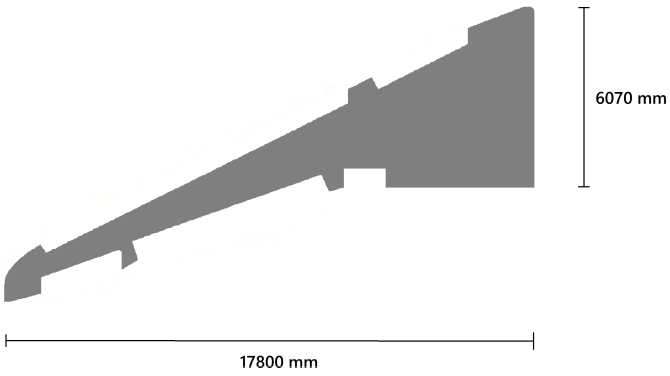

Figure 6.8: Wing skin part geometry.

Table 6.21: Model results ATL vs AFP - Wing skin.

Symbol	A_{orig}	A_{offs}	Mat_{dep}	$Tech_{scrap}$	$\%_{scrap}$	$Mass_{dep}$	$Mass_{scrap}$	$Scrap_{cost}$	Mat_{cost}
ATL	32.23	33.07	1477.8	188.5	12.76	886.7	113.11	339.3	62953
AFP			1326.3	36.98	2.79	795.8	22.19	66.57	56498
Unit	m^2	m^2	m^2	m^2	%	kg	kg	€	€

Table 6.22: Model detailed results - Wing skin.

Symbol	ATL single	ATL two	ATL two bi-dir.	AFP		AFP bi-dir.		Unit
$Course_{s/f}$	2	-	-	1	2	1	2	
$Cycle_{time}$	15.208	11.33	9.817	10.648	10.482	9.799	9.634	h
$Layup_{time}$	11.541	7.663	6.15	5.831	5.666	4.983	4.817	h
$T_{on_{part}}$	5.567	1.830	1.830	1.529	1.364	1.529	1.364	h
$T_{off_{part}}$	5.974	5.833	4.32	4.302	4.302	3.454	3.454	h
T_{trans}	2.045	1.999	0.486	1.244	1.244	0.396	0.396	h
$T_{app/ret}$	3.929	3.834	3.834	3.058	3.058	3.058	3.058	h
$T_{c_{rolls}}$	1.667	1.667	1.667	2.817	2.817	2.817	2.817	h
N_{rreq}	21	21	21	448	448	448	448	-
$Layup_{rate}$	58.302	78.261	90.316	74.735	75.913	81.193	82.587	kg/h

6.3.5 Results comparison

In this section the results from the previous examples are compared in order to assess the evolution of the outputs with the increase in part area and through the multiple machine systems. Only the most important outputs were considered for the graphics, i.e, the cycle time, lay-up time, time on part, time off part, transitional time, technical scrap percentage and finally the lay-up rates. Furthermore, not all systems were displayed, as only relevant contrasting information was selected. Regarding ATL technology systems, as depicted in Figure 6.9, it is possible to conclude that all parameters increase with part area increase, except for the technical scrap percentage that usually decreases with part size increase. Although being the standard rule, some examples can be the exception as is the case of the wing skin, which has a much larger area when comparing to the vertical stabilizer but carries a higher technical scrap percentage as well. This is due to the complex geometry of the wing skin comparing to the simpler geometry of the vertical stabilizer. The more complex geometry, usually, the more technical scrap produced.

Comparing systems within the ATL technology, the only relevant difference, which affects consequent parameters, is once more in the time on part parameter which is significantly higher for the ATL single-phase machine. This is majorly due to the high starting and cutting times characteristic of these systems. All other parameters are as expected, being the cycle time and lay-up time higher in ATL single-phase, time off part slightly higher in ATL single-phase and finally the lay-up rate is higher for the ATL two-phase system. Comparing ATL two-phase uni-directional with ATL two-phase bi-directional lay-up, not shown in the figure, the major difference is in the time off part parameter which is evidently lower for the latter.

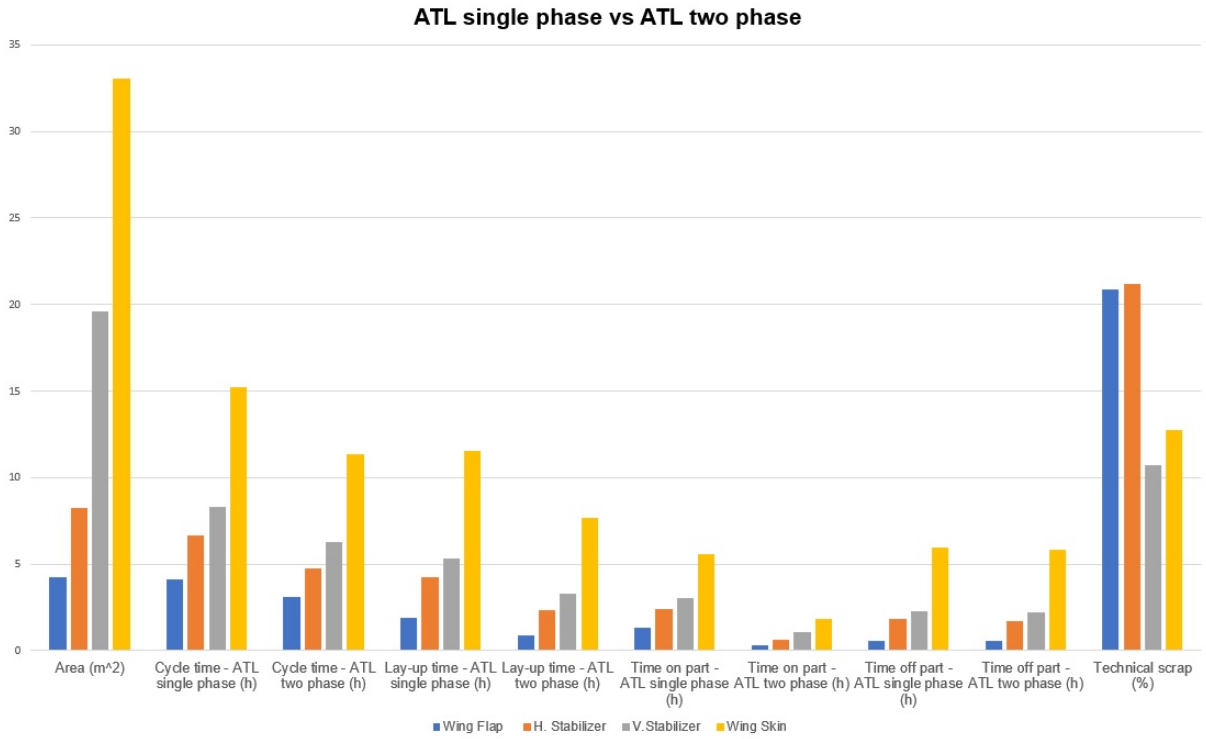

Figure 6.9: Comparison between ATL single-phase system and ATL two-phase system results.

Figure 6.10 illustrates the simulation results for AFP 2 and AFP 2 bi-directional systems. When comparing these AFP systems, by analyzing the figure, it's a quick realization that the major difference is on the transitional time which is much smaller for bi-directional systems. Consequently, all other time parameters will be smaller for AFP 2 bi-directional lay-up for the exception of the time on part parameter which is not shown as it is equal for both systems. The difference between AFP 2 and AFP (1) is in the time on part parameter, being lesser for AFP 2. Comparing AFP 2 system with ATL systems from previous figures it is possible to conclude that the cycle times are much lower for all parts simulated when comparing to ATL single-phase systems and slightly lower than ATL two-phase uni-directional systems. However, when comparing cycle times between AFP 2 and ATL two-phase bi-directional systems the first is only lower for the smaller part simulated, the wing flap. Comparing AFP 2 bi-directional lay-up with all other systems, the first has a smaller cycle time for the smaller wing flap, horizontal stabilizer and wink skin but is surpassed by the ATL two-phase bi-directional system for the vertical stabilizer, in which the latter is the fastest system of all simulated. This happens because, although lay-up times are all faster for all AFP systems, the time difference in the time to change tape rolls is lesser than the difference in lay-up time for the particular case of the vertical stabilizer making the ATL two-phase bi-direction systems the most efficient for that lay-up in terms of time spent.

Finally, the material costs, as expected, are higher for ATL technology than for AFP and are directly proportional to the material deposited as the price per kg was set as the same for both technologies.

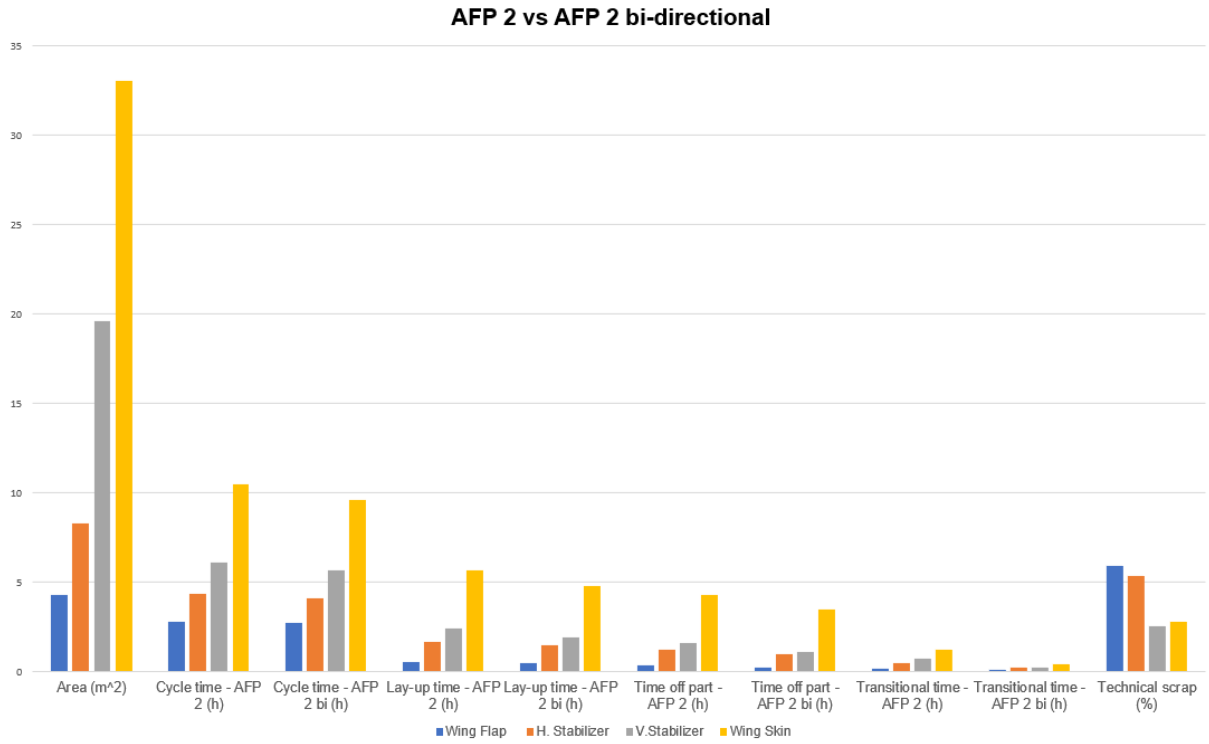

Figure 6.10: Comparison between AFP 2 system and AFP 2 bi-directional system results.

By analyzing Figure 6.11, some observations can be made. The first, and the most evident, is that the lay-up rate increase, as discussed in theory, with part size for the same machine systems. Although most cycle times are lower for AFP, as discussed in previous paragraphs, ATL machines lay down more material because they do not possess the ability to cut and restart individual tows and therefore produce more technical scrap.

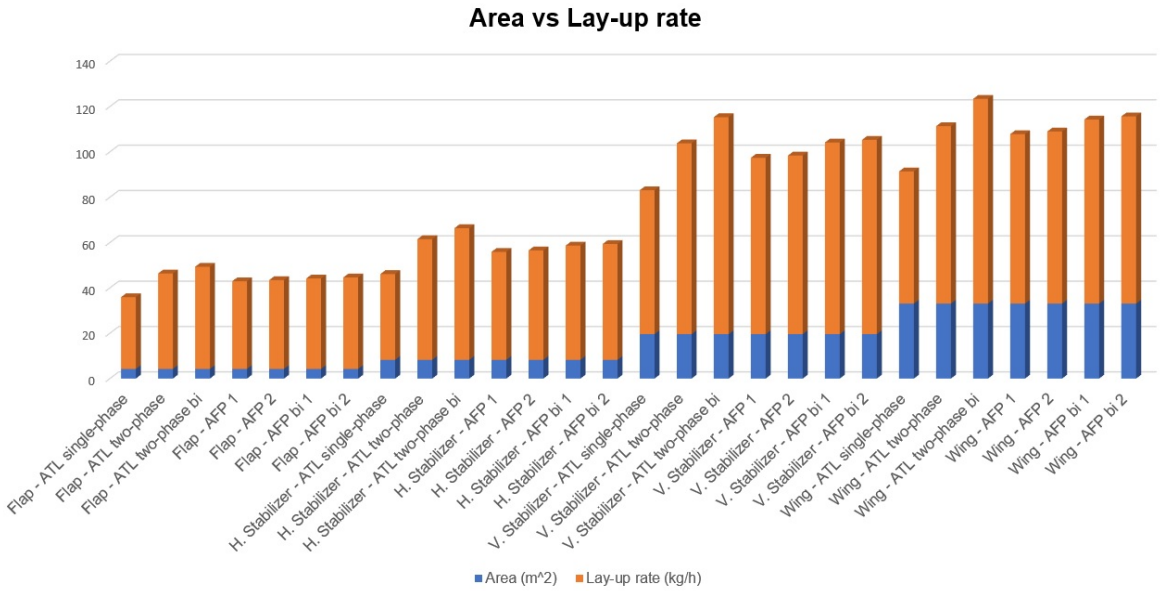

Figure 6.11: Area vs lay-up rate for all ATL and AFP machine systems.

By laying down more material in more, although almost similar time, the difference in material deposited has a bigger impact than the difference in cycle times for ATL two-phase systems. They then possess the highest lay-up rates for all part sizes being the ATL two-phase bi-directional system the most efficient one. As seen in the figure the difference between lay-up rate for the ATL two-phase bi-directional systems and AFP bi-directional systems increases slightly with the increase in part size. In contrast the difference between ATL two-phase uni-directional system and the same AFP bi-directional systems decreases with the increase in part size. The systems can be generally ranked in order of productivity from ATL dual-phase bi-directional system, followed by ATL two-phase uni-directional (smaller parts), AFP bi-directional 2 and 1 (larger parts), AFP uni-directional 2 and 1 and finally ATL single-phase.

6.4 First tape offset study results

The results of the study regarding the potential reduction on material deposited with an offset of the first tape laid are shown in this segment. The first scenario to be studied was the horizontal stabilizer seen in Figure 6.3. The results utilizing the model developed were 89.02 m^2 of technical scrap when laying the first tape aligned with the part's boundary as exemplified in Figure 5.4 - Figure 5.7 and 88.89 m^2, a negligible saving of 0.13 m^2 or 0.15%, when using an offset on the first tape laid in each ply. The plies that had its first tape require an offset were plies number 2, 6, 10, 14, 18, 27, 35 (Figure 6.12), 21 (Figure 6.13), 22 (subsection A.1.5), 23, 31 and 39 also shown in (subsection A.1.5). The plies that remained the same did not improve on its technical scrap savings when implementing an offset on its first tape. The first tapes suffering an offset are illustrated in red in the previously referred images. For Figure 6.12 and all the plies it represents, the offset corresponded to 26 pixels which translates to an offset of 82.55 mm. For Figure 6.13 and Figure A.2 the offset was 78 pixels, which equals 247.65 mm. For Figure A.3 the offset was 34 pixels, or 107.95 mm. The direction of the lay-up is described in the figure's subtitles. The ply sequence used was [0 90 45 -45] x 5, symmetric. Material cost and scrap disposal cost are 71 a 3 €/kg.

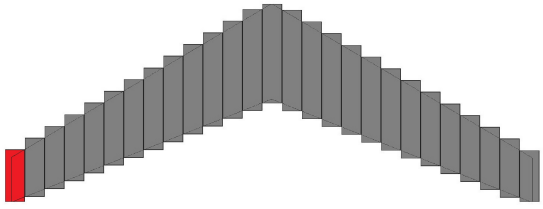

Figure 6.12: Offset study - ATL Ply Lay-up 90º (left to right).

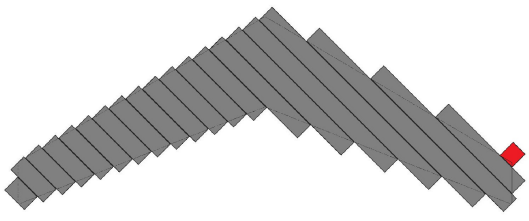

Figure 6.13: Offset study - ATL Ply Lay-up -45º (right to left).

In a second scenario, the same Figure 6.3 was modified as to include gaps in the direction of lay-up of the machine. This approach tries to describe a situation where this study could have a greater potential than the one observed in the previous scenario. This kind of example can be seen when certain plies have areas which require strength reinforcement. For this example, there are three first tape studies

to do if the machine is laying material longitudinally and two tape offset studies if the machine is laying material horizontally which potentially enhances the material savings in technical scrap. The standard lay-up for this part was already shown as an example for the 0º ply in Figure 5.15 (with longitudinal gap alignment). The total technical scrap obtained for the standard lay-up configuration was 76.37 m^2 and for the offset study the same parameter suffered a slight decrease, as expected, to 74.57 m^2. The difference was 1.8 m^2, or 2.36%, which corresponds to approximately 77 euros in material savings for this lay-up.

The plies in which the offset was indeed required were 1 and 24, with 29 and 43 pixels (92.075, 136.525 mm) to the first tape of two of each sections shown in Figure 6.14. Also plies 2, 6, 10, 14, 18, 27, 31, 35 and 39 (Figure 6.15) got and offset of 7 and 52 pixels (22.225, 165.1 mm). Furthermore, plies 3, 7, 11, 15, 19, 26, 30, 34, 38 have two first tape offsets of 92 and 31 pixels (292.1, 98.425 mm) to two of its sections shown in Figure 6.16. In addition, plies 4, 8, 12, 16, 20, 25, 29, 33, 37 (Figure 6.17) also require an offset of 40 pixels, or 127 mm. Finally, plies 21 (subsection A.1.5), 22 (subsection A.1.5) and 23 subsection A.1.5) with 65 (206.375 mm), 93 (295.275 mm), 58 and 1 (184.15 mm, 3.175 mm) pixels, correspondingly. All the above described offsets are shown in red in the corresponding images and the direction of the lay-up is described in the figure's subtitles.

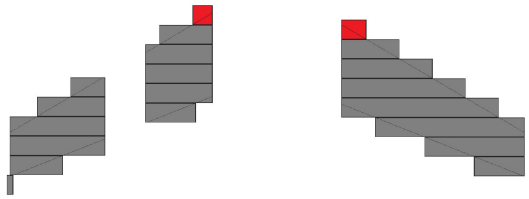

Figure 6.14: Offset study - ATL Ply Lay-up 0º (top to bottom).

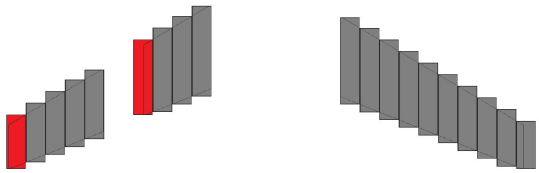

Figure 6.15: Offset study - ATL Ply Lay-up 90º (left to right).

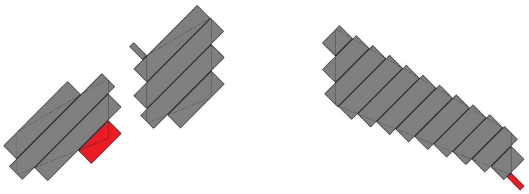

Figure 6.16: Offset study - ATL Ply Lay-up 45º (right to left).

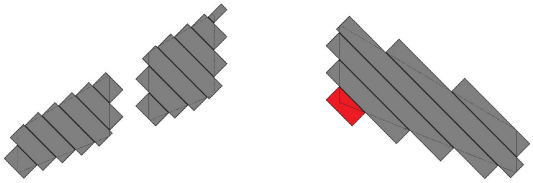

Figure 6.17: Offset study - ATL Ply Lay-up -45º (left to right).

By analyzing both scenarios it can be concluded that an offset must be provided when the first edge, i.e, the side where the machine lays material first, has a smaller course length than the outer or final edge. For the first scenario, the savings in material were negligible, but for the second scenario this study revealed more potential as the material cost savings were 2.36% translating to around 80 euros per part production which is not a very high value, but it is, nonetheless, a cost that can be saved.

7. Conclusions and Future work

The main focus of this thesis was to assess material costs and deposition rates of automated lay-up composite technologies for parts with planar complexity found in real aerospace components. Therefore, a study regarding these technologies was performed, clarifying the requirement of an analysis and simulation tool to accomplish the proposed goals. A complex mathematical basis was developed through equations that describe the calculation of several parameters, which can be divided in three major categories: times, distances and costs. The computing of the distance parameters was possible through thorough research and the observation, *in locu*, of a composite part lay-up at Embraer Évora. These equations were critical for the algorithm developed in this work.

With the tool developed and working for any kind of flat part geometry, its validation was required. This was done in two stages. The first was using the tool to simulate a lay-up with a geometry that is utilized in real aerospace composite manufacturing. The Embraer specimen test part, consisting of a simple small rectangle, was then used and its real lamination results, provided to me by Embraer and performed in an AFP system, were compared to the ones from the tool. The comparison produced an almost perfect agreement, with less than 1% difference. In this first validation test, parameters like the part area, the material deposited, its percentage of technical scrap and the time on part were successfully validated. This revealed that the part image processing is performing accurately as geometrical constraints were well computed and translated to real values. It also demonstrated that the correct relation between machine lay-up path projections and part boundaries was achieved due to the agreement in material deposited and technical scrap percentage. Finally, the time on part parameter validation, which comprises the time the machine is actually laying down material, indicates that the relation between axis speeds, accelerations, machines constraints like the minimum course length or the cut restart length and the part geometry is working properly. Furthermore, the tool was validated with a horizontal stabilizer, a more complex geometry from Soares et al. [104], on both AFP and ATL technology, revealing it had a solid working foundation with differences not higher than 1.76% except from the technical scrap that, by being small in absolute value, had a larger difference of about 1.3 m^2, or 35%.

On a second stage, the tool was validated trough a comparison with Lukaszewicz [83] benchmark studies which are highly relevant in the aerospace composite field of study, as this work is cited multiple times in other articles and research papers. This model, also simple in geometry, enabled the validation of the same parameters for both technologies, which are described in that work through more simplistic equations. In addition, other parameters like the time to change tape and tow rolls and the number of rolls required per lay-up were also validated. Furthermore, it enhanced the tool's reliability as Lukaszewicz [83] results are specified by ply orientation providing a more detailed description of the calculations. The time off part parameter, which includes the time the machine spends transitioning between lay-up courses, plies, approaching and retracting the mold was not able to be validated as there was no data available for comparison. However, by validating all other time parameters, there is a strong premise to consider the values obtained by tool for the time off parameter as viable since the equations in which both

are based on are the same. As a consequence, the deposition rates were only eligible for comparison using the time on part value and not, as standard procedure, the cycle time.

With the tool validated, several representative aircraft parts were simulated in order to assess its material costs and deposition rates. These parts were a wing flap, a horizontal stabilizer, a vertical stabilizer and a wing skin. These are ordered by increase in part size. Also, machine technology comparison for each part and between parts was performed. The systems simulated with the tool were the ATL single-phase system, ATL two-phase system with uni and bi-directional lay-up and also AFP uni and bi-directional systems.

It was plausible to conclude that, as a general rule and as stated in Grimshaw et al. [54], the lay-up rate increase with part area increase. The lay-up rates were found to be higher for ATL two phase bi-directional systems, that although had a higher cycle time than AFP bi-directional systems, the larger difference in material deposited in favor of the first, made them the most productive system of all simulated. They were followed by AFP bi-directional system for the two larger parts, being the wing skin and vertical stabilizer, and ATL two phase uni-directional for the two smaller ones. Next in order is the AFP uni-directional and finally, the least productive system, the ATL single phase machine. Once more, as a general rule, scrap rates decrease with part size increase. However, for the larger and more complex part simulated, a wing skin, of about 32.23 m^2, the scrap rate increased when comparing to the smaller vertical stabilizer. This is justified by the higher complexity of the wing's geometry. Moreover, material costs are higher for ATL systems as they deposit more material being the cost per kg of material set as equal for both systems.

One of the objectives proposed in this thesis was to discover news ways to reduce material costs through an optimization of the lay-up paths selection. It was then decided to include an option for technical scrap reduction on the tool that inspects each ply geometry and assesses if an offset of the first tape is required (only ATL technology was found to be advantageous for this scenario due to the larger tape width). The feature was included and the results proved to be negligible for simple geometries as an horizontal stabilizer, with 8.27 m^2, attained a material cost reduction of 0.15%. For more complex geometries, with similar area, the cost reduction was a more promising 2.36%. This value is strongly dependent on material areal weight, part size, and the material cost per kg as the savings are likely proportional to the increase of these values.

With the validations and analysis performed, the developed model presents itself as a tool capable of estimating material costs and deposition rates using current machine technology for real world parts with complex planar shapes. The potential of this tool is untapped as further developments can take it to a far broader utilization. The tool can be adapted to work for any kind of three-dimensional parts which would increase its utility and also an interface could be created with other computer aided design and manufacturing software to further enhance its capabilities.

Bibliography

[1] D. K. Rajak, D. D. Pagar, R. Kumar, and C. I. Pruncu. Recent progress of reinforcement materials: a comprehensive overview of composite materials. *Journal of Materials Research and Technology*, 2019.

[2] K. K. Chawla. *Composite Materials*. Springer, 4^{th} edition, 2019. ISBN:978-3-030-28982-9.

[3] L. Ilcewicz and C. Ashforth. *Comprehensive Composite Materials II*, chapter Scaling Crucial to Integrated Product Development of Composite Airframe Structures, pages 26–90. Elsevier, 2018.

[4] G. Marsh. Automating aerospace composites production with fibre placement. *Reinforced Plastics*, 2011.

[5] M. K. Hagnell and M. Åkermo. A composite cost model for the aeronautical industry: Methodology and case study. *Composites Part B: Engineering*, 2015.

[6] D. Gates. Electroimpact to build fiber-laying machines for boeing's 777x. Online, 2014. `https://www.seattletimes.com/business/electroimpact-to-build-fiber-laying-machines-for-boeingrsquos-777x/`, last accessed 14 August 2020.

[7] W.-P. Tang, B. Johnson, and D. E. Gonsor. *Optimizing non-productive part motion in an automated tape. Patent US 7,720,561 B2*, 18th May 2010.

[8] P. Zhang, Z. Zhou, G. Chen, and S. Chen. Optimizing the lay-up of composite tapes based on improved geodesic strategy for automated tape placement. *Journal of Mechanical Engineering Science*, 2017.

[9] C. R. Pupo. Continuous tow path generation for constant and variable stiffness composite laminates on single and double curved surfaces. Master's thesis, College of Engineering and Computing, University of South Carolina, 2017.

[10] D. Brosius. Aerospace and industrial composites: Now on divergent paths? Online, 2016. `https://www.compositesworld.com/articles/aerospace-and-industrial-composites-now-on-divergent-paths`, last accessed 16 August 2020.

[11] G. Gardiner. Increasing access to afp. Online, 2019. `https://www.compositesworld.com/articles/increasing-access-to-afp`, last accessed 17 August 2020.

[12] U. P. Breuer. *Commercial Aircraft Composite Technology*, chapter Introduction, pages 1–23. Springer, 2016.

[13] P. McMullen. *Composites, Volume 15, (3)*, chapter Fibre/resin composites for aircraft primary structures: a short history, 1936-1984, pages 222–230. Butterworth Co Ltd, 2018.

[14] C. Soutis. Carbon fiber reinforced plastics in aircraft construction. *Materials Science and Engineering A*, 412(1-2):171–176, 2011.

[15] W. G. Roeseler, B. Sarh, and M. U. Kismarton. Composite structures: The first 100 years. In *16th International Conference of Composite Materials*. The Boeing Company, 2007.

[16] A. C. M. Association. Commercial aircraft. Online. `https://discovercomposites.com/transportation/commercial-aircraft/`, last accessed 17 August 2020.

[17] G. Dorey. Carbon fibres and their applications. *Journal of Physics D: Applied Physics*, 20(3): 245–256, 1987.

[18] C. Red. 777x: Bigger-than-expected carbon fiber impact. Online, 2016. https://www.compositesworld.com/articles/777x-bigger-than-expected-carbon-fiber-impact, last accessed 22 August 2020.

[19] M. S. Loukil. *Experimental and Numerical Studies of Intralaminar Cracking in High Performance Composites*. PhD thesis, Université de Lorraine, 2013.

[20] G. Goebel. The embraer bandeirante, xingu, brasilia. Online, 2018. https://www.airvectors.net/avbrasil.html, last accessed 26 July 2020.

[21] J. Croft. Embraer phenom 300: bolder big brother. Online, 2008. https://www.flightglobal.com/embraer-phenom-300-bolder-big-brother/80192.article, last accessed 17 August 2020.

[22] L. S. Marques. Composites rd challenges for embraer aerostructures. In *SAMPE Brazil congress*. Embraer, 2017.

[23] B. Inc. Bombardier aerospace granted authority to offer cseries aircraft to customers. Online, 2005. https://www.bombardier.com/en/media/newsList/details.158-bombardier-aerospace-granted-authority-to-offer-cseries-aircraft-to-customers.bombardiercom.html, last accessed 26 July 2020.

[24] A. Inc. A220-100 purpose built for efficiency. Online, 2020. https://www.aerospace-technology.com/projects/airbus-a220-100-jetliner/, last accessed 17 August 2020.

[25] I. Composites. New irkut mc-21 aims to outperform airbus and boeing. Online, 2017. https://www.insidecomposites.com/new-irkut-mc21-aims-to-outperform-airbus-and-boeing/, last accessed 10 August 2020.

[26] S. Govindasamy. Aa09: Mitsubishi unveils major changes to mrj programme. Online, 2009. https://www.flightglobal.com/aa09-mitsubishi-unveils-major-changes-to-mrj-programme/88890.article, last accessed 30 July 2020.

[27] L. Commercial Aircraft Corporation of China. Comac rolls out first c919 in shanghai. Online, 2015. http://english.comac.cc/news/mc/201511/02/t20151102_3033164.shtml, last accessed 30 July 2020.

[28] I. Grand View Research. Global composites market size — industry report, 2020-2027. Technical report, Grand View Research, Inc, 2020.

[29] M. Sauer and M. Kühnel. The global cf- und cc-market 2018 - market developments, trends, outlook and challenges. Technical report, Carbon Composites e.V, 2018.

[30] M. Sauer. Composites market report 2019 - the global cf- und cc-market 2019 - market developments, trends, outlook and challenges. Technical report, Carbon Composites e.V, 2019.

[31] M. Intelligence. Carbon fiber market - growth, trends, and forecast (2020 - 2025). Technical report, Mordor Intelligence, 2020.

[32] H. Corp. Vestas supply agreement. Online, 2017. https://www.hexcel.com/News/News-

Releases/2573/hexcel-and-vestas-expand-composite-materials-supply-agreement-for-wind-blades, last accessed 19 August 2020.

[33] D. Knab, S. C. Baban, D. A. Schlosser, D. P. Seidel, C. Lök, and T. Knoblinger. What's next for aerospace composites? Technical report, Artur D.Little Luxembourg S.A, 2018.

[34] S. Research. Advanced composites market. Online, 2019. https://www.stratviewresearch.com/836/advanced-composites-market.html, last accessed 10 August 2020.

[35] K. Pulidindi and S. Mukherjee. Aerospace composites market size share — global forecasts 2026. Technical report, Global Market Insights, 2020.

[36] A. Inc. Airbus aircraft deliveries in 2019. Online, 2020. https://www.airbus.com/newsroom/press-releases/en/2020/01/airbus-delivers-strong-2019-commercial-aircraft-performance.html, last accessed 28 July 2020.

[37] H. Corp. Airbus helicopter h160 supply agreement. Online, 2017. https://www.hexcel.com/News/News-Releases/2544/airbus-helicopters-selects-hexcel-as-supplier-of-advanced-composite-materials-for, last accessed 19 August 2020.

[38] H. Corp. Utc aerospace systems supply agreement. Online, 2017. https://www.hexcel.com/News/News-Releases/2577/hexcel-and-utc-aerospace-systems-extend-existing-contract-through-2030, last accessed 19 August 2020.

[39] T. I. for Advanced Composites Manufacturing Innovation IACMI. Space x. Online, 2018. https://iacmi.org/2018/02/12/spacex-falcon-heavy-launch-holds-promise-for-carbon-fiber-composites/, last accessed 19 August 2020.

[40] S. Francis. Composites in the race to space. Online, 2020. https://www.compositesworld.com/articles/composites-in-space(2), last accessed 22 August 2020.

[41] K. Schlegel, D. P. Parlevliet, D. C. Weimer, D. A. Schuster, and M. Kupke. On the interply friction of different generations of carbon/epoxy prepreg systems. *Journal of Plastics Technology*, 15(6): 393–436, 2019.

[42] N. Gharabegi. Composite laminates made by automated fiber placement of dry fibers and vacuum assisted resin transfer molding. Master's thesis, Concordia University, 2018.

[43] G. Gardiner. Dry fiber placement: Surpassing limits. Online, 2016. https://www.compositesworld.com/articles/dry-fiber-placement-surpassing-limits, last accessed 16 August 2020.

[44] A. McIlhagger, E. Archer, and R. McIlhagger. *Polymer Composites in the Aerospace Industry*, chapter Manufacturing processes for composite materials and components for aerospace applications, pages 59–81. Elsevier, 2 edition, 2020.

[45] CompositesWorld. Fabrication methods (2015). Online, 2015. https://www.compositesworld.com/articles/fabrication-methods-2015, last accessed 16 August 2020.

[46] H. Mason. Hyundai motor co., uber unveil air taxi model. Online, 2020. https://www.compositesworld.com/news/hyundai-motor-co-uber-unveil-air-taxi-model, last accessed 19 August 2020.

[47] H. Mason. Porsche, boeing to partner for premium urban air mobility. Online,

2019. https://www.compositesworld.com/news/porsche-boeing-to-partner-on-premium-urban-air-mobility-market, last accessed 19 August 2020.

[48] J. Sloan. The markets: Aerospace (2020). Online, 2020. https://www.compositesworld.com/articles/the-markets-aerospace, last accessed 31 July 2020.

[49] C. Grant. Automated processes for composite aircraft structure. *Industrial Robot: An International Journal*, 33(2):117–121, 2006.

[50] S. Research. Afp/atl machines market size, share, trend, forecast, competitive analysis: 2019-2024. Technical report, StratView Research, 2019.

[51] B. E. Chitwood and M. S. Howeth. *Composite tape laying machine with pivoting presser member. Patent 4627886*, 6th April 1971.

[52] W. B. Goldsworthy. *Geodesic path length compensator for composite-tape placement method. Patent US 3810,805*, 14th May 1974.

[53] D. H.-J. A. Lukaszewicz, C. Ward, and K. D. Potter. The engineering aspects of automated prepreg layup: History, present and future. *Composites*, Part B(43):997–1009, 2011.

[54] M. N. Grimshaw, C. G. Grant, and J. M. L. Diaz. Advanced technology tape laying for affordable manufacturing of large composite structures. In *SAMPE; 2001: a materials and processes odyssey*, volume 2, pages 2484–2494. SAMPE, 2001. ISBN:0938994905.

[55] J. Frketic, T. Dickens, and S. Ramakrishnan. Automated manufacturing and processing of fiber-reinforced polymer (frp) composites: An additive review of contemporary and modern techniques for advanced materials manufacturing. *Additive Manufacturing*, 14:69–86, 2017.

[56] R. J. Grone and M. N. Grimshaw. *Composite tape laying machine with pivoting presser member. Patent US 4627886*, 30th May 1985.

[57] A. Goel. Economics of composite material manufacturing equipment. Master's thesis, Massachusetts Institute of Technology, 2000.

[58] J. A. Zaffiro. *Control of radiation heating system for thermoplastic composite tape. Patent 5177340*. Cincinnati Milacron Inc, 5th January 1991.

[59] C. B. Anderton and A. Colvin. A roadmap to automated composites. Technical report, CGTech, 2017.

[60] Fives. Cincinnati charger tape layers. Online, 2020. https://metal-cutting-composites.fivesgroup.com/products/composites/tape-layer-systems/cincinnati-charger-tape-layers.html last accessed 7 August 2020.

[61] M. D. I. SAU. Torreslayup - productivity and flexibility together in a perfect solution. Online, 2020. https://www.mtorres.es/en/aeronautics/products/carbon-fiber/torreslayup, last accessed 7 August 2020.

[62] A. Crosky, C. Grant, and D. Kelly. *Wiley Encyclopedia of Composites*, volume 2, chapter Fibre placement processes for composites manufacture, pages 945–950. John Wiley Sons, Inc, 2 edition, 2012.

[63] D. O. Evans, M. M. Vaniglia, and P. Hopkins. Fiber placement process study. In *34th International SAMPE symposium*, pages 1822–1833. SAMPE, 1989.

[64] C. Composites. Coriolis c1 - the reference in automated fiber placement. Online, 2020. https://www.coriolis-composites.com/fiber-placement-machines/coriolis-c1/, last accessed 8 August 2020.

[65] R. Calawa and J. Nancarrow. Medium wave infrared heater for high-speed fiber placement. Technical report, SAE Aerofast, 2007.

[66] *Faserstreifenverbinder fuer Bandwickler. Patent DE 10 2008 010 424 A1*. Torres Martinez M., 2nd October 2008.

[67] T. Oldani. *Visual Fiber Placement Inspection. Patent US 7,835,567 B2*. Ingersoll Machine Tools, Inc., 16th November 2010.

[68] T. Oldani and D. Jarvi. *Automated Fiber Placement Using Multiple Placement Heads, Replaceable Creels, and Replaceable Placement Heads. Patent US 7.407,556 B2*. Ingersoll Machine Tools, Inc., 5th August 2008.

[69] T. Oldani and D. Jarvi. *Performing High-Speed Events "On The Fly" During Fabrication Of A Composite Structure By Automated Fiber Placement. Patent US 7.513,965 B2*. Ingersoll Machine Tools, Inc., 7th April 2009.

[70] A. Manufacturing and Design. Airbus orders six fiber placement systems for a350 xwb fuselage. Online, 2008. https://www.aerospacemanufacturinganddesign.com/article/airbus-orders-six-fiber-placement-systems-for-a350-xwb-fuselage/, last accessed 8 August 2020.

[71] F. Group. Cincinnati viper™ fiber placement systems. Online, 2020. https://metal-cutting-composites.fivesgroup.com/products/composites/fiber-placement-systems/cincinnati-viper-fps.html, last accessed 8 August 2020.

[72] F. Group. Cincinnati gemini atl/afp. Online, 2020. https://metal-cutting-composites.fivesgroup.com/products/composites/tape-layer-systems/cincinnati-gemini-dockable-gantry-system.html, last accessed 8 August 2020.

[73] M. Company. Torres newsletter. Online, 2016.

[74] C. M. T. Division. Mongoose hybrid™. Online, 2020. https://en.machinetools.camozzi.com/products/composite-manufacturing/all-products/mongoose-hybrid.kl, last accessed 8 August 2020.

[75] E. Inc. Composite manufacturing. Online, 2020. https://www.electroimpact.com/Products/Composites/Overview.aspx, last accessed 8 August 2020.

[76] Mikrosam. Automated tape laying. Online, 2020. https://mikrosam.com/new/article/en/automated-tape-laying-atl/, last accessed 22 August 2020.

[77] F. Group. Forest-liné atlas. Online, 2020. https://metal-cutting-composites.fivesgroup.com/products/composites/tape-layer-systems/forest-line-atlas.html, last accessed 10 August 2020.

[78] H. Lengsfeld and J. Lacalle. *Composite Technology: Prepregs and Monolithic Part Fabrication Technologies*, chapter Prepregs: Processing Technology, pages 47–113. Hanser, 2015.

[79] R. J. Grone, L. R. Schnell, and L. Vearil. *Composite tape laying machine and method. Patent US 4557783*, 5th December 1983.

[80] T. M. M. *Tape laying unit for depositing a band of composite material. Patent EP 1097 799 A1*, 9th May 2001.

[81] M. Grimshaw. *Machine for applying composite and presser assembly therefor. Patent EP 0371289-A1*, 8th November 1989.

[82] M. Grimshaw and J. Hechtt. *Method and apparatus for laying composite material. Patent EP 0644040-A1*, 8th November 1994.

[83] D. H.-J. A. Lukaszewicz. *Optimisation of high-speed automated layup of thermoset carbon-fibre preimpregnates*. PhD thesis, University of Bristol, 2011.

[84] R. J. Crossley, P. J. Schubel, and N. A. Warrior. Experimental determination and control of prepreg tack for automated manufacture. *Plastics, Rubber and Composites*, 40(6/7):363–368, 2011.

[85] S. Khan. Thermal control system design for automated fiber placement process. Master's thesis, Concordia University, 2011.

[86] J. Sloan. Afp/atl evolution. Online, 2014. `https://www.compositesworld.com/articles/afpatl-evolution`, last accessed 16 August 2020.

[87] J. Sloan. Narrow ud tapes to bridge the atl-afp gap. Online, 2020. `https://www.compositesworld.com/articles/narrow-ud-tapes-to-bridge-the-atl-afp-gap`, last accessed 16 August 2020.

[88] R. DeVlieg, K. Jeffries, and P. Vogeli. High-speed fiber placement on large complex structures. In *SAE Technical Paper Series*. Eletroimpact, Inc, AeroTech Congress Exhibition, 2007.

[89] A. SAS. Boeing 787 – lessons learnt. Online, 2008. `https://www.slideshare.net/aergenium/b787-lessons-learnt-presentation`, 10 August 2020.

[90] A. Crosky, C. Grant, D. Kelly, X. Legrand, and G. Pearce. *Advances in Composites Manufacturing and Process Design*, chapter Fibre placement processes for composites manufacture, pages 79–92. Elsevier, 2015.

[91] M. Szcesny, F. Heieck, S. Carosella, P. Middendorf, H. Sehrschön, and M. Schneiderbauer. The advanced ply placement process – an innovative direct 3d placement technology for plies and tapes. *Advanced Manufacturing: Polymer Composites Science*, 3(1):2–9, 2017.

[92] J. Rybicka, A. Tiwari, P. A. del Campo, and J. Howarth. Capturing composites manufacturing waste flows through process mapping. *Journal of Cleaner Production*, 91:251–261, 2014.

[93] M. Tyrrell. Automated layup systems – sweating the assets. Online, 2017. `https://www.composites.media/automated-layup-systems-sweating-assets/`, last accessed 10 August 2020.

[94] B. Denkena, C. Schmidtb, and P. Weberb. Automated fiber placement head for manufacturing of innovative aerospace stiffening structures. In *Procedia Manufacturing*, volume 6, pages 96–104. 16th Machining Innovations Conference for Aerospace Industry - MIC 2016, Elsevier B.V., 2016.

[95] J. Sloan. Evolving afp for the next generation. Online, 2019. `https://www.compositesworld.com/articles/evolving-afp-for-the-next-generation`, last accessed 16 August 2020.

[96] K. Kozaczuk. Automated fiber placement systems overview. *Transactions of the institute of aviation*, 4(245):52–59, 2016.

[97] K. Mason. Smarter, integrated data for atl/afp. Online, 2019. https://www.compositesworld.com/articles/smarter-integrated-data-for-atlafp, last accessed 15 August 2020.

[98] K. Potter. *The Structural Integrity of Carbon Fiber Composites*, chapter But How Can We Make Something Useful Out of Black String?' The Development of Carbon Fibre Composites Manufacturing (1965–2015), pages 29–57. Springer, 2015.

[99] A. Oy. Carbon fiber composites: Processing guide. Online, 2019. https://www.addcomposites.com/post/carbon-fiber-composites-processing-guide, last accessed 27 November 2020.

[100] N. S. Rao, A. Simha, P. K. Rao, and V. R. Kumar. *Carbon Composites are becoming competitive and cost effective*. Infosys Ltd., 2018.

[101] H. Corp. *HexPly® Prepreg Technology*. Hexcel, 2013.

[102] H. Corp. Carbon fiber reinforcements. Online, 2020. https://www.hexcel.com/Products/Fabrics-Reinforcements/Carbon-Fiber-Reinforcements, last accessed 30 August 2020.

[103] A. Oy. Virtual demo: How to make flat laminate using afp-xs. Online, 2019. https://www.addcomposites.com/post/virtual-demo-how-to-make-flat-laminate-using-afp-xs, last accessed 28 August 2020.

[104] B. Soares, E. Henriques, I. Ribeiro, and M. Freitas. Cost analysis of alternative automated technologies for composite parts production. *International Journal of Production Research*, 2018.

A. Annex

A.1 Main script structure

A main script was created where the main loops of the tool run. Only the most important parts of the script will be referred in order to give a wide understanding of the algorithm's logic. Most relevant functions and inputs/outputs will also be referred in this section. The main script, as illustrated in Figure 5.1, starts with a setup phase where the user provides the necessary inputs, as explained in the previous section, for the model to function. Then, the composite part drawing is processed in an image processing section of the script. After that, the core of the tool is called into action where the simulation of the part manufacturing is performed. Finally, the results are processed and the outputs saved and presented. The following paragraphs will provide further insight in each one of these script sections.

A.1.1 Image Processing

The first step to take is to pre-process the input variables in order to make them useful in the form the algorithm is set. The tape/tow width, the minimum course length, the minimum cut-restart length and the part offset are all provided in mm. For these measures to work in the algorithm they need to be converted into the pixel resolution scale. If the values given for these measures are not a multiple of the pixel resolution provided, the tool terminates and a warning message appears as to correct this situation. If this problem is solved, they are then divided by the pixel resolution, P_{res}. As previously discussed, this is crucial to the correct and plausible functioning of the model due to working with discrete pixels values. They are stored in the variables ***tape_width_pixel***, ***min_course_length_pixel***, ***min_cut_restart_pixel*** and ***offset_pixel***, correspondingly. Following that, a directory called "Files" is created within the path where the tool's executable is stored in the computer where each simulation image(s) and excel file are saved. This is done through a created function called ***createDirectory***.

The next step is to read the composite image(s), stored in the variable ***Part_images***, using *MATLAB*'s function ***imread*** as the basis for the creation of a larger function called ***readImages***. The image information is then stored in the variable ***Fig_rgb*** as a three dimensional matrix, each dimension associated with a color, red, green, and blue. The data is stored as uint8 - Unsigned Integers of 8 bits. This matrix, along with the variable ***offset_pixel***, are then called to a function called ***imageProcesing***. Colors are not important in the subject at matter, as such, the *MATLAB*'s function ***rgb2gray*** is used to convert the matrix ***Fig_rgb*** into a new black and white image with one dimension stored in the variable ***Fig_calc***. After, that variable is updated using a function created called ***binarize*** which, as the name indicates, takes the matrix stored in ***Fig_calc*** and translates it to binary numbers. An uint8 data type contains all numbers from 0 to 255 and, as such, the referred function transforms every number with value 255 in the matrix to 0 and the ones with value 0 equal to 1. This makes the values which represent the area of the part ready to be manipulated which is crucial to make calculations and logical operations as they get a 1 value.

A developed function named ***boundaryImage*** is then called in order to detect the part's boundary. A grey line is attributed to the image contour with the interior and exterior in white. This new matrix is called ***Fig_display***. This matrix is then centered in the white canvass in order to avoid orientation misplacement of the tape in the algorithm. This is done through the created function ***centering***. Furthermore, if a part offset is provided, the image is re-sized to that length using the created function ***resizing***. This surface increase is needed and very important because it prevents any defect that may appear near the edges of the part. Three matrices are produced as outputs of the ***imageProcesing*** function, ***Fig_display***, ***Fig_area_calc*** and ***Fig_rsized_boundaries***. The first is the matrix where each ply deposition will be "stored" and displayed throughout the script. The second is a matrix storing original part information for further original part area calculation. The last matrix has multiple purposes such as calculation of the resized area, serving as basis for further processes as a figure without any material deposited. In a way, its the anchor of the algorithm providing the boundaries of the part to be laminated as reference. Its original and resized perimeter is also obtained in this function. After this, the part's area before applying composite material, meaning its original area, and the resized one are calculated. This is done by summing all the entries with the value 1 in the matrices described above for the purpose. The ply deposition loop can now be started.

A.1.2 Part Manufacturing simulation

A loop is performed for each ply lay-up. This loop starts with the value stored in the variable ***Ply_index*** of the current ply number being simulated. The loops reaches its end when ***Ply_index*** reaches the full length of the variable ***Full_ply_Sequence*** which contains the angle orientation of all plies. If necessary, the matrices representing the simulated lay-up part and the basis re-sized part are rotated using the *MATLAB* function ***imrotate*** according to the variable ***Full_ply_Sequence*** and then updated and allocated in a new variable ***Fig_display*** and ***Fig_current_ply***, respectively. The same logic applies if the matrix needs to be flipped horizontally. This happens if the finish location side of one ply course makes the machine start on that side on the next ply for transitional time saving purposes. If this side is the right side of the part's image, the image needs to be flipped because the algorithm has the lay-up starting on the left side of each ply in order to reduce the algorithm's complexity. The flipping decision is made in the end of each loop and will be further explained down this section. The variable ***Fig_calc_transitional_time*** is created by subjecting ***Fig_current_ply*** to the functions ***boundaryImage*** which, as explained, takes a matrix image and transforms it in its grey color boundaries and a white background. Also, the created function ***negativeTransf*** is applied to that same matrix which transforms it in its negative colors. This happens because its values, which represent the area of the part, need to become positive value 1 instead of a 0 value. Then they can be used for calculations purposes in the functions used to calculate transitional tape/tow distances which will explained further down this section as well. This all happens when calling the created function ***imageRotatorFlipper***.

Inside each ply loop a tape/tow loop is performed. This is done in order to jump from column to column of the matrix ***Fig_current_ply*** and start the part lay-up. A function called ***first_entry_detection*** was created to detect the first column with a non-zero entry. It returns the number of that column and stores in

the loop variable ***index*** which functions as an internal clock for the whole script because it represents the location status of the lay-up at each moment of the loop. Following this, the function ***lamination*** is used. It is responsible, as the explicit name indicates, for the composite lamination itself. It takes as major inputs the matrices ***Fig_current_ply***, ***Fig_display***, ***Fig_calc_transitional_time***, the ***tape_width_pixel***, ***min_course_length_pixel***, ***min_cut_restart_length_pixel*** and the column where to start the deposition, the ***index***. Also the ***Current_T_number***, which represent the current number of tapes/tows, is an input of this function. As most important outputs the function returns the updated ***Current_T_number***, the area of the deposited composite tapes/tows, ***T_area***, its tape/tows minimum and maximum row and column coordinates, ***T_coords*** and its length, ***T_length***. It also updates the image matrix ***Fig_display*** with the current deposited tape/tows as well as the index to start the next tape/tow loop. This is done by adding the tape width to the current ***index***. Also, the variable ***Fig_display_transitional_time*** is created here for each tape/tow deposition by applying the function ***negativeTransf*** to ***Fig_display*** for transitional time between tape/tows courses calculation purposes. If a course deposition has any longitudinal gaps, its distance is also calculated in the ***lamination*** function and stored in the variable ***transitional_longitudinal_distance***.

Consequently, the variables ***Current_area***, which indicate the area sum of all the current deposited tapes/tows and the created variable ***longitudinal_transitional_time_per_ply*** is also updated with the time necessary to transition the longitudinal gap distance. This time is calculated using the created function ***time_Calc***. This function basically uses the acceleration and speed (inputs) for that movement, in this case, the ***Transitional_acceleration*** and ***Transitional_speed*** as well as the distance travelled in that movement, here, the ***transitional_longitudinal_distance***. It also takes into account the initial speed of that movement which can be from idle position or other determined speed, depending of the technology chosen and the machine configuration. If the variable ***display_index*** equals 1, which is consequence of the user option, then the lamination is displayed with the corresponding updated tows with current lay-up area and ply orientation angle in the image title using the created function ***imageDisplay***.

If the deposition reaches an horizontal gap or the end of the part lay-up, translating to the variable ***T_coords*** having its first two entries with value zero, the function ***first_entry_detection*** is called again to assess the new ***index*** after the gap and determine the ***Gap_distance***, if that is the case. This gap distance takes into account machine configuration, meaning if the machine has uni or bi-directional lay-up or the machine technology selected. This gap transition distance is given as the shortest distance between the four options described in chapter 4 for optimal time saving purposes. The function ***first_entry_detection*** also returns the the row and column number where the machine last deposited before the horizontal gap in the variables ***Finishing_row*** and ***Finishing_column***, correspondingly. This is important for the case of the script reaching the end of the part layup because that point, where the machine finished the lay-up, will be used further down the algorithm to assess the transitional ply distance, meaning the distance the machine has to travel between finishing one ply and starting another. After, if the case is of a horizontal gap, the ***Horizontal_transitional_time_per_ply*** variable is updated with the corresponding gap machine transitional time, also calculated through the function ***timeCalc***.

Proceeding, the transitional distance for the next tow or tape deposition is calculated using created functions ***transitionalTowDistanceAFP*** and ***transitionalTapeDistanceATL*** according to the technology used. Here, the discussed ***Fig_calc_transitional_time*** and ***Fig_display_transitional_time*** are used as inputs for that purpose. Following, transitional tape/tow time time is calculated and added to ***AFP_transitional_time_per_ply*** or ***ATL_transitional_time_per_ply*** in the same fashion using ***timeCalc***, same acceleration and speed and using the created output variables ***Tow_transitional_distance_AFP*** or ***Tape_transitional_distance_ATL***. To finalize each tape/tow loop, its coordinates are stored in variable ***Total_T_coords*** and its length in ***Total_T_length***.

When the variable ***index*** reaches the last column of the matrix ***Fig_current_ply*** the tape/tow deposition loop is broken. Following, if variables ***Fig_display*** and ***Fig_current_ply*** were horizontally flipped they are flipped back to its original rotated state. After this, they are rotated back to its original angle so they can be rotated to its corresponding next ply orientation angle. Then, the function ***flipping*** is used to determine if the next ply image needs to be horizontally flipped. This is important because there is a need to determine the distance between the last machine location and the following ply machine start location. As there are always four options for this location starting point, as explained in chapter 4, it requires the determination of these distances so that the the shortest one can be selected. If the shortest distance means the deposition starts on the left side of the original image there is no need for the image, ***Fig_display***, to be flipped because, as explained, the algorithm detects the first column entry from left to right of the referring matrix. If the shortest distance from one ply's end to the next means the deposition must start on the right side of the original image then there is a need to flip the image horizontally on the start of the next ply loop and the value stored in the variable ***Flip_index*** is 1, otherwise is 0. After this, ***Ply_transition_distance*** is calculated. Consequently the time to perform plies transition is calculated and then added to ***Ply_transitional_time_per_ply***.

Furthermore, the total area deposited in this ply is stored in ***Total_material_deposited_per_ply***. One of the most important and complex functions is now reached that computes the time it takes for the machine to perform a lay-up course. Course time comprehends the time the machine spends from the moment it touches the deposition plane in the beginning of the lay-up process to the moment it finishes the tapes/tows and lifts off the deposition plane. The created function, ***courseTimeCalc***, is responsible for not only calculating each ply course time, ***Total_course_time***, but also for the number of ***Courses_number*** the machine takes in each ply deposition. The lay-up time per ply, ***Total_course_time***, also includes the calculated initiation, cutting time and lay-up speed time of each tape/tow stored in variables ***Initiation_time_per_ply***, ***Cutting_time_per_ply*** and ***Layup_speed_time_per_ply***. The latter constitutes the time time the part is at or reaching the desired lay-up speed. The time on part, ***Time_on_part_per_ply*** is then updated with the ***Total_course_time***. In the next step, the total material deposited per machine creel is calculated using the created function ***depositionPerCreel*** and stored in ***Total_deposition_per_creel_per_ply***. To finish one ply loop cycle, ***Total_approach_retract_time_per_ply*** is calculated and the total lay-up time, ***Total_layup_time_per_ply***, which sums up ***Time_on_part_per_ply***, the ***Total_approach_retract_time_per_ply*** and the ***Total_transitional_time_per_ply*** is finally obtained by summing all the previous mentioned transitional time related variables. The loop then jumps to next ply

and the process repeats. When all the ply's have went through both cycles the major loop is terminated.

A.1.3 Results Processing

The last section of the algorithm is responsible for processing the results using the function ***resultsProcessing***. Some important outputs are the ***Total_material_deposited***, ***Total_scrap***, ***Total_scrap_percentage***, ***Total_mass***, ***Scrap_mass, Layup_time***, ***Cycle_time***, ***Total_initiation_time***, ***Total_cutting_time***, ***Total_transitional_time***, ***Total_approach_retract_time***, ***Total_cost***, ***Material_cost***, ***Scrap_Cost*** and ***Layup_rate***, ***Time_on_part_per_ply***, ***Number_of_rolls_req*** among others. These variables evaluate material and time parameters and are displayed in the *command window* with the function ***printing***. Total scrap material per ply as well as its percentage with respect to the original area is calculated. The total lay-up time and cycle time are also obtained. Finally, the lay-up ratio is provided making the algorithm reach its objectives. The two last functions are then reached. The first, called ***plotting***, is responsible for plotting the bars graphic illustrating the total material deposited per machine creel and the second, ***excelCreator***, creates an excel file with all the results from the simulation and also saves the simulation image(s). The flowchart of Figure A.1 summarizes all steps explained above.

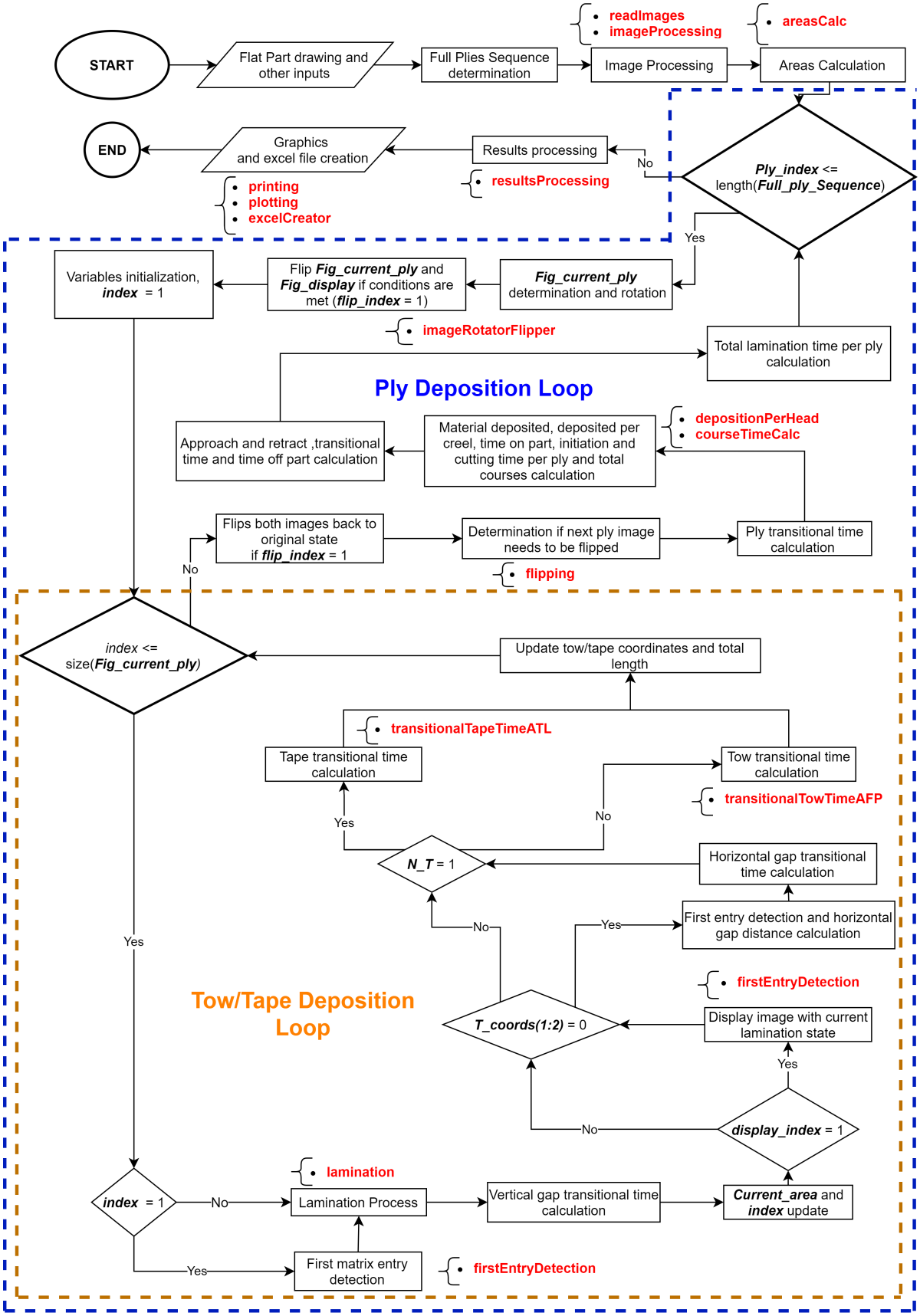

Figure A.1: Main script flowchart.

A.1.4 Lay-up and Scrap rates for aeronautical representative composite parts

Table A.1: Machine data for aeronautical representative parts simulation.

Parameter	ATL single	ATL two	ATL two bi-dir.	AFP	AFP bi-dir.	unit
a_{lay}	1000	1000	1000	2000	2000	mm/s^2
a_{tr}	1000	1000	1000	2000	2000	mm/s^2
a_{vert}	1000	1000	1000	2000	2000	mm/s^2
v_{lay}	1000	1000	1000	1000	1000	mm/s
v_{tr}	1000	1000	1000	1000	1000	mm/s
v_{init}	-	600	600	600	600	mm/s
v_{cutt}	-	700	700	700	700	mm/s
v_{app}	200	200	200	200	200	mm/s
v_{ret}	400	400	400	400	400	mm/s
$Layup_d$	Uni dir.	Uni dir.	Bi dir.	Uni dir.	Bi dir.	-
$Course_{start/finish}$	At part's edge (2)	-	-	Both	Both	-

A.1.5 First tape offset study results

First scenario:

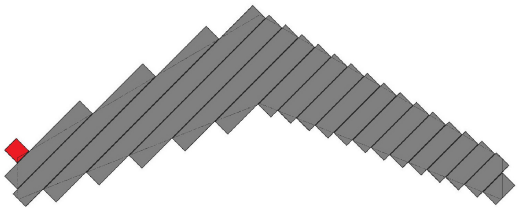

Figure A.2: Offset study - ATL Ply Lay-up 45º (left to right).

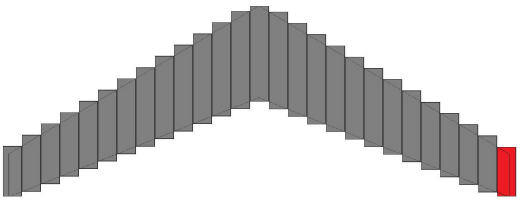

Figure A.3: Offset study - ATL Ply Lay-up 90º (right to left).

Second scenario:

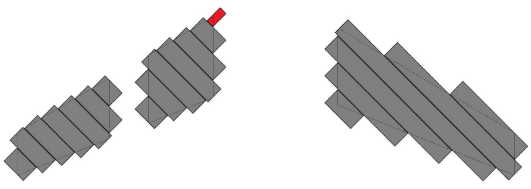

Figure A.4: Offset study - ATL Ply Lay-up -45º (right to left).

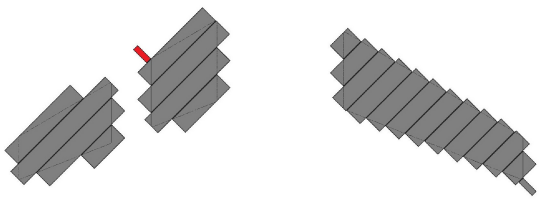

Figure A.5: Offset study - ATL Ply Lay-up 45º (left to right).

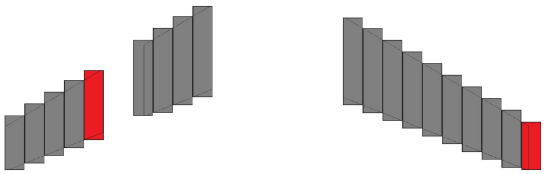

Figure A.6: Offset study - ATL Ply Lay-up 90º (right to left).